ADMET AMPHIPHILES

By

ERIK BENJAMIN BERDA

A DISSERTATION PRESENTED TO THE GRADUATE SCHOOL
OF THE UNIVERSITY OF FLORIDA IN PARTIAL FULFILLMENT
OF THE REQUIREMENTS FOR THE DEGREE OF
DOCTOR OF PHILOSOPHY

UNIVERSITY OF FLORIDA

2008

To Dana, the love of my life, for her sacrifices, love, support, and understanding and to Bethy, Patty, and Mikey for lots of help along the *way*.

ACKNOWLEDGMENTS

There are many a great folken whom helped me along the *way*, both here in Gainesville and back in Pennsylvania, say thankya. I'll start in Gainesville and work my way backwards in a pseudo-chronological fashion.

First I'd like to acknowledge the Department of Chemistry, in particular Ben Smith, Ken Wagener, John Reynolds, and Randy Duran. They saw potential when no other institution would give me a chance. I am eternally grateful for your confidence.

I would again like to thank Ken Wagener for his patience; I am a stubborn and often intolerable student. He forgave my frequent trespasses, and I learned a great deal about mentoring from him. I would also like to acknowledge John Reynolds. It has been a pleasure working under two capable advisors and I truly appreciate the opportunities I was presented with working in the Butler Labs (a.k.a. the artist formerly known as Polymer Floor). Also I would like to thank George Butler, rest peacefully, and his wife Josephine for their contributions to our program. I would like to thank the rest of my committee: Bill Dolbier, Mike Scott, and Tony Brennan for there time, effort, and advice. I would especially like to thank Bill Dolbier; I really began to understand organic chemistry during his 5224 class. I would also like to acknowledge Tammy Davidson and Eric Scriven, it has been a pleasure serving as a TA for both of you.

The *road* through Gainesville would not have been tolerable if it were not for great friends. Thank you to Travis Baughman for splitting the rent, talking Wagener group, and rocking the endless blues in E. Thank you to Jeremiah Tipton for the best rendition of *Spoonman* ever. Thanks to Ben Reeves for low key low tones, the Wednesday jams are severely missed. Thanks to his lovely wife Jenny for beating me Texas Hold'em repeatedly. Thank you to Josh McClellan for philosophical discussions while nearly freezing to death in the November North Georgia woods. Thanks to Piotr and Nela Matloka for good lunches, good parties, and being great hosts

in Belgium. I'd like to thank James Leonard for showing me that you can actually load 2 20 ga. Rounds into a 12 ga. Shotgun, pull the trigger, and live to laugh about it. Thanks to Giovanni Rojas for tons of laughs in Pasadena. I'd like to thank Flo Courchay for consistent kind remarks. Thank you to Kate Opper for turtle sitting, dog lending, and spilling appletinis on my carpet. Thank you to Sam Popwell for good laughs during the summer 07 teaching labs, What Would Bear Do? Thank you to YuYing Wei for an analytical chemist's perspective on synthetic chemistry, I'll stop cleaning spatulas with my gloves now. Thanks to Paula Delgado for showing me the inherent flaws in the DSC sample press design. I would like to thank Zach Kean for good times at T&T's. Thank you to the newest members of the Wagener Mafia: Bora and Brian, it was nice to get to know you over the past several months. I'd like to thank Bob Brookins and Tim Steckler for good laughs at the Seminole Hard Rock Casino. Thanks to The German for sharing a few small pitchers between enormous chromatography sessions. Thank you to Pierre, Jianguo, June, and Prasad for making 322/324 a great place to make polymers. Thanks to Merve Ertas for constructive criticism and entertaining use of the English language. Thank you to Sophie Bernard for being just sarcastic enough. I'd like to thank JJ Cowart for help with some polymerizations. Also, thank you to Eva and Mike hanging out and listening to the Beatles. Thanks to Violeta Petkovska for great conversation and even headed advice. I can't forget to thank Rachel Lande for being a great student, even when I was not such a great mentor.

The gentle way kept me sane during my tour of duty in Gainesville. I would like to thank Matt and Lauren, Davis and Virginia, Ed and Carissa, Thomas and Cathy, Larry and Ana, Weber, Chris, Chan, and Natty for being great teachers and great friends. Thank you to the entire UF Judo club past and present, it has been exceptional to train with such superb judoka.

Thank you to all of my colleagues from the Polymer Floor, Organic Division, and the rest of the department that I may have inadvertently neglected to mention. I could fill an entire dissertation thanking such a wonderful group of individuals.

Work would come to a grinding halt in this place if it weren't for the efforts of some amazing administrative assistants. In the polymer office Sara Klossner and Gena Borrero, we know who really runs the show, thank you for your hard work. Also, thank you to Lori Clark in the Graduate Office and Maribel Lisk in the Chairman's office for all of your help as well.

Special thanks go to Toshio Masuda, Fumio Sanda, Masashi Shiotsuki, Kimiko Tada, Kayo, Suzuki, Matty, the rest of the Masuda Lab, and Kazushi Mashima for being great hosts and great friends during my trip to Kyoto. I can't wait to return.

From Pennsylvania there are a number of people to whom I am forever in debt. Of course, my parents Pat and Marybeth, one couldn't ask for better teachers and friends. Also, thanks are in order for my brother and best friend Mike Berda. I couldn't leave out Clarkie, thanks for all your love and support, nor the GrandBerdas, thanks for the prayers. Of course this section wouldn't be complete without thanking the rest of the "family," Jay DeFrangesco, Nick Pisano, and Dan Watson. My mind wanders to Norristown circa 1997 often, thank you for being great friends. In addition, I would like to thank Lynn Hinely, Joseph DeFrancesco, and Ron Petruso for being great teachers and really shaping what would be my career choice.

From Penn State I would like to acknowledge Harry Allcock, Bob Morford, and Eric Powell for my introduction to polymer research. Also, I would like to thank Bob Minard for giving me a shot at teaching organic lab, also Dan Sykes for being a patient educator. I would like to thank Steven Babcock for the only F I had to fight to recieve.

From Watts Hall to 333 thank you to Tom Riccairdi, Brian Boyle, Mark Lupinacci, Bryan Koval, Aaron Pressman, Mike Carroll, Patty Salimone, Jessica Summers, and Hillary Ryan. My memories of this time are fond and I think of you all often. I wouldn't have made it through PSU without you. The thirty pounds I gained eating DP dough was worth it. I would also like to thank Arie Hawkins and the crew at the college formerly known as WMC. Westminster Maryland was an experience in and of itself.

Thank you to the I&C group at Limerick Generating Station, the opportunity to work here was amazing and I will never forget it. I totally understand *Dilbert* and *Office Space* after this experience.

From 1011 to UC building C I'd like to thank Geoff Faden, Jason Drews, E, Rob Lanning, Steve Kulada, Tracey Johnson, Josie, Luis "Tito," Santana, Punishment, Ace, Tre Diggs, Laura Merrick, and of course "Mecca." These times were unforgetable. The extra semester it cost was worth it.

There are some people from Mario's that can not go unmentioned. Thank you to Melody Phillips, Michelle, Scott, Ralph, Linda, Gail, and Tracey Faye; it was awesome to meet and work with you. Of course I can not forget Tom at the end of the bar for good conversation over several glasses of vino.

Mario's is special to me for another reason; this is where I met Dana. I knew from the moment I met you. Thank you for your constant love and encouragement; you mean the world to me. Of course I can't leave out my family on Elm Street: Denny, Judy, and Erin. Thanks for sharing your lives; I am actually growing to enjoy playing board games.

Science is the pursuit of the truth; however the truth itself is unapproachable by any one *path*. To me, this is the meaning of the degree Doctor of Philosophy; the art we choose is simply the *way* we *walk*. My deepest gratitude for *walking* with me, I could not have done it alone.

TABLE OF CONTENTS

page

LIST OF TABLES

LIST OF FIGURES

Abstract of Dissertation Presented to the Graduate School
of the University of Florida in Partial Fulfillment of the
Requirements for the Degree of Doctor of Philosophy

ADMET AMPHIPHILES

By

Erik B. Berda

May 2008

Chair: Kenneth B. Wagener
Major: Chemistry

Acyclic diene metathesis (ADMET) allows for the synthesis of perfectly linear polyolefins with precisely controlled distribution of some exactly defined functional group, either within or pendant to the polymer backbone. The materials produced in this fashion possess properties that are tunable synthetically, accomplished by changing the identity of the regularly appearing moiety or the frequency of its appearance. A wide range of materials have been produced in this fashion, resulting in a catalogue of polymers displaying various morphologies and material responses. The ADMET polymerization and subsequent hydrogenation strategy when applied to the synthesis of model polymers facilitates the systematic study of various structural manipulations and their relationship to property.

Here we describe the incorporation of hydrophilic pendant defects, namely short chain polyethylene glycol branches, onto the backbone of polyethylene using ADMET polycondensation chemistry. The motivation behind this work is to create semi crystalline materials, intentionally excluding this hydrophilic moiety from the crystal, thereby isolating the behavior of the methylene sequences between glycol branches. The immiscibility of the hydrophobic backbone and hydrophilic defects induces folding of the backbone about the pendant defect allowing the clustering of the PEG branches to minimizing contact between each

segment. This work demonstrates that by carefully planning the identity of the pendant defect it can be excluded from the crystal and induced to aggregate; excluded and induced to crystallize separately, or excluded and re-included back into the polymer backbone crystals. The crystallization of the backbone excluding the PEG branches to the amorphous regions, or even the formation of bicontinuous PE and PEG phases could result in a layered or channeled morphology that may find utility in advanced applications.

CHAPTER 1
INTRODUCTION

The Evolution of ADMET

By the mid 1980s considerable advancements had been made in the field of olefin metathesis chemistry.[1] This mild carbon bond forming reaction was discovered by accident in the late 1960s when researchers at Goodyear exposed a mixture of 1-olefins to a combination of tungsten hexachloride and a lewis acid with the intent to find a new catalyst for the polymerization of vinyl olefins.[2, 3] Instead of high polymer the research team observed a complex mixture of scrambled olefin products. The mechanism of this reaction, first proposed by Yves Chauvin[4] in 1971 and later confirmed by Thomas Katz[5] in 1975, involves the 2+2 cyclo addition of an olefin to a metal carbene to form a metallocyclobutane, followed by a 2+2 cyclo reversion to yield a new olefin and metal carbene. A majority of the research in the years to follow involved the development of stable metal carbenes that could facilitate this useful transformation, which has become an indispensable tool to the synthetic organic chemist (Figure 1-1).[1, 6]

This reaction was used from its inception in the synthesis of polymers. Despite the lack of well defined catalyst systems, a large volume of work had been produced by the mid 80s on the ring opening polymerization of strained cyclic olefins.[6] This reaction, coined ROMP (ring opening metathesis polymerization) has become one of the most useful methods in the fabrication of functionalized polymers for use in every imaginable application. Although it was proposed early on that this reaction could also be used in the polycondensation of a linear diolefin, it wasn't until 1987 when the first study proving the feasibility of this concept appeared.[7] In this report the Wagener Group at the University of Florida attempted the polymerization of 1,9 decadiene using an ill defined tungsten hexachloride /lewis acid mixture,

resulting in viscous oil and an intractable solid. Monitoring the disappearance of terminal olefin signal via ^{13}C NMR and IR confirmed that the polymerization had occurred. Since any polycondensation requires that the reaction involved proceeds quantitatively, the self metathesis of styrene to stilbene was attempted as a test reaction. The isolated product in this case was polystyrene, rather than stilbene, due to the cationic polymerization of styrene initiated by the lewis acid present in the ill defined catalyst system. The authors were quick to realize that while the concept was feasible, a well defined metal carbene catalyst would be necessary to prevent this detrimental side reaction.[7]

Fortunately, excellent progress was being made in catalyst design at this time. Professor Wagener was so excited by the outlook for this reaction that he called Richard Schrock at MIT and Bob Grubbs at Cal Tech to request assistance in the area of well defined catalysts and give this acyclic diene metathesis (ADMET) a second try. Armed now with the right carbene for the job, the Wagener group successfully synthesized stilbene from styrene in quantitative yields and reported the first viable ADMET of 1,9 decadiene to polyoctenamer.[8] Examples of well-defined metal carbene metathesis catalysts are shown in Figure 1-3.

It was obvious even in the initial ADMET report that this reaction could have utility in the fabrication of unique structures.[7, 8] Virtually any moiety that can be functionalized with two olefins could potentially become an ADMET monomer. Not surprisingly early efforts in the Wagener group involved the synthesis of a variety of functionalized polymers using this chemistry ("what could 'R' be"). As metathesis catalysts became increasingly robust and tolerant of functional groups the number of moieties that could be used in this reaction increased and the library of ADMET polymers grew considerably. Simultaneously, research on the mechanism of this reaction ensued (Figure 1-4). By attacking ADMET from both practical and fundamental

aspects the Wagener research group was able to carve a niche in the olefin metathesis story. Several review articles have been published on this topic.[9-11]

More recently research in the Wagener group has moved specifically towards the study of precise structure (Figure 1-5). In particular, ADMET has the unique ability of producing structures that mimic copolymers of ethylene and vinyl comonomers.[9-20] These ethylene based copolymers are typically made using chain propagation techniques, which are subject to uncontrollable side reactions that create unwanted defects. These defects in turn have adverse effects on polymer performance.[9] Perfectly linear defect free model polymers can be created using ADMET. This is accomplished by synthesizing a symmetrical terminal diene with a pendant functional group, polymerizing, and exhaustively hydrogenating the resulting unsaturated polyolefin backbone, allowing "defects" to be introduced in a controlled manner. Knowing exactly what the identity of this defect is and where it occurs along the backbone provides a systematic way to study this aspect of structure-property in ethylene based materials.[9] This chapter describes the evolution of this study. Research on various materials from linear polyethylene free of defects, through the addition of halogen atoms and alkyl branches of increasing size has displayed that not only do the precise structures created using ADMET possess unique properties, but that these properties are highly controllable. The library of polymers that has been created in this fashion and the information these polymers have provided about structure and property have led us to a new frontier: synthesis of precisely tunable polyolefins for advanced applications. For simplicity of discussion, the polymers described in this introduction will follow a systematic nomenclature: the identity of the pendant moiety is named first, followed by its frequency of its appearance along the polyethylene backbone (Figure 1-6).

Linear ADMET Polyethylene

Unbranched, or perfectly linear, polyethylene is of considerable interest, particularly for studying the behavior of this homopolymer during crystallization. Much of this work has been conducted on large *n*-paraffins (monodisperse PE oligomers) up to 390 carbons long, since defect free high-molecular weight PE is an elusive goal. While small molecule paraffin compounds allow in-depth study of structurally perfect model materials, end group concentration becomes a problem and leads to irregularities when trying to extrapolate morphological behavior to a macromolecular system. The methyl endgroups present in *n*-paraffins are regarded as defects that hinder crystallization. Polymer chains up to millions of grams per mol, on the other hand, possess an infinitesimal number of methyl end groups relative to backbone carbons, and comparisons between these two systems can lead to ambiguous results.

The synthesis of linear ADMET PE is important in this work to prove that the structures created are indeed effective as models of the commodity materials they mimic. Perfectly linear ADMET is prepared via the polymerization of 1,9 decadiene followed by saturation of the product polyoctenamer with hydrogen. While high molecular weight samples exhibit thermal behavior similar to that of high density polyethylene, molecular weights of products can be controlled by regulating reaction time, temperature, and the monomer/catalyst ratio affording a family of ADMET PE polymers with varied thermal responses. Despite the relatively low molecular weight (between 2000 and 15000 g/mol) for some ADMET PEs, these polymers all display sharp DSC melting transitions above 130 °C (Table 1-1). While the peak melting point increases with increased molecular weight, the polymer of M_n = 15,000 shows a peak melt of 134 °C, exactly that of high density polyethylene. It is evident based on this work that beyond the

molecular weight threshold of M_n = 15,000 ADMET polymers can effectively model analogous commercial materials.

Model Polyolefins with Precisely Placed Halogen Atoms

ADMET polyolefins with precisely placed halogen atoms (Figure 1-7) provide a unique system for studying crystallization and melting behavior of precision polyolefins. By synthesizing polymers decorated with fluorine, chlorine, and bromine the effect of this systematic increase in pendant defect size can be probed. Four separate studies[13, 14, 16, 21] were conducted on this class of materials. In the first the static methylene sequence length between defects was held constant (18 backbone carbons) and the defect identity altered.[16] In the other three the defect was held constant (fluorine, chlorine, or bromine) and the distance between defects altered.[13, 14, 21] In the first study it was found, not surprisingly, that with the increased defect size came a decrease in melting temperature and enthalpy.[16] When the defect identity was held constant melting temperature and enthalpy decreased with decreasing distance between defects,[13, 14] the notable exception being the fluorine containing polymers which all have approximately the same melting temperature despite differences in defect distribution.[21] Table 1-2 summarizes the DSC data for the precise halogenated polyethylenes.

Precise Fluorine Placement.

Regardless of branch distribution the melting points of ADMET polymers containing precisely placed fluorine atoms are consistent with what is witnessed for linear ADMET PE, evidence that the orthorhombic crystal structure of HDPE is unaffected by the addition of the fluorine atom.[21] This result was confirmed by WAXS. This is not surprising; considering the similarity in size between hydrogen and fluorine the steric requirements for housing this defect in the crystal shouldn't be significantly different. The melting enthalpy of this family of copolymers does however decrease with increasing fluorine content. This is much more significant in the

cases of F15 and F9 than in the cases of F19 and F21. The decrease in enthalpy for the higher defect concentration is evidence that electronic repulsions and bond polarity, as well as sterics, play an important role in the crystallization behavior for ADMET polymers.[16, 21]

Precise Chlorine Placement.

The consequences for the incorporation of chlorine atoms at precise intervals along polyethylene's backbone are more severe. There is a marked decrease in melting temperature from ADMET PE and the precise fluorine family. There is also a change in crystal structure, from orthorhombic to triclinic. These data show that the distribution of chlorine atoms in the crystalline and amorphous regions is uniform. Further, the lamellar thickness (estimated using atomic force microscopy) far exceeds the distance between defects on the backbone. This confirms that the chlorine atoms are included within the crystal. The steric requirements, however, are too severe for the orthorhombic crystal structure to remain intact. This behavior is solely a result of the uniform defect distribution, as random analogues with similar branch content possess broadened melting profiles with higher peak melting temperatures.[22] This is indicative of populations of lamella with different thicknesses, typical of copolymers with random branch distribution and quite unlike the homopolymer type crystallization and melting witnessed in ADMET systems.[13, 21, 22]

Precise Bromine Placement.

ADMET models with precise bromine placement represent the upper size limit for our study of halogen containing polymers, as nature resisted efforts to produce iodine containing ADMET polymers. As expected, the increased size of the bromine atom results in a decrease in melting temperature and enthalpy compared with the other halogenated ADMET polymers.[14] Like the precision chlorine polymers a triclinic crystal structure was assigned for the bromine containing polymers. The distribution of the bromine atoms was uniform in both crystalline and

amorphous regions like the chlorine polymers, and like the random chlorine polymers the random bromine polymers exhibited copolymer type methylene sequence selection when crystallizing.[22] Based on AFM measurements, as is the case for chlorine, the bromine atom resides within the crystal. Perhaps the most interesting feature of the precision bromine polymers is their similarity in thermal response to ADMET polymers with precise methyl branch placement (discussed in the following section). Based on these findings along with the data reported for the fluorine polymers, it appears that defect steric requirements are the most important factor in dictating the melting point of the resulting ADMET polymer crystal. Or, more simply put: a defect is a defect, regardless of its identity.[14] It could be a coffee cup!

Model Polyolefins with Precisely Placed Alkyl Branches

For more than half a century studies on structure and morphology have been central to polyolefin research. Discoveries in this area have allowed for the synthesis of materials with wide range of properties and behaviors. This is exemplified in the case of poly(ethylene-*co*-1-olefins), where the behavior of the polymer can be greatly altered simply by varying the content and identity of the comonomer chosen.

Precise Methyl Placement: ADMET Ethylene Propylene (EP) Copolymers.

Besides being commercially significant, EP copolymers can provide a general insight to the structure property relationship when viewed as model systems. Consider polypropylene: highly crystalline when the orientation of the pendant methyl group is highly regular (syndiotactic or isotactic), however completely amorphous when backbone methyl groups are randomly oriented (atactic); a simple structural difference resulting in significantly altered behavior. Linear defect free polyethylene, the other extreme, is highly crystalline. However, this crystallinity can be disrupted by the incorporation of defects, clearly evident in the aforementioned halogen work. Between the extremes of amorphous attactic polypropylene and

highly crystalline, defect free polyethylene lie EP copolymers. Simply varying the amount and placement of the incorporated methyl defect allows the response of the final material to be significantly altered and ultimately controlled.[9]

Although numerous methods are available for producing model polymeric systems, ADMET modeling controls comonomer content and distribution, therefore leading to fewer ambiguities relative to other model systems when relating structure on the molecular level to macroscopic properties.[9, 19, 23, 24] Polymerization of symmetrical methyl branched terminal dienes, followed by exhaustive saturation of the resultant polymer, afford these precise EP models (Figure 1-8).[19] These models are named according to the frequency of the pendant defect, i.e. Me21 for a methyl branch every 21st backbone carbon, Me15 for every 15th and so on. To date Me5, Me7, Me11, Me15, Me19, and Me21 have been investigated. The syntheses of Me11 through Me21 are rather straight forward using this simple yet elegant polymerization/hydrogenation approach.[19] Placing branches every 5th or 7th backbone carbon requires the synthesis of a symmetrical diene dimer, as the corresponding diene monomers undergo ring closing metathesis rather than ADMET.[24] Attempts to place methyl groups every third backbone carbon, using a diene trimer, were unsuccessful due to the placement of the methyl group in the allylic position. This allylic methyl decreases the yield of the cross metathesis reaction allowing for only the partial oligermerization of the diene (Figure 1-9).[25]

The effects of branch distribution are clear when examining the thermal behavior of the precision EP copolymer family.[19] As defect content increases melting temperature and enthalpy decrease. These precise models are semicrystalline even at branch contents high enough to render random EP copolymers completely amorphous. Not until methyl groups are placed on

every 5th carbon do these precise ADMET EP copolymers lose the ability to crystallize.[24] Table 1-3 summarizes the DSC data for the precise methyl family.

Copolymerization of ADMET EP monomers with 1,9 decadiene, thereby forming linear EP copolymers with random branch distribution, has also been accomplished.[23] In this study it was again found that as the branch content increased, over all crystallinity as well as the melting temperatures and enthalpies decreased. In the cases of the highest amount of branch incorporation the random materials exhibited a broad, ill defined melting behavior quite unlike the sharp melting endotherm observed for the precise models with similar branch content. This drastic difference in the behavior between precise and random models punctuates the effect of precise branch placement (Figure 1-10).[19, 23]

Me21 and Me15 have been further characterized by Wegner et al. using X-ray diffraction, TEM, and Raman spectroscopy to further understand their structure and morphology.[26] TEM results indicate a lamellar thickness far exceeding the inter branch distance along the backbone, proving that like chlorine and bromine atoms the methyl group must be included within the crystal. The diffraction work elucidated crystal structure. This data showed that the chains pack into a triclinic lattice which allows inclusion of methyl branches as lattice defects. Further, it was found that methylene sequences between defects participate in a hexagonal sublattice. In order for the chains to pack in this way the defects must be contained within plains oblique to the chain stems, leading to conformationally distorted crystals. This is more prevalent in the case of Me15 than in Me21 due to the greater defect content, a result confirmed by Raman spectroscopy. The melting point depression witnessed is no surprise given these observations. Further scattering experiments and exhaustive DSC experiments performed on Me21 by Wunderlich et al. lead to the same conclusion involving defects concentrated in planes between stacks of hexagonally

packed methylene sequences; however a monoclinic lattice rather than triclinic was used to describe the main unit cell within which the defects planes and hexagonal sublattice resides.[27]

ADMET Polyolefins with Larger Alkyl Defects.

To further understand the morphology of these precise materials and probe the size limit for inclusion of defects within the crystal, ADMET models with precisely placed ethyl, hexyl, and geminal dimethyl branches have been examined.

Precise Geminal Dimethyl Placement.

Precision geminal dimethyl ADMET models (Figure 1-11) display the effect increasing steric bulk has on the polymer's thermal behavior.[20] The addition of the second methyl group when moving from Me9 to 2Me9 disrupts the polymers ability to pack into crystals resulting in an amorphous material for 2Me9. Extending the inter defect sequence length to 14 or 20 carbons renders the polymer semicrystalline with a depressed melting temperature when compared to the analogous EP models. Interestingly, 2Me15 shows much less melting point depression from Me15 than does 2Me21 from Me21. Further, 2Me21 shows thermal behavior unlike either 2Me15 or any of the EP family. Exhaustive DSC studies on this material reveal that much of this behavior is dependant on thermal history. WAXD studies show reflections associated with hexagonal, monoclinic, and triclinic packing pointing towards polymorphism as a possible cause of this complex behavior. The melting behavior was found to be incident with the melting of eicosane (a 20 carbon *n*-paraffin), suggesting that crystallization behavior of 2Me21 is strongly related to the branch to branch distance.[27] The DSC data for this family of polymers is shown in Table 1-4.

Precise Ethyl Branch Placement.

Ethylene butene (EB) copolymers featuring precisely placed ethyl branches (Figure 1-12) were the next logical step in this study; moving from two single carbon defects to a single two

carbon defect.[17] These are of particular interest as EB copolymers are important materials commercially. Like 2Me9, Et9 is fully amorphous. Again, extending the space between defects allows for crystallization in both Et15 and Et21. Like the geminal dimethyl models the EB models show greatly depressed melting temperatures when compared to the EP models. Another point of interest is the difference in the observed thermal behavior from both the geminal dimethyl family and the EP family. EB copolymers exhibit bimodal melting profiles very much unlike the sharp, uniform melt exhibited by the EP family.[17]

WAXD investigations,[17] as well as exhaustive DSC analysis[27] have helped in explaining this behavior. Like 2Me21, the melting behavior of Et21 can be correlated with that of eicosane and is therefore very much dependant on the branch to branch distance. The WAXD results shows some lattice expansion implying the partial inclusion of ethyl groups into the crystal, however to a lesser extent than in EP21. Comparing these results for 2Me21 and Et21 imply that much of the melting behavior is attributed to crystallization of methylene sequences between defects. The bimodal melt could therefore be a result of polymorphism involving the inclusion and exclusion of these defects, or a melting and simultaneous crystallization mechanism. In or out of the crystal, the effect of increased volume requirements of the defect when increasing the size by just one methylene unit is obvious. Table 1-5 summarizes the DSC data for the precise ethyl family.

Precise Hexyl Branch Placement.

ADMET Ethylene Octene (EO) models serve as LLDPE models with precise hexyl branch placement (Figure 1-13).[12] These precise EO models follow a similar trend in behavior as the previously discussed families; that is with increasing branch content decreasing melting temperature and enthalpy are observed. It is no surprise that Hex9 is totally amorphous, as the much smaller ethyl branch is able to completely disrupt crystallinity at this branch concentration.

A semicrystalline morphology is observed for Hex15; an interesting result considering all other known EO copolymers with similar branch content are amorphous.[12] Hex21 is as well semicrystalline. The very low melting temperature (16 °C) is indicative of very small crystallites. Interestingly the melting enthalpy of Hex21 is similar to that of Et21, which is likewise surprising considering the notable decreases in enthalpy from Me21 to 2Me21 to Et21. The melting profile of the Hex21 closely mimics that of Me21 with a single sharp melting endotherm, rather than the complex endotherms displayed by 2Me21 and Et21. One possible explanation is that the hexyl branch is of sufficient size to be completely excluded from the crystal, owing the observed behavior to the crystallization of the inter defect methylene units. The inclusion of the branch resulting in a single crystal form as seen in Me21 is another possibility. With no scattering data available for this polymer conclusions on whether or not the hexyl branch is included or excluded from the crystal in these precise EO models based on thermal behavior alone. Table 1-6 summarizes the DSC data for this group of polymers.

Some reasonable conclusions can be drawn by comparing the DSC heating traces of Et21 and Hex21 (Figure 1-14).[12, 17] The lower melting mode of the bimodal melting endotherm for Et21 perfectly overlaps with the melting endotherm for Hex21. Taking the similarity of melting enthalpies into consideration as well is seems possible that at defect sizes beyond the ethyl group the inter defect methylene sequences can crystallize and exclude the branch to the amorphous regions. For these larger defects it would mean that these crystals do not organize into well defined lamella as the ADMET EP's do. It is possible that there are fewer carbons in the paraffinic crystal structure for Hex21 than for the other alkyl branched ADMET models (based on the decreased melting temperature), where the defect itself as well as the point at which the branch connects to the backbone would be excluded form this crystal, creating pockets of

uniform nanocrystallites randomly oriented in a matrix of amorphous hydrocarbon. This model for the crystallization of ADMET polyolefins is illustrated in Figure 1-15.

Precise Ether Placement

Model polymers with the precise placement of ether moieties along a PE backbone (Figure 1-16) represent the first examples of linear ethylene-co-vinyl ether polymers ever made.[28, 29] Difference in reactivity ratios between ethylene and vinyl ethers prevented the synthesis of this type of material via chain propagation chemistry until very recently.[30] These polymers differ from their alkyl branched cousins only by the exchange of the methylene unit directly off the backbone for an oxygen atom, which allows for some intriguing comparisons. Looking at the thermal behavior of OMe21 and Et21, shown in Figure 1-10, reveals a very interesting result.[9] The addition of the oxygen results in a slight increase of the peak melting temperature and melting enthalpy. The melting temperature for OMe21, like several of the previous examples, is incident with that of eicosane. As the steric requirements are roughly the same for these two polymers it can be concluded that the polarity of the bond and the electronics of the oxygen create a favorable place to initiate a fold in the polymer backbone, allowing for a more complete crystallization of the inter defect paraffic unit cell. The DSC data for this group of precision polyolefins are shown in Table 1-7.

Toward Advanced Applications

Precise Carboxylic Acid Placement.

A family of polymers with precise placement of carboxylic acids made using ADMET (Figure 1-18) were synthesized to model commercial analogues.[31] The resulting material produced some very significant data concerning the morphology of ADMET polymers. One of the most interesting features of these polymers is the fact that all of the carboxylic acid groups are dimerized based on the FTIR spectra. Based on SAXS measurements on these polymers it

was found that they contain a high degree of order that corresponds directly to the inter defect distance. WAXS data confirms that the paraffinic crystal structure is uninterrupted by the incorporation of these defects. The melting point of COOH21, like the 2Me21, is incident with eicosane. Correlating this data confirms that the methylene sequences between acids organize into a paraffin like crystal with the dimerized carboxylic acids concentrated in defect planes, similar to what was observed for the Me21. Diffraction experiments on a drawn sample of COOH21 provide even more compelling evidence for this; several concentric reflections were observed, corresponding to 1, 2, and 3 parallel stacks of crystallized inter-acid methylene sequences. This behavior is in sharp contrast to that of the random analogues, again highlighting the ability of ADMET to impart unique morphological features into polymeric systems by perfectly controlling microstructure.[31] Table 1-8 summarizes the DSC data for these polymers.

Precise Ionomers

A family of precise ADMET ionomers was examined by neutralizing the above carboxylic acid polymers with various amounts of zinc salt.[32] As seen in the other ADMET studies presented here, these materials did not behave at all like their random counterparts. In DSC experiments the first heating trace of these materials resulted in liquid crystalline like thermograms due to the melting of the well ordered interdefect paraffinic structures, resulting in an LC like phase, before entering an isotropic melt. This behavior was not repeatable on subsequent cooling and heating, implying that the ionic clusters and carboxylic acid dimers dominate the morphology when the material is cooled after the initial heating cycle. Long term annealing experiments were not conducted, however to see if the re-ordering of the inter defect methylene sequences could occur.

Purpose of Study

The question of whether or not large defects are included or excluded from the crystals of these ADMET polymers is central to our work in the Wagener research group. While the alkyl branching work is interesting and provides insight into the unique behavior of ADMET polymers, the composition of the defect is still identical to that of the backbone, and therefore there remains the propensity for the inclusion of such a defect into the polymer unit cell. This dissertation describes the incorporation of hydrophilic pendant defects, namely short chain polyethylene glycol branches, onto the backbone of polyethylene using ADMET polycondensation chemistry. The motivation in this work is to intentionally exclude the defect from the crystal, thereby isolating the behavior of the inter defect methylene sequences. Phase separation and self assembly of PE-co-PEG block copolymers and block oligomers is well known.[31-49] However this strategy has not been applied to precision polyolefins with any well defined goal in mind. The immiscibility of the hydrophobic backbone and hydrophilic defects should induce a specific behavior: the PE backbone chains should fold to allow the clustering of the PEG branches, minimizing contact between each segment. The crystallization of the backbone while excluding the PEG branches to the amorphous regions, or even the formation of bicontinuous PE and PEG phases could result in a layered or channeled morphology (depicted by a simple cartoon in Figure 1-19) that may find utility in advanced applications such as polymer electrolytes or membrane technologies.

Chapter 2 describes the synthesis of a series of ADMET polymers with hydroxy terminated PEG branches. A protecting group was used to ensure the absence of side reactions during monomer synthesis and polymerization. The thermal behavior of the polymer with and without the protecting group was evaluated; it was found that the identity of the graft end group can significantly alter the behavior of these polymers. Analysis of the data collected for this family

revealed that the polymer backbone forms crystallites while excluding the PEG branches to amorphous regions. Chapter 3 describes the synthesis of a series of ADMET polymers with methoxy terminated glycol branches. Methyl groups are small enough as not to disrupt backbone crystallization, but lack the ability for hydrogen bonding possessed by the polymers in chapter 2. Three parameters are altered in this study: the length of the PEG graft, the manner in which the branch is connected to the backbone, and the distribution of the branch along the backbone. Doing so isolates the effect all three features have on the ability of the backbone to crystallize. These polymers were analyzed both before and after hydrogenation to understand the effect the site of unsaturation (essentially a defect) has on the crystallization of the backbone. Chapter 4 examines whether or not self assembly or aggregation of functional groups attached to the end of the PEG chains is possible. This is an important question- if this concept is proven tailoring these polymers for application has promise. First, the end of the PEG chain was labeled with a pyrene unit. Fluorescence measurements confirm excimer formation and therefore the interactions of the pyrene groups. Although this aggregation results in an increase in glass transition temperature relative to the corresponding unlabeled polymer, the crystallinity of the polymer backbone remains intact displaying that the amorphous content can be altered independently of the crystalline regions. Two different *n*-paraffin end groups are also studied, the goal being to induce self assembly of the branches and thus alter the crystallization behavior. This chapter demonstrates that by carefully planning the identity of the pendant defect it can be excluded from the crystal and induced to aggregate; excluded and induced to crystallize separately, or cocrystallized with the polymer backbone crystals. Chapter 5 describes the synthesis of deuterium labeled polymers analogous to the materials described in chapter three. By labeling the polymer at 3 different locations information about molecular motion at these points above

and below the polymer's glass transition and melting temperatures can be accessed by solid state deuterium NMR. The solid state NMR experiments themselves are, however, beyond the scope of this dissertation and are therefore not discussed.

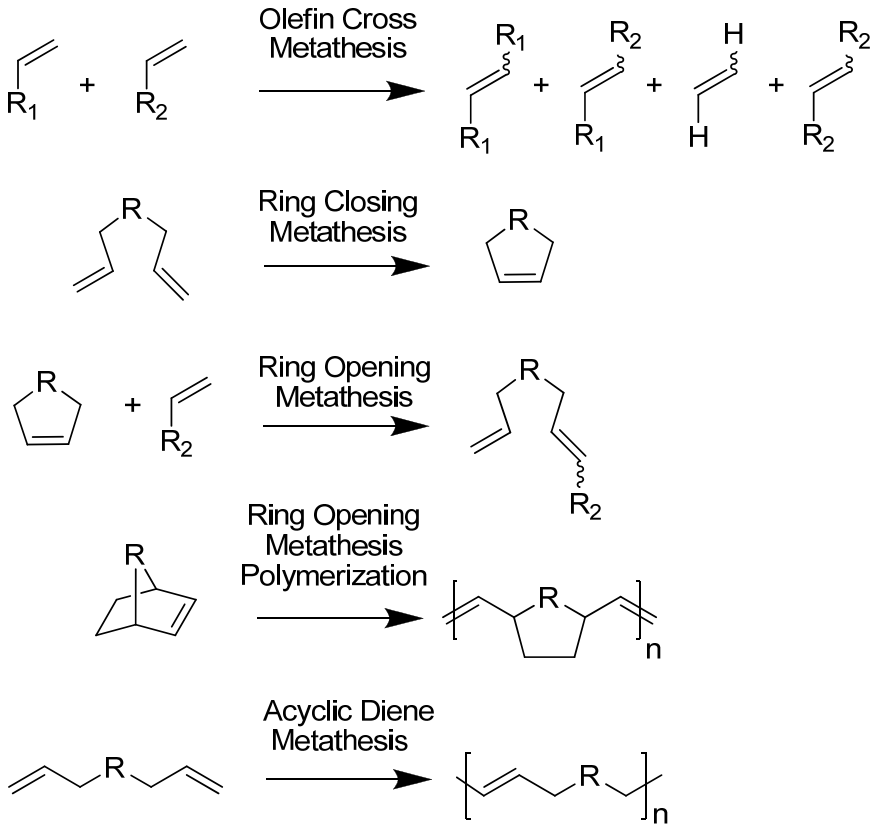

Figure 1-1: Olefin metathesis reactions

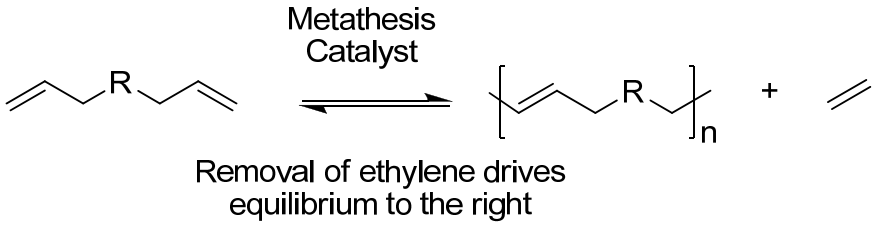

Figure 1-2: The ADMET polycondensation reaction.

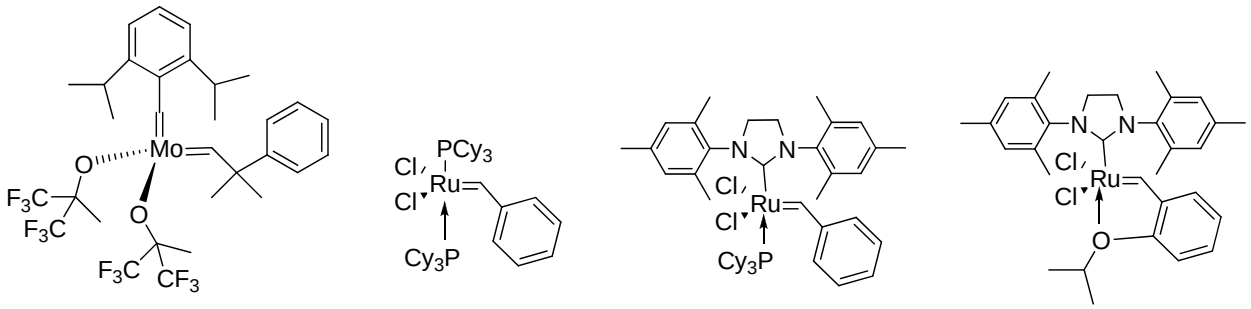

Schrock's Molybdenum Catalyst | Grubbs' First Generation Catalyst | Grubbs' Second Generation Catalyst | Grubbs Hoyveda Catalyst

Figure 1-3: Well defined metathesis catalysts

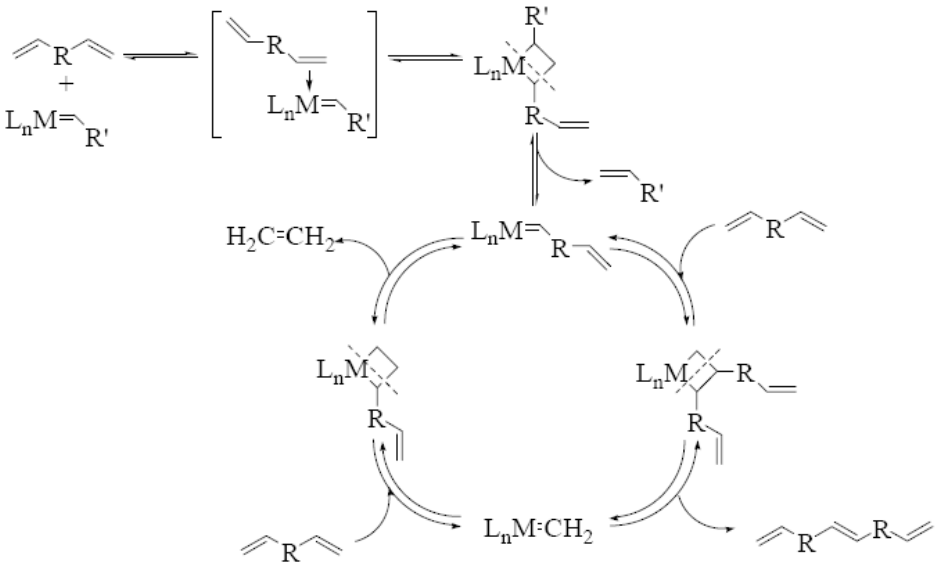

Figure 1-4: The ADMET mechanism

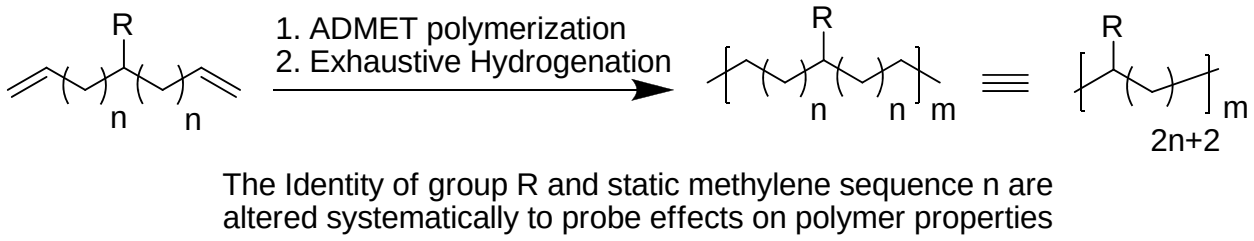

Figure 1-5: ADMET polymerization/hydrogenation strategy for precision polyolefin models

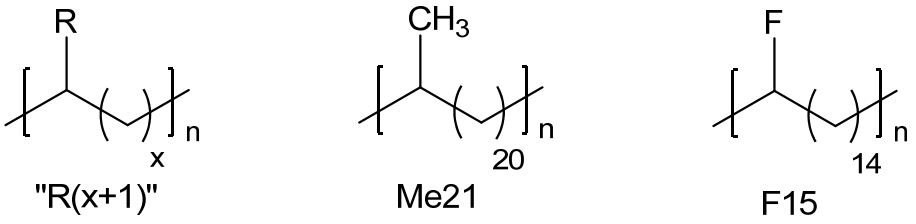

Figure 1-6: Nomenclature used in this introduction for ADMET polymers

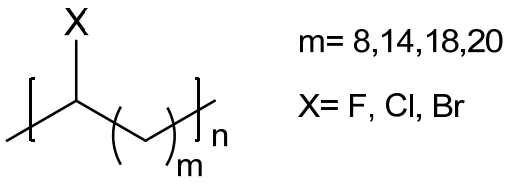

Figure 1-7: Precise halogen family

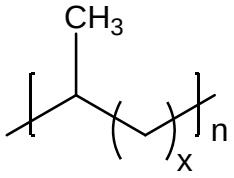

x= 4,6,8,10,14,17,20

Figure 1-8: Precise methyl family

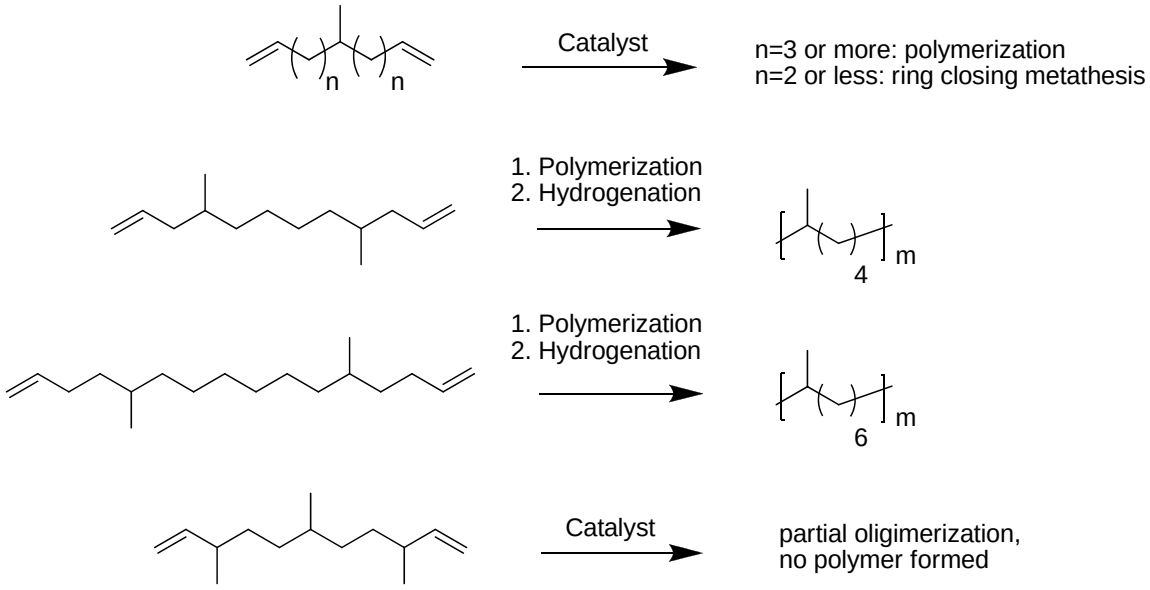

Figure 1-9: Synthesis of ADMET EP models. Shorter run lengths require the use of "ADMET dimmers." The use of ADMET trimers for placing groups every 3rd is complicated by the presence of the allylic methyl groups.

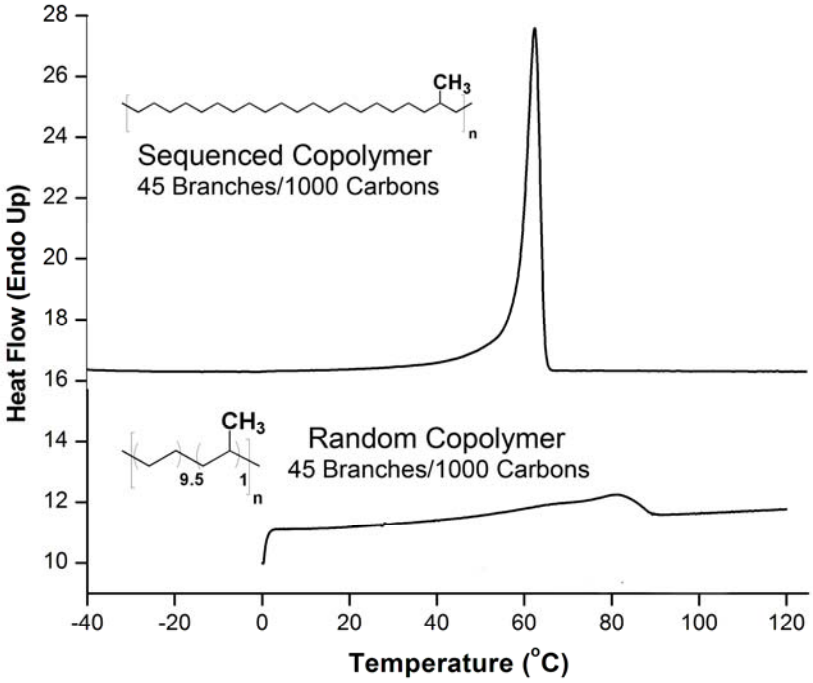

Figure 1-10: DSC comparison of random and precise EP polymers with similar branch content.

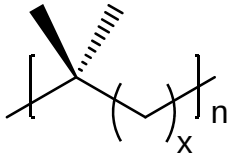

x= 8, 14, 20

Figure 1-11: Precise *geminal*-dimethyl family

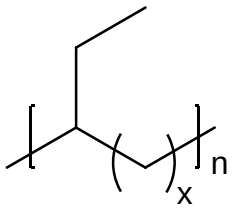

x= 8, 14, 20

Figure 1-12: Precise ethyl family

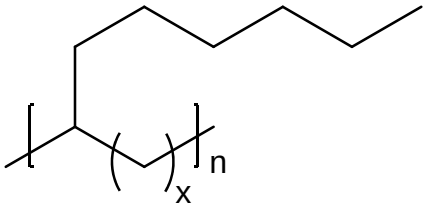

x= 8, 14, 20

Figure 1-13: Precise hexyl family

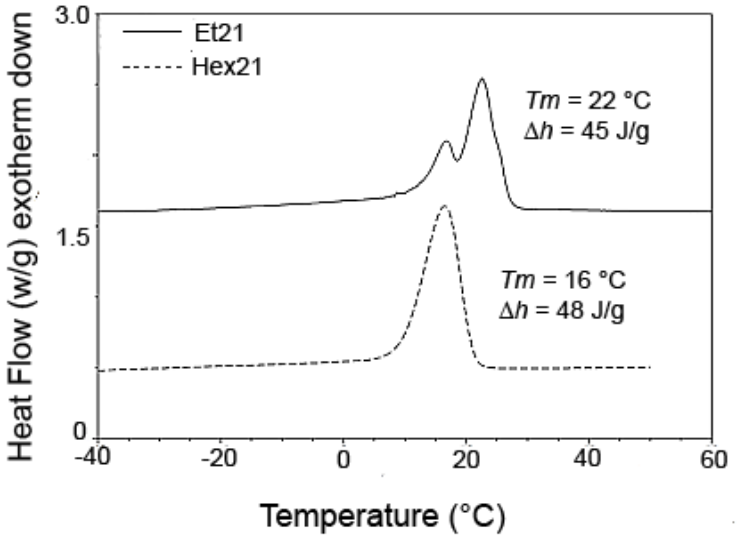

Figure 1-14: DSC comparison of Et21 and Hex21 (data taken consecutively on the same DSC independent of references 13 and 18)

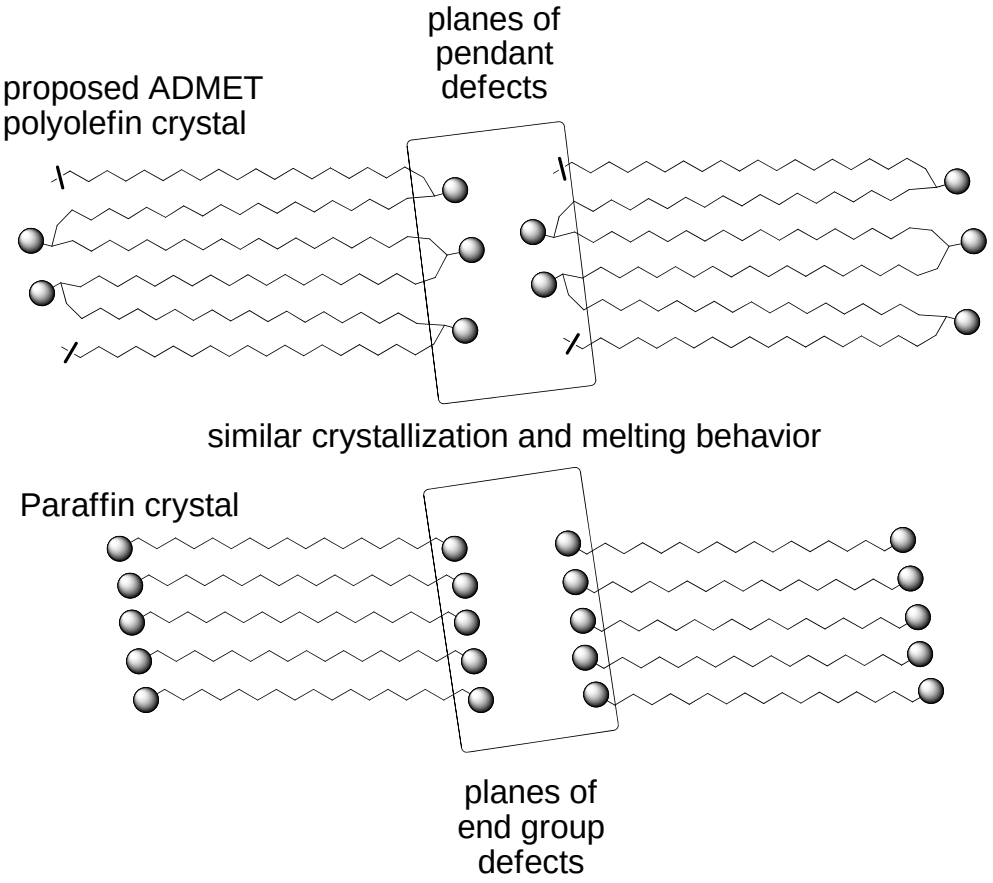

Figure 1-15: Model for the crystallization of ADMET polyolefins with larger defects

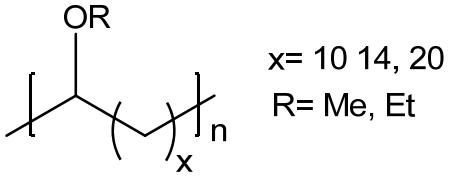

Figure 1-16: Precise ether family

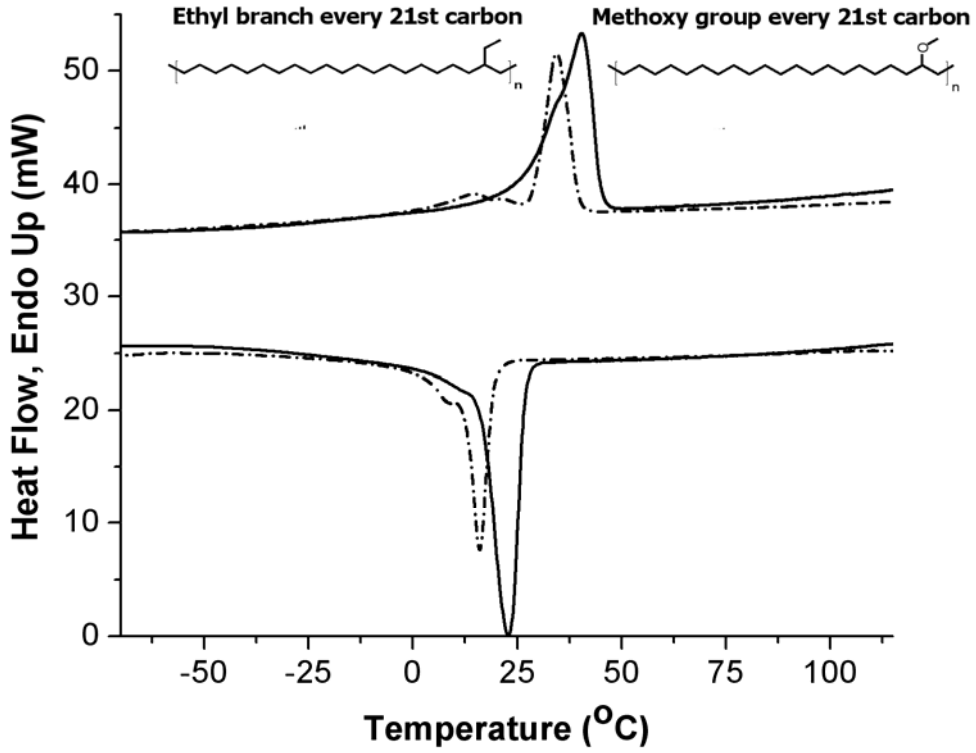

Figure 1-17: DSC comparison of OMe21 and Et21

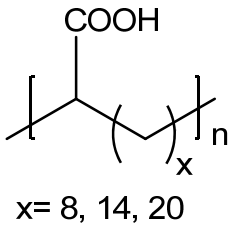

Figure 1-18: Precise carboxylic acid family

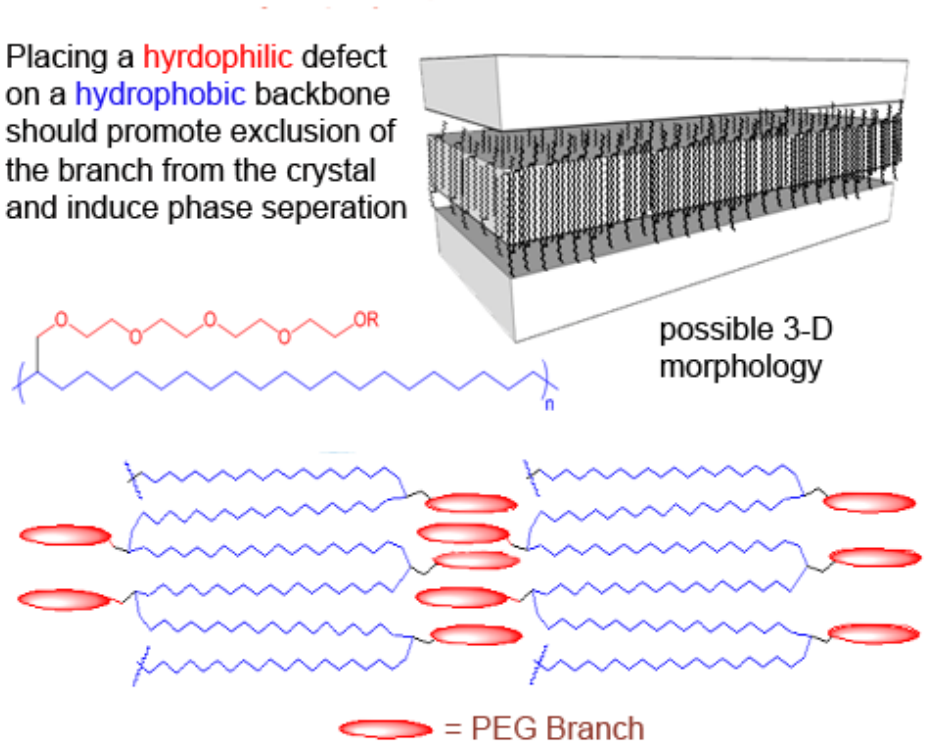

Figure 1-19: Target morphology

Table 1-1**:** Effect of molecular weight on thermal behavior in linear ADMET polyethylene

M_n	Polydispersity Index (PDI)	T_m (°C) (peak)	Δh_m (J/g)
2400	2.4	130.7	252
7600	2.4	131.3	213
11000	1.9	132.0	221
15000	2.6	133.9	204

Table 1-2: DSC data for precise halogen family

Polymer	T_m (°C)	Δh_m (J/g)
F9	124	137
F15	124	174
F19	127	207
F21	124	205
Cl 9	41	27
Cl 15	63	87
Cl 19	72	105
Cl 21	81	11
Br9	-14	21
Br15	49	35
Br19	63	55
Br21	70	48

Table 1-3: DSC data for precise methyl family

Polymer	T_m (°C)	Δh_m (J/g)
Me5	Amorphous	
Me7	-60	19
Me9	-14	28
Me11	11	66
Me15	39	82
Me19	57	96
Me21	63	103

Table 1-4: DSC data for precise *geminal*-dimethyl family

Polymer	T_m (°C)	Δh_m (J/g)
2Me9	Amorphous	n/a
2Me15	32	40
2Me21	45	61

Table 1-5: DSC data for precise ethyl family

Polymer	T_m (°C)	Δh_m (J/g)
Et9	Amorphus	n/a
Et15	-33 & -6	Not reported
Et21	17&34 (ref 18)	48

Table 1-6: DSC data for precise hexyl family

Polymer	T_m (°C)	Δh_m (J/g)
Hex9	Amorphus	n/a
Hex15	-48	19
Hex21	16	53

Table 1-7: DSC Data for precise ether family

Polymer	T_m (°C)	Δh_m (J/g)
OMe11	-41	35
OMe15	-10	62
OMe21	40	78
OEt11	-4	66
OEt15	-33	82
OEt21	28	96

Table 1-8: DSC data for precise carboxylic acid family

Polymer	T_m (°C)	Δh_m (J/g)
COOH9	Amorphous	n/a
COOH15	Amorphous	n/a
COOH21	45	42

CHAPTER 2
ADMET AMPHIPHILES: POLYETHYLENE WITH PRECISELY PLACED HYDROPHILIC DEFECTS

Introduction

Amphiphilic copolymers receive considerable attention in the literature due to the vast array of compositions, morphologies, and properties available in these materials.[33-40] Systems featuring hydrophilic segments, often poly(ethylene glycol) (PEG), and lipophilic segments such as polyethylene (PE) are of interest due to their biocompatibility, propensity for phase segregation, and ability to self assemble into higher ordered structures.[33-44] Block copolymer architectures are by far the most investigated, which is not surprising as advances living polymerization techniques have facilitated the synthesis of numerous systems with well defined structures.[35, 36, 38, 40, 41, 45-48] Amphiphilic graft copolymer architectures have received less attention, likely due to the inability to control composition and structure with the same precision available in block copolymer synthesis. This is particularly true for PE-g-PEG systems where only a few examples exist, most of which lack structural control in terms of graft incorporation or distribution.[42]

Well defined microstructures are essential to fully understand the behavior of amphiphilic graft copolymer model systems. Acyclic diene metathesis (ADMET) polycondensation chemistry is an excellent tool to model polymeric systems that lack such structural regularity when synthesized through other means. A number of ethylene based copolymers have been modeled in this fashion, from simple ethylene-co-α-olefin systems made to mimic industrial polyethylene[9] to materials inaccessible through other means such as poly(ethylene-co-vinyl ether)[9, 28, 29] and so called "bio-olefins."[49, 50]

The synthesis of PEG grafted unsaturated polyolefins with controlled placement of PEG grafts has been previously reported.[43] These polymers contained an overwhelming weight

percentage of polyether, and the properties reported reflected this. In that study the polyolefin backbone remained unsaturated; this site of unsaturation in the backbone repeat unit serves as a defect well known to impede the crystallization of PE.[9] Recent success in controlling the crystallization behavior and morphology of polyethylene through the incorporation of pendant moieties of various size and polarity[13, 14, 16, 28, 31] inspired this study, which investigates fully saturated versions of these PEG grafted polyethylenes. This chapter describes the synthesis of a family of polymers with short glycol chains (4 oxyethylene repeat units) attached every 9th, 15th, and 21st carbon along a backbone of polyethylene. By precisely controlling structure, the relative weight percentages of PE and PEG can be varied and the morphological effects of this architecture systematically probed. The goal is that by incorporating a pendant group that is immiscible with the PE backbone it may be possible to build a layered or channeled morphology that would have utility in advanced applications.

The precise polymer structures have been confirmed by NMR (^{1}H and ^{13}C). Thermal characterization by differential scanning calorimetry (DSC) reveals properties ranging from semi crystalline to fully amorphous. When the PE and PEG content are nearly equal, the polymer contains a high degree of amorphous content, as well as crystalline regions that display variable melting behavior based on thermal history. For the case of the highest amount of polyether incorporation, the material is completely amorphous. The lowest amount of polyether incorporation results in a semicrystalline material; the melting temperature incident with n-paraffin molecules of length similar to the static methylene sequence length between PEG branches. X-ray diffraction experiments confirmed that the crystallinity is a result of the PE backbone, which crystallizes excluding the PEG graft, creating crystalline phases of pure polyolefin dispersed in a matrix of amorphous PEG and PE phases.

Experimental Section

Instrumentation.

All ^{1}H NMR (300 MHz) and ^{13}C NMR (75 MHz) spectra were recorded on a Varian Associates Mercury 300 spectrometer. Chemical shifts for ^{1}H and ^{13}C NMR were referenced to residual signals from CDCl3 (^{1}H: δ= 7.27 ppm and 13C: δ = 77.23 ppm) with 0.03% v/v TMS as an internal reference. Thin layer chromatography (TLC) was performed on EMD silica gel coated (250 μm thickness) glass plates. Developed TLC plates were stained with iodine adsorbed on silica to produce a visible signature. Reaction conversions and relative purity of crude products were monitored by TLC and 1H NMR. Fourier transform infrared (FT-IR) measurements were conducted on polymer films cast from chloroform onto KBr plates using a Bruker Vector 22 Infrared Spectrophotometer. High resolution mass spectrometry analyses were performed on a Bruker APEX II 4.7 T Fourier Transform Ion Cyclone Resonance mass spectrometer (Bruker Daltonics, Billerica, MA) using electrospray ionization (ESI). The XRD measurements were taken using a Philips X'Pert MRD system using grazing incidence (omega=3°). Elemental analysis was carried out at Atlantic Microlab Inc. (Norcross, GA).

Molecular weights and molecular weight distributions (M_w/M_n) were determined by gel permeation chromatography (GPC) using a Waters Associates GPCV2000 liquid chromatography system with an internal differential refractive index detector (DRI) and two Waters Styragel HR-5E columns (10 microns PD, 7.8 mm ID, 300 mm length) at 40 °C. HPLC grade tetrahydrofuran was used as the mobile phase (flow rate = 1.0 mL/minute). Retention times were calibrated against polystyrene standards (Polymer Laboratories; Amherst, MA).

Differential scanning calorimetry (DSC) and temperature modulated differential scanning calorimetry (MDSC) were performed on a TA Instruments Q1000 equipped with a liquid

nitrogen cooling accessory calibrated using sapphire and high purity indium metal. All samples were prepared in hermetically sealed pans (4-7 mg/sample) and were referenced to an empty pan. Samples were run under s purge of helium gas. A scan rate of 10 °C per minute was used unless otherwise specified. Modulated experiments were scanned with a 3 °C per minute linear heating rate with modulation amplitude of 0.4 °C and period of 80 seconds. Melting temperatures are taken as the peak of the melting transition, glass transition temperatures as the mid point of a step change in heat capacity. Annealing experiments were conducted as follows: samples were heated through the melt at 10 °C per minute to erase thermal history, followed by cooling at 10 °C per minute to -150 °C, heated at 10 °C per minute to the annealing temperature, held isothermally for 1 hour, cooled rapidly to -150 °C, and heated through the melt at 10 °C per minute. Data reported reflects this final heating scan.

Materials.

Unless otherwise specified all reagents were purchased from Aldrich and used without further purification. Grubbs' 1st generation catalyst was a gift from Materia, Inc. Diene tosylates 1a-c and tetra(ethylene glycol) monotrityl ether were synthesized according to the literature.[17, 19, 40, 44]

General Procedure for the Synthesis of Trityl Protected Tetra(ethylene glycol) Monomers

Anhydrous DMF (250 ml) was cannula transferred into an oven dried, 3 neck round bottom flask equipped with a magnetic stirrer, gas inlet, and charged with sodium hydride (1.3 eq, 60% dispersion in mineral oil). The slurry was cooled to 0°C and 1.2 equivalents of tetra ethylene glycol monotrityl ether in 30 mL of anhydrous DMF were added via syringe. Hydrogen evolution was monitored by bubbler; when gas evoulution ceased 1 equivalent of 1 in 30 mL of anhydrous DMF was added via syringe. The reaction was stirred for 17 hours at 0 °C and quenched by pouring into 600 mL of water. The resulting mixture was extracted with diethyl

ether and the combined organics washed with brine. Concentration afforded a yellow oil which was further purified by column chromatography.

2-(4-pentenyl)-6-heptenyl-1-tetra(ethylene glycol) monotrityl ether (2-2a).

Column Chromatography: 55% diethyl ether 45% hexane eluent yielded 3.2g (55% yield) of colorless oil. ^{1}H NMR ($CDCl_3$): δ (ppm) 1.21-1.52 (br, 9H), 1.98 (q, 4H), 3.21 (t, 2H), 3.29 (d, 2H), 3.50-3.75 (br, 14H) 4.98 (m, 4H), 5.82 (m, 2H), 7.19 (m, 9H), 7.43 (d, 6H). 13C NMR (CDCl3): δ (ppm) 26.09, 30.83, 34.09, 37.86, 63.19, 70.15, 70.35, 70.44, 70.51, 70.56, 74.53, 86.28, 113.92, 126.68, 127.51, 128.48, 138.97, 143.91. ESI/HRMS: $[M+NH4]^+$ calcd for $NH_4C_{39}H_{52}O_5$, 618.4153; found 618.4128. Anal. (CH) calcd for $C_{39}H_{52}O_5$: C, 77.96; H, 8.72. Found C, 77.91; H, 8.82.

2-(7-octenyl)-9-decenyl-1-tetra(ethylene glycol) monotrityl ether (2-2b).

Column Chromatography: 25% ethyl acetate 75% hexane eluent yielding 4.0g (60% yield) of colorless oil. ^{1}H NMR ($CDCl_3$): δ (ppm) 1.21-1.52 (br, 21H), 1.98 (q, 4H), 3.21 (t, 2H), 3.29 (d, 2H), 3.50-3.75 (br, 14H) 4.98 (m, 4H), 5.82 (m, 2H), 7.19 (m, 9H), 7.43 (d, 6H). ^{13}C NMR ($CDCl_3$): .δ (ppm) 26.52, 28.71, 28.92, 29.70, 31.08, 33.58, 37.86, 63.09, 70.13, 70.36, 70.43, 70.50, 70.57, 74.54, 86.29, 113.90, 126.67, 127.52, 128.49, 138.98, 143.92. ESI/HRMS: $[M]^+$ calcd for $C_{45}H_{64}O_5$, 684.48; found 684.4753. Anal. (CH) calcd for $C_{45}H_{64}O_5$: C, 78.90; H, 9.42. Found C, 78.96; H, 9.48.

2-(10-undecenyl)-12-tridecenyl-1-tetra(ethylene glycol) monotrityl ether (2-2c).

Column Chromatography 15% ethyl acetate 85% hexane eluent afforded 1.01g (34% yield) of colorless oil. ^{1}H NMR ($CDCl_3$): δ (ppm) 1.21-1.52 (br, 33H), 1.98 (q, 4H), 3.21 (t, 2H), 3.29 (d, 2H), 3.50-3.75 (br, 14H) 4.98 (m, 4H), 5.82 (m, 2H), 7.19 (m, 9H), 7.43 (d, 6H). ^{13}C NMR ($CDCl_3$): δ (ppm) 27.03, 29.14, 29.35, 29.71, 29.82, 29.85, 30.28 31.52, 34.01, 38.29, 63.51,

70.57, 70.78, 70.86, 70.92, 70.99, 74.98, 86.71, 114.28, 127.08, 127.92, 128.90, 139.41, 144.32 ESI/HRMS: $[M+NH4]^+$ calcd for $NH_4C_{51}H_{76}O_5$, 786.6031; found 786.6037. Anal. (CH) calcd for $C_{51}H_{76}O_5$: C, 79.64; H, 9.96. Found C, 79.46; H, 10.03.

General Procedure for ADMET Polymerizations

Monomers were dried under vacuum at 80 °C for 48 hours prior to polymerization and transferred to a 50 ml round bottom flask equipped with a magnetic stir bar. Grubbs 1st generation catalyst (300:1 monomer catalyst ratio) was added and the flask placed under vacuum at 45 °C for 4 days. Polymerizations were quenched with ethyl vinyl ether (5 drops in degassed toluene), precipitated into acidic methanol to remove catalyst residue, and isolated as an adhesive gum.

Polymerization of 2-(4-pentenyl)-6-heptenyl-1-tetra(ethylene glycol) monotrityl ether (TEGOTr9u, 2-3a).

^{1}H NMR ($CDCl_3$): δ (ppm) 1.21-1.52 (br, 9H), 1.98 (q, 4H), 3.21 (t, 2H), 3.29 (d, 2H), 3.50-3.75 (br, 14H), 5.35 (br, 2H), 7.19-7.36 (m, 9H), 7.43 (d, 6H). ^{13}C NMR ($CDCl_3$): δ (ppm) 26.09, 30.83, 34.09, 37.86, 63.86, 70.72, 71.01, 71.13, 71.27, 71.33, 75.15, 86.67, 127.14, 128.15, 129.15, 130.06 (cis olefin), 130.79 (trans olefin), 144.68. IR (ν cm-1) 2924, 2852, 1488, 1462, 1447, 1106, 1032, 1010, 966, 745, 760, 705. GPC (THF vs. polystyrene standards): M_w = 9100 g/mol; PDI (M_w/M_n) = 1.89

Polymerization of 2-(7-octenyl)-9-decenyl-1-tetra(ethylene glycol) monotrityl ether (TEGOTr15u, 2-3b).

^{1}H NMR ($CDCl_3$): δ (ppm) 1.21-1.52 (br, 21H), 1.98 (q, 4H), 3.21 (t, 2H), 3.29 (d, 2H), 3.50-3.75 (br, 14H), 5.35 (br, 2H), 7.19-7.36 (m, 9H), 7.43 (d, 6H). ^{13}C NMR ($CDCl_3$): δ (ppm) 27.40, 27.84, 29.87, 29.95, 30.32, 30.40, 30.58, 31.96, 33.25, 38.71, 63.91, 70.93, 71.16, 71.23, 71.30, 71.37, 75.32, 87.09, 127.48, 128.32, 129.29, 130.15 (cis olefin), 130.90 (trans olefin),

144.71. IR (ν cm-1) 2923, 2853, 1489, 1463, 1448, 1108, 1033, 1011, 967, 746, 761, 706. GPC data (THF vs. polystyrene standards): M_w = 47300 g/mol; P.D.I. (M_w/M_n) = 1.85

Polymerization of 2-(10-undecenyl)-12-tridecenyl-1-tetra(ethylene glycol) monotrityl ether (TEGOTr21u, 2-3c).

^{1}H NMR ($CDCl_3$): δ (ppm) 1.21-1.52 (br, 33H), 1.98 (q, 4H), 3.21 (t, 2H), 3.29 (d, 2H), 3.50-3.75 (br, 14H), 5.35 (br, 2H), 7.19 (m, 9H), 7.43 (d, 6H). ^{13}C NMR ($CDCl_3$): δ (ppm) 27.08, 29.49, 29.80, 29.93, 30.33, 31.62, 32.87, 38.39, 63.56, 70.58, 70.81, 70.88, 70.95, 71.02, 75.08, 86.76, 127.10, 127.95, 128.95, 130.09 (cis olefin), 130.54 (trans olefin), 144.37 IR (ν cm-1) 2923, 2853, 1489, 1463, 1448, 1108, 1033, 1011, 967, 746, 761, 706. GPC data (THF vs. polystyrene standards): M_w = 49900 g/mol; P.D.I. (M_w/M_n) = 1.71

General Procedure for Parr Bomb Hydrogenation of Unsaturated Polymers

Unsaturated, trityl protected polymers were dissolved in toluene and added to a glass lined Parr bomb. Wilkinson's catalyst was added and the bomb charged with 700 psi of H_2. The reaction was stirred for 3 days at room temperature. The resulting polymers were purified by precipitation into acidic methanol to remove catalyst residue and isolated as an adhesive gum.

TEGOTr9 (2-4a).

^{1}H NMR ($CDCl_3$): δ (ppm) 1.21-1.52 (br, 17H), 1.98 3.21 (t, 2H), 3.29 (d, 2H), 3.50-3.75 (br, 14H), 5.35 (br, 2H), 7.19-7.36 (m, 9H), 7.43 (d, 6H). ^{13}C NMR ($CDCl_3$): δ (ppm) 26.19, 30.86, 34.14, 37.82, 63.76, 70.63, 71.05, 71.17, 71.23, 71.41, 75.21, 86.63, 127.16, 128.12, 129.21, 144.68. IR (ν cm-1) 2924, 2852, 1488, 1462, 1447, 1106, 1032, 1010, 745, 760, 705. GPC (THF vs. polystyrene standards): M_w = 9300 g/mol; PDI (M_w/M_n) = 1.63

TEGOTr15 (2-4b).

^{1}H NMR ($CDCl_3$): δ (ppm) 1.21-1.52 (br, 29H), 3.29 (t, 2H), 3.21 (d, 2H), 3.50-3.75 (br, 14H), 7.19-7.36 (m, 9H), 7.43 (d, 6H). ^{13}C NMR ($CDCl_3$): δ (ppm) 27.12, 30.03, 30.42, 31.62, 63.55, 70.57, 70.82, 70.90, 70.96, 71.03, 127.13, 127.97, 128.96, 144.38. IR (ν cm-1) 2923, 2853, 1489, 1463, 1448, 1108, 1033, 1011, 746, 761, 706. GPC (THF vs. Polystyrene standards): M_w = 45100 PDI (M_w/M_n) = 1.99

TEGOTr21 (2-4c).

^{1}H NMR ($CDCl_3$): δ (ppm) 1.21-1.52 (br, 41H), 3.21 (t, 2H), 3.29 (d, 2H), 3.50-3.75 (br, 14H), 5.35 (br, 2H), 7.19-7.36 (m, 9H), 7.43 (d, 6H). ^{13}C NMR ($CDCl_3$): δ (ppm) 27.08, 29.98, 30.37, 31.62, 38.38, 63.57, 70.58, 70.82, 70.89, 70.96, 71.02, 75.02, 86.76, 127.11, 127.95, 128.95, 144.37 IR (ν cm-1) 2923, 2853, 1489, 1463, 1448, 1108, 1033, 1011, 967, 746, 761, 720, 706. GPC data (THF vs. polystyrene standards): M_w = 51700 g/mol; P.D.I. (M_w/M_n) = 1.77

General Procedure for the Removal of the Trityl Protecting Group

The saturated, trityl protected polymers 4a-c were dissolved in THF, acidified with concentrated HCl, and refluxed for 5 hours. The resulting polymers were precipitated into hexane to remove triphenyl methane and dried under vacuum at 80 °C over night to afford an adhesive, elastic gum.

TEGOH9 (2-5a).

^{1}H NMR ($CDCl_3$): δ (ppm) 1.21-1.52 (br, 17H), 3.29 (d, 2H), 3.50-3.75 (br, 16H). ^{13}C NMR (d4-methanol): δ (ppm) 26.75, 29.57, 30.53, 31.31, 38.29, 61.08, 70.28, 70.47, 72.56, 74.42. IR (ν cm-1) 3424, 2924, 2854, 1465, 1351, 1116, 886, 722. GPC (THF vs. polystyrene standards): M_w = 9500 g/mol; PDI (M_w/M_n) = 1.57

TEGOH15 (2-5b).

^{1}H NMR ($CDCl_3$): δ (ppm) 1.21-1.52 (br, 29H), 3.29 (d, 2H), 3.50-3.75 (br, 16H). ^{13}C NMR (d8-THF): δ (ppm) 27.93, 30.76, 31.16, 32.52, 39.49, 62.29, 71.50, 71.62, 74.09, 75.03. IR (ν cm-1) 3423, 2923, 2853, 1464, 1350, 1115, 886, 721. GPC (THF vs. Polystyrene standards): M_w = 48700; PDI (M_w/M_n) = 2.13

TEGOH21 (2-5c).

^{1}H NMR ($CDCl_3$): δ (ppm) 1.21-1.52 (br, 41H), 3.29 (d, 2H), 3.50-3.75 (br, 16H), ^{13}C NMR (CDCl3): δ (ppm) 27.34, 29.95, 30.35, 31.55, 38.29, 62.00, 70.60, 70.87, 72.80, 75.04, IR (ν cm-1) 3422, 2923, 2852, 1463, 1351, 1114, 887, 720. GPC data (THF vs. polystyrene standards): M_w = 63200 g/mol; PDI (M_w/M_n) = 2.19

Results and Discussion

Synthesis and Structural Analysis

Synthesis of these precise amphiphilic copolymers involves well known chemistry (Figure 2-1). Diene tosylates 2-1a-c (prepared as previously described[19]) were coupled with the PEG branch via Williamson etherification. Tetra ethylene glycol (TEG) was monoprotected with the bulky trityl (Tr) group before the Williamson etherification to avoid side reactions and enhance solubility in organic media. The structures of monomer 2-2a-c were confirmed by NMR (^{1}H and ^{13}C), HRMS, and elemental analysis. Following polymerization the unsaturated, trityl protected polymer was fully hydrogenated using Wilkinson's catalyst. The protecting group remained untouched during this reaction and required subsequent acidification for removal. Polymer structures 2-3a-c and 2-4a-c were confirmed by NMR (^{1}H and ^{13}C) and FTIR. Molecular weight data (GPC versus polystyrene standards) is summarized in Table 2-1.

For simplicity of discussion, a systematic nomenclature is used for these ADMET amphiphilic copolymers and monomers. Monomers are named first by the number of methylene carbons between the terminal olefin and branch point followed by the identity of the pendant group, for example 6,6TEGOTr for structure 2-2b. Polymers are named first for the identity of the pendant group, followed by the frequency of its appearance along the backbone, e.g. TEGOH15 for structure 2-5b. Unsaturated polymers are denoted with the suffix "u." Figure 2-2 shows the ^{1}H NMR spectrum of 6,6TEGOTr (arbitrarily chosen as an example) with peaks assigned: trityl protecting group (7.2-7.6 ppm), terminal olefin (5.8 and 4.9 ppm), glycol protons (3.5-3.8 ppm), branch point methylene unit (3.3 ppm), methylene unit adjacent to the protecting group oxygen (3.2 ppm), allylic protons (2.1 ppm), and internal methylene protons (1.2-1.6 ppm).

The progression from monomer (6,6TEGOTr) to fully saturated, deprotected polymer (TEGOH15) by ^{1}H NMR is shown in Figure 2-3. After polymerization with first generation Grubbs catalyst the terminal olefin signals at 4.9 and 5.8 ppm in the monomer spectrum converge to one signal for internal olefin at 5.4 ppm in the spectrum of the unsaturated, protected polymer 2-3b. Following hydrogenation, this internal olefin peak completely disappears in the spectrum of the saturated but still protected polymer 2-4b. Deprotection with HCl results in the loss of trityl protecting group signal at 7.2-7.6 ppm as seen in the spectrum for the final polymer 2-5b. The pristine structures of the fully saturated, deprotected polymers were confirmed by ^{13}C NMR. The spectrum for polymer 2-5b is shown in Figure 2-4, only resonances predicted by the repeat unit are present confirming the absence of side reactions and structural defects.

Thermal Analysis

Figure 2-5 shows the differential scanning calorimetry (DSC) cycle (first cooling scan from the melt, second heating scan) for the series of saturated, deprotected polymers. TEGOH21 is semi crystalline with a peak melting temperature of 29 °C. Decreasing the space between PEG grafts when moving from TEGOH21 to TEGOH15 results in a decrease in melting temperature from 29 °C to -3 °C, as well as a decrease in melting enthalpy. Both polymers exhibit glass transitions at the same temperature, -63 °C. The marked change in the melting behavior coupled with no change in the thermal response of the amorphous character implies that the crystallinity is solely a result of the PE backbone. This is punctuated by the thermal behavior of TEGOH9, where further decreasing the number of backbone carbons between grafts results in a completely amorphous material. The glass transition temperature for TEGOH9, -65 °C, is only slightly depressed from the other polymers in this series, again indicating similar amorphous character. It can be concluded when examining the whole series that for the case of TEGOH21 and TEGOH15 the backbone of the polymer is able to form crystallites while totally excluding the PEG grafts to the amorphous regions. In the case of TEGOH9, the close proximity of the PEG groups along the backbone is disrupting the ability of the backbone to order into crystallites. All three polymers therefore must contain amorphous regions with high polyether content, confirmed by the nearly identical glass transitions. Table 2-2 summarizes the presented thermal data.

The melting profile of TEGOH15 is particularly interesting as it contains a second, lower temperature endothermic shoulder. Since this material shows only a single, sharp crystallization upon cooling this shoulder is surprising. Various annealing experiments were conducted to further understand this behavior (Figure 2-6).

Annealing just below this shoulder induces a significant increase in its intensity without altering the higher temperature endotherm. Annealing just above the shoulder completely

suppresses this behavior while slightly affecting the higher temperature endotherm. Annealing first above, then below induces the same effect on the high temperature peak, but also the reappearance of the lower temperature peak. These annealing treatments should decrease this lower melting transition in all cases as the crystallites formed during cooling would provide the template for crystal growth. The low temperature peak must therefore be an artifact of smaller, less stable crystallites formed after the initial cooling scan.

This behavior was investigated in more depth using temperature modulated DSC (MDSC). MDSC can provide a wealth of information on overlapping thermal transitions by separating reversible and irreversible processes.[51] Based on the MDSC plot (Figure 2-7), crystallization is occurring simultaneously along with melting, beginning just above the glass transition temperature. PE segments that are locked in the amorphous regions upon cooling gain sufficient mobility to crystallize above T_g. As temperature increases this annealing process continues until finally a maximum melting temperature is reached and the crystallites formed on cooling melt with no simultaneous crystallization occurring. The low temperature peak is therefore a result of these smaller crystallites undergoing an annealing process during heating, the higher temperature peak due to the melting of crystallites formed during the cooling scan. Crystallization of the PEG grafts can be ruled out as this phenomenon is not witnessed in the other polymers of this series.

Similar behavior is witnessed when annealing experiments are conducted on TEGOH21. Annealing at room temperature for several days TEGOH21 results in an increase in peak melting temperature, resulting in a melt that is incident with *n*-paraffin molecules with lengths similar to the static methylene sequence length between grafts (Figure 2-8). This result provides more compelling evidence that the crystallinity witnessed in these materials is wholly due to the PE backbone.

Although thermal analysis can provide excellent information on the dynamic crystallization behavior, it provides no information on the structure of the crystallites formed. The thermal data strongly suggests that the PEG graft exclusion model is correct. To be certain TEGOH21 was studied by x-ray diffraction. TEGOH21 was chosen over TEGOH15 because its melting temperature allows for measurements to be taken at room temperature. The diffraction pattern of TEGOH21 is shown in Figure 2-9.

A single diffraction is seen at 2Θ= 21.6°, which lies in between the known diffraction patterns for orthorhombic paraffins[27] and the (100)*h* reflection at 2Θ=20.5° for hexagonal polyethylene.[52] This implies a contracted hexagonal unit cell tending towards the paraffinic orthorohombic unit cell, almost identical to the results obtained by Wunderlich et. al. for poly(octedecyl acrylate),[27] also in agreement with Wegner's[26] assessment of precise alkyl branched polyethylenes prepared by ADMET where the methylene sequences between branches organize into a hexagonal sub lattice within a triclinic unit cell. By correlating the XRD and DSC results obtained for these ADMET amphiphiles it can be concluded that the PE backbone is indeed forming crystallites and excluding the glycol grafts to the amorphous regions.

The terminus of the PEG graft seems to play an extremely important role in this unique behavior. Clustering of the PEG grafts, likely forming a pure polyether phase is evident by the broad hydrogen bonding peak in the IR spectrum for these polymers (Figure 2-10).

Replacing the hydroxyl end group with the bulky trityl protecting group when going from TEGOH15 to TEGOTr15 disrupts all crystallinity and increases the glass transition temperature by 30 °C (Figure 2-11A). The results are similar when moving from TEGOH21 to TEGOTr21; in this case crystallization is not totally disrupted, but it is significantly hindered as noted by a decrease in melting temperature and enthalpy (Figure 2-11B). At this point it is unclear whether

the lack of hydrogen bonding, the shear steric bulk of the trityl group, or a combination of both are responsible for the difference in behavior between the TEGOH and TEGOTr series.

Conclusions

In summary, amphiphilic PE-g-PEG copolymer models with precisely defined structures can be synthesized via metathesis polycondensation chemistry; thermal data suggest that the PE backbones crystallize excluding the PEG graft, a result that is confirmed by x-ray diffraction. Thermal history has a significant effect on behavior of these materials. The identity of the graft end group clearly plays an important role in the morphology of such systems; the copolymer can be made semicrystalline or rendered completely amorphous simply by altering this group. The following chapter describes the effects of changing the size of the PEG graft and the manner in which it is connected to the backbone. Methoxy terminated PEG chains are examined to rule out hydrogen bonding or end group steric requirements as the cause of the behavior witnessed in this chapter. The effect of backbone saturation is also evaluated.

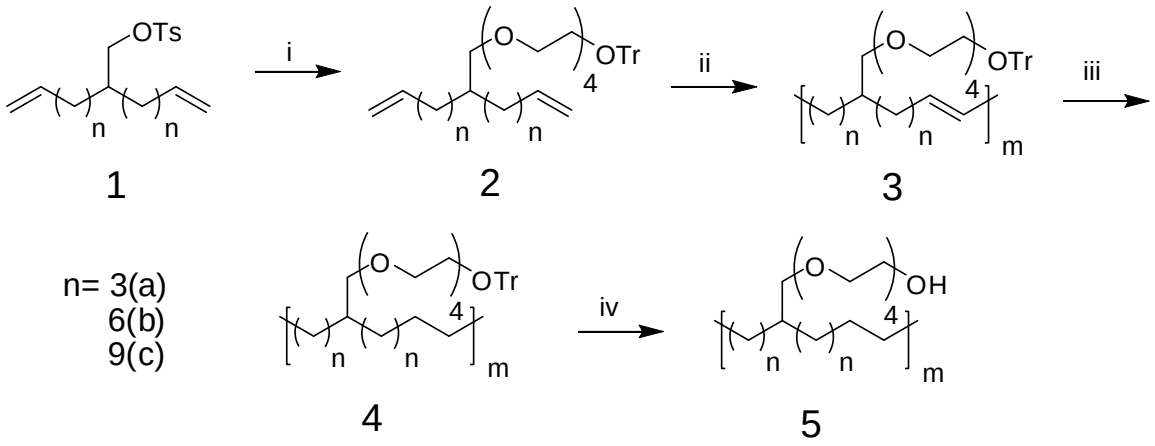

Figure 2-1: Polymer Synthesis. i: NaH, DMF, tetra ethylene glycol monotrityl ether; ii: Grubbs' 1st generation, 45°C, vacuum; iii: Wilkinson's Catalyst, toluene, H2 700psi; iv: THF, HCl.

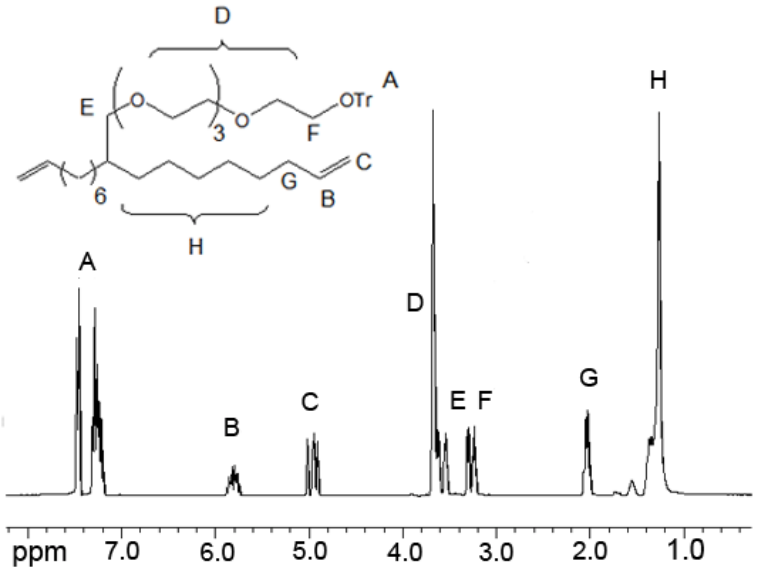

Figure 2-2: ^{1}H NMR spectrum of 6,6TEGOTr.

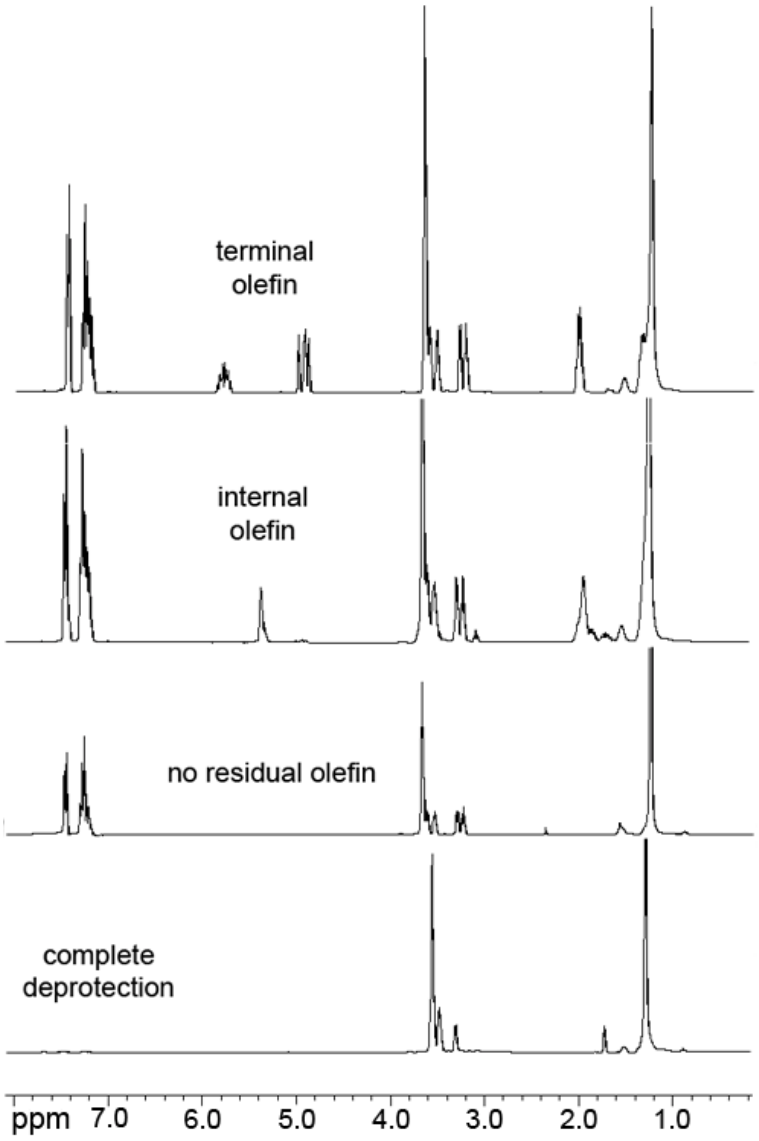

Figure 2-3: Progression of monomer (6,6TEGOTr) to polymer (TEGOH15) monitored by ^{1}H NMR.

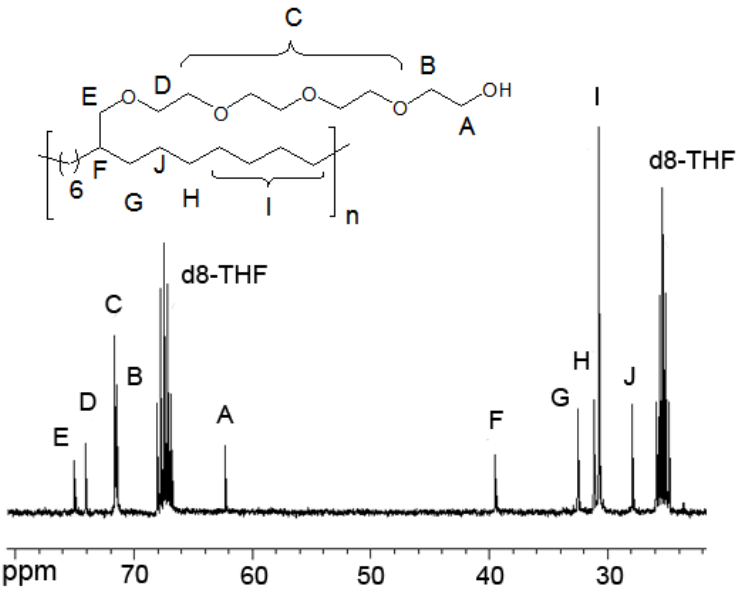

Figure 2-4: ^{13}C spectrum of TEGOH15.

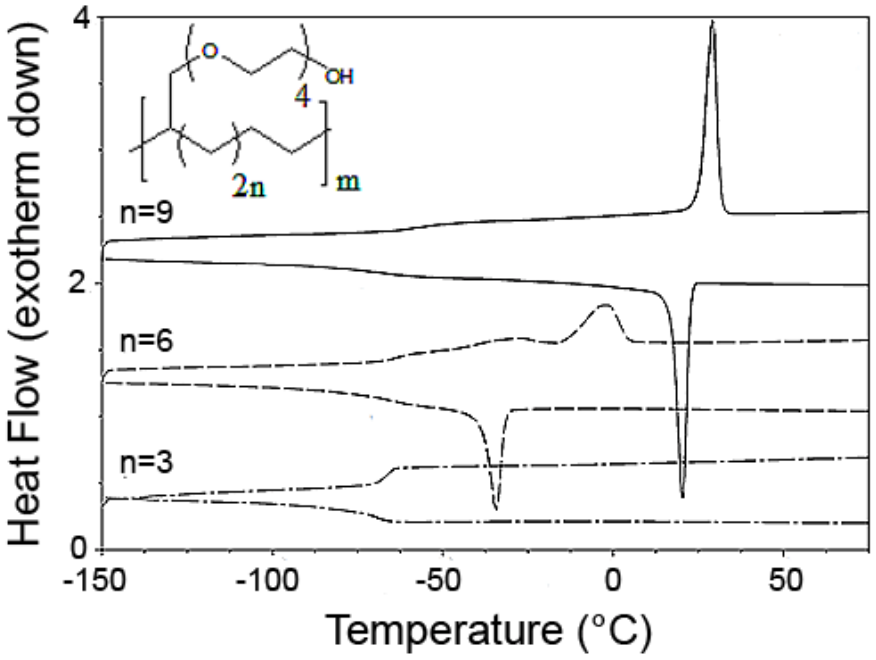

Figure 2-5: DSC heating and cooling profiles for TEGOH family.

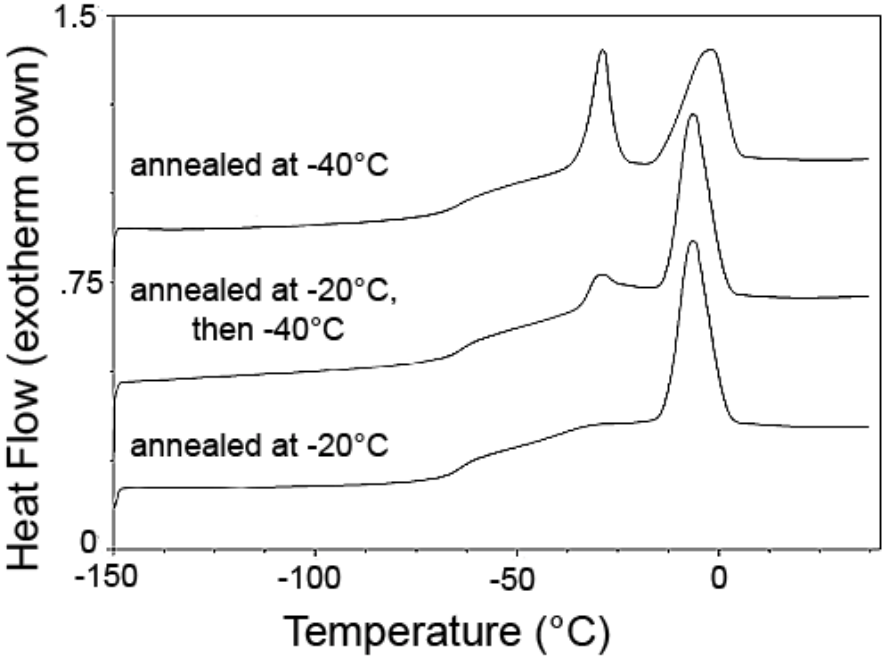

Figure 2-6: Annealing TEGOH15.

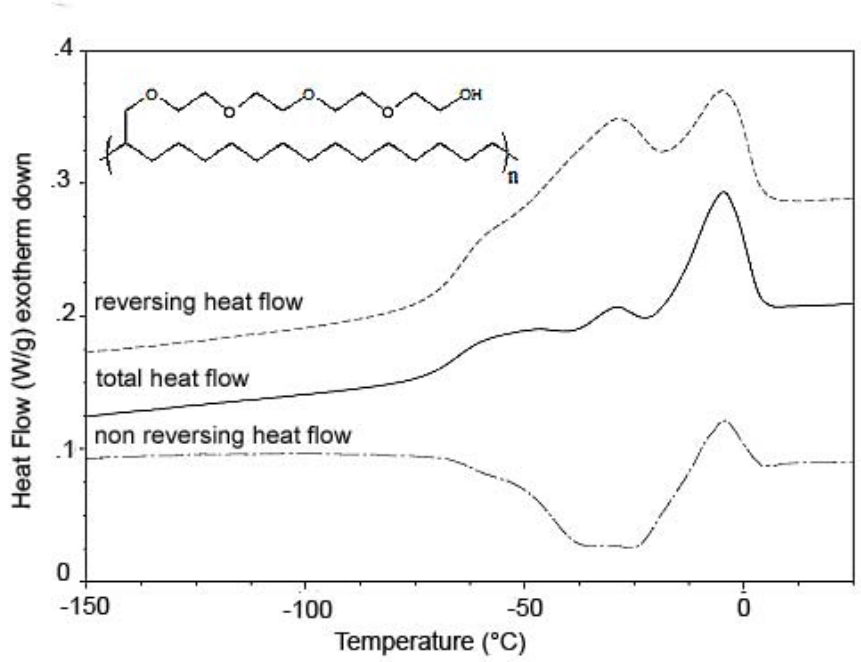

Figure 2-7: MDSC of TEGOH15

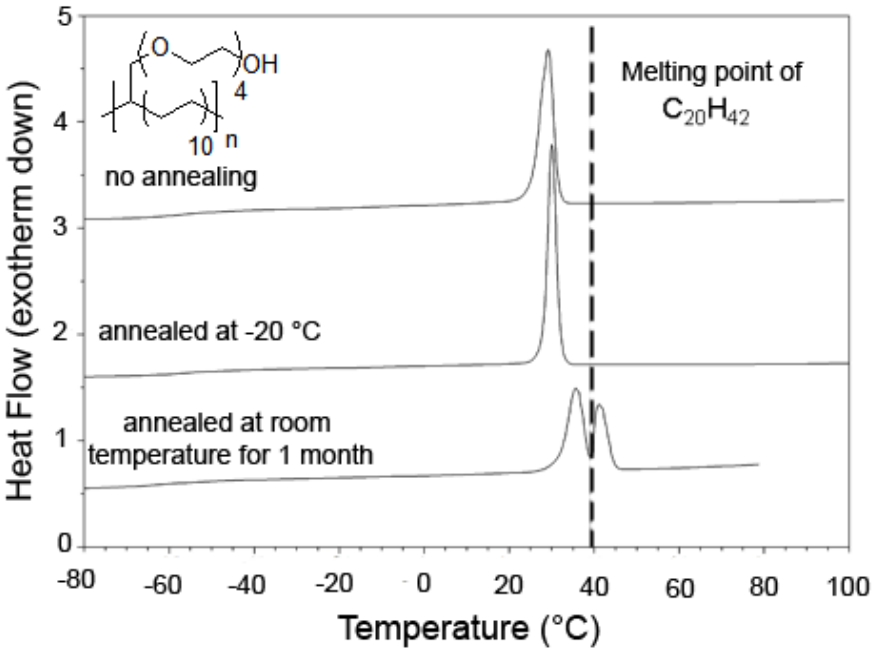

Figure 2-8: Annealing TEGOH21

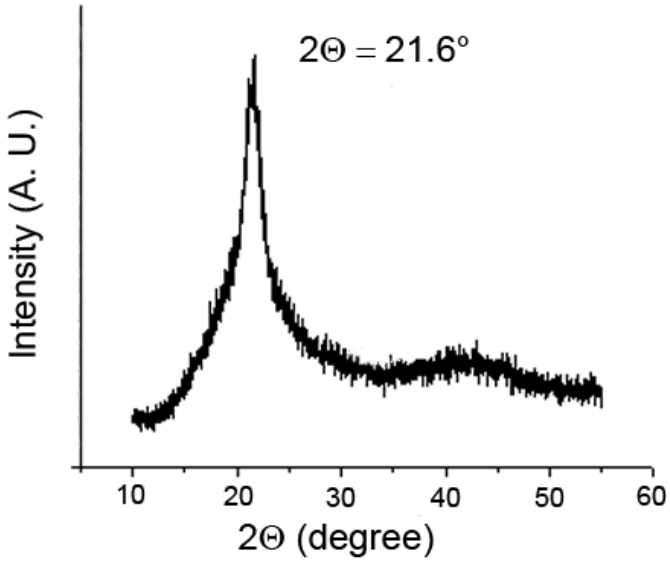

Figure 2-9: X-ray diffraction pattern for TEGOH21.

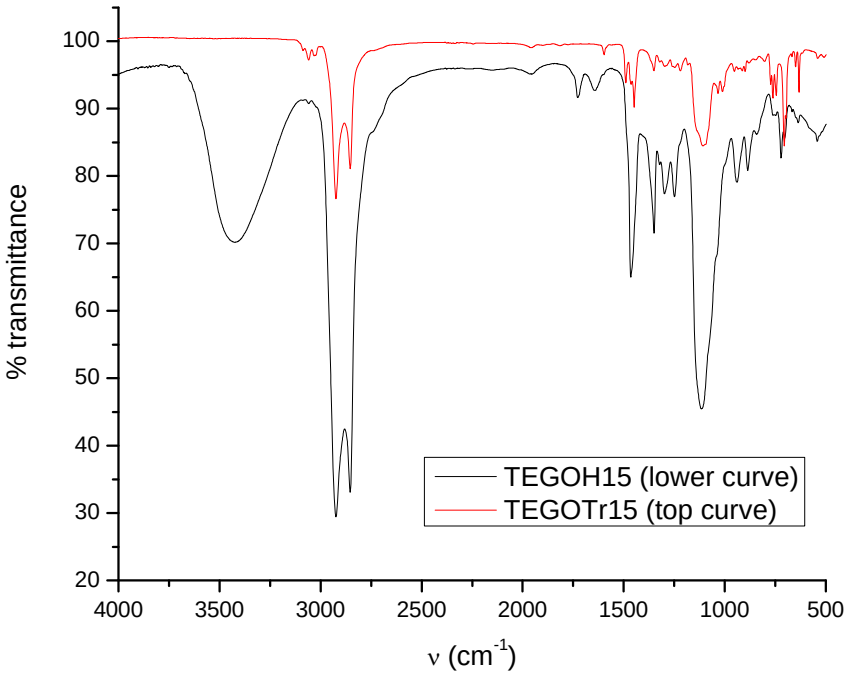

Figure 2-10: IR spectrum of TEGOH15 and TEGOTr15 (arbitrarily chosen as examples) showing clear hydrogen bonding stretch at ~3500 cm-1 in 2-5b but absent in 2-4b.

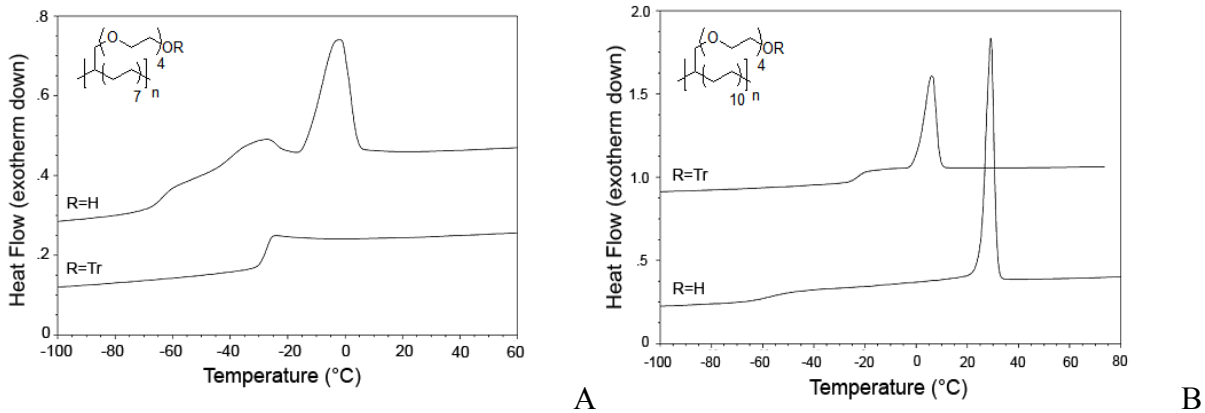

Figure 2-11: DSC comparisons for protected and deprotected polymers. A) TEGOTr15 and TEGOH15. B) TEGOTr21 and TEGOH21.

Table 2-1: Molecular weight data for polymers described in chapter 2.

Polymer	M_n[a] (kg/mol)	M_w[a] (kg/mol)	PDI[b]
TEGOTr9u	4.8	9.1	1.89
TEGOTr15u	25.6	47.3	1.85
TEGOTr21u	29.2	49.9	1.71
TEGOTr9	5.7	9.3	1.63
TEGOTr15	22.7	45.1	1.99
TEGOTr21	29.2	51.7	1.77
TEGOH9	6.1	9.5	1.57
TEGOH15	22.9	48.7	2.13
TEGOH21	28.8	63.2	2.19

[a] GPC vs. polystyrene standards; b M_w/M_n

Table 2-2: DSC data for polymers described in chapter 2.

Polymer	T_g (°C))	ΔC_p (J/g·°C)	T_m (°C)	ΔH_m (J/g)	T_c (°C)	ΔH_c (J/g)
TEGOH9	-65	.73	n/a	n/a	n/a	n/a
TEGOH15	-63	.28	-3	19	-34	21
TEGOH21	-63	.26	29	36	20	36

CHAPTER 3
PROBING THE EFFECTS OF PENDANT BRANCH LENGTH, DISTRIBUTION, AND CONNECTIVITY IN ADMET AMPHIPHILES

Introduction

The manipulation of morphology via synthetic control over microstructure spearheads research in polymer chemistry. The design of novel materials for advanced applications and the study of commodity materials to improve commercial products both require an understanding of the relationship between structure and material behavior. Acyclic diene metathesis (ADMET) has been utilized extensively for the modeling of polymeric systems,[9-11] where linear, defect-free polymers produced by this method serve as pristine models of commercial materials or as novel materials for advanced applications.[13, 14, 31, 49, 53, 54] Research in this area has shown that imparting these materials with such structural regularity results in behavior unique to this class of polymers.[9, 12, 13, 31, 53]

A recent area of effort in our laboratory has been the synthesis of polyethylene with precise placement of hydrophilic branches. Although these polymers resemble traditional amphiphilic graft copolymers, there are a number of notable differences. First, ADMET amphiphiles possess a perfectly uniform distribution of hydrophilic grafts (polyethylene glycol, PEG) along a hydrophobic (polyethylene, PE) backbone, architecture which is typically inaccessible for PE-*g*-PEG systems.[39, 42, 55] The distance between branches (14 and 20 backbone carbons apart in this study) is tunable synthetically by altering the size and symmetry of the diene monomer. Second, the length of the graft is precisely defined, thereby differing from traditional amphiphilic graft copolymers.[39, 42, 55, 56] Precise placement of hydrophilic branches on the hydrophobic backbone induces a phase separated morphology that may be desirable in advanced applications.

Our recent synthesis of hydroxyl terminated tetra ethylene glycol grafted PE was the first to demonstrate such morphological control.[15] In that study we concluded that the polyethylene

backbone crystallized by excluding the PEG branch based on thermal and structural investigations.[15] We believe for this to occur, the PEG branch must be inducing a fold in the PE backbone, thereby allowing for the clustering of the branches and allowing the backbone to form small, isolated paraffin like crystallites (Figure 3-1). While the domain sizes that would result from this model are quite small in comparison to other amphiphilic PE-*co*-PEG block and graft copolymer systemes,[33, 38, 39, 42, 55, 57] this behavior is well documented for alternating block oligomers[44, 45, 58] of PEG and PE having blocks of similar size to the branch to branch distance and PEG graft lengths of our polymers.

This chapter describes a family of polymers designed to test this model. First, the size of PEG branch is altered. If the crystallinity is solely a result of the backbone then the crystallization and melting behavior should be independent of branch length, which is indeed the case. Second, if the folds in the chain are occurring at the site of the PEG branch then the manner in which the branch is connected to the backbone should alter the behavior as well. In this report we present polymers in which the first atom of the branch is either a carbon (methylene group) or an oxygen atom. This alters both the sterics and electronics at this point in the chain thereby altering the ability of the chain to fold, a result confirmed by thermal investigations. Finally, altering the architecture of the backbone should effect changes in the behavior according to this model. We examine this in two ways: by changing the static methylene sequence length between branches and by investigating the effect a site of unsaturation (seen as a defect) has on the crystallization and melting behavior. Both parameters prove significant in influencing the behavior of the polymers presented.

The pristine nature of the monomer structures (shown in scheme 1) are confirmed by NMR (^{1}H and ^{13}C), high resolution mass spectrometry, and elemental analysis. Corresponding

unsaturated and fully saturated polymer structures are confirmed by NMR (^{1}H and ^{13}C), and FTIR. The thermal behavior is thoroughly investigated by differential scanning calorimetry (DSC) and temperature modulated DSC (MDSC). The thermal stability of the materials is also assessed using thermogravimetric analysis (TGA).

The thermal analysis results indicate that the architecture of the PE backbone as well as the manner in which the PEG branch is connect to the backbone play an important role in the crystallization and melting behavior of these materials. The size of the PEG branch, however, does not affect this behavior. This provides compelling evidence that our model for the chains folding about the defects, as presented in Figure 3-1, is correct.

Experimental Section

Instrumentation

All ^{1}H NMR (300 MHz) and ^{13}C NMR (75 MHz) spectra were recorded on a Varian Associates Mercury 300 spectrometer. Chemical shifts for ^{1}H and ^{13}C NMR were referenced to residual signals from $CDCl_3$ (^{1}H: δ= 7.27 ppm and ^{13}C: δ = 77.23 ppm) with 0.03% v/v TMS as an internal reference. Thin layer chromatography (TLC) was performed on EMD silica gel coated (250 μm thickness) glass plates. Developed TLC plates were stained with iodine adsorbed on silica to produce a visible signature. Reaction conversions and relative purity of crude products were monitored by TLC and ^{1}H NMR. Fourier transform infrared (FT-IR) measurements were conducted with a Bruker Vector 22 Infrared Spectrophotometer using polymer films cast from chloroform onto KBr plates. High resolution mass spectrometry analyses were performed on a Bruker APEX II 4.7 T Fourier Transform Ion Cyclotron Resonance mass spectrometer (Bruker Daltonics, Billerica, MA) using electrospray ionization (ESI). Elemental analysis was carried out at Atlantic Microlab Inc. (Norcross, GA).

Molecular weights and molecular weight distributions (M_w/M_n) were determined by gel permeation chromatography (GPC) using a Waters Associates GPCV2000 liquid chromatography system with an internal differential refractive index detector (DRI) and two Waters Styragel HR-5E columns (10 micron particle diameter, 7.8 mm ID, 300 mm length) at 40 °C. The mobile phase was HPLC grade tetrahydrofuran at a flow rate of 1.0 mL/minute. Retention times were calibrated versus polystyrene standards (Polymer Laboratories; Amherst, MA).

Differential scanning calorimetry (DSC) and temperature modulated differential scanning calorimetry (MDSC) were performed on a TA Instruments Q1000 equipped with a liquid nitrogen cooling accessory and calibrated using sapphire and high purity indium metal. All samples were prepared in hermetically sealed aluminum pans (4-7 mg/sample) and were referenced to an empty pan. Samples were run under s purge of helium gas. Scan rates of 10ºC/min and 3ºC/min were used for DSC and MDSC, respectively. The MDSC modulation amplitude and period were 0.4º and 80 s, respectively. Melting temperatures were evaluated as the peak of the melting transition and glass transition temperatures as the mid-point of a step change in heat capacity. Annealing experiments were conducted as follows: samples were heated through the melt to erase thermal history, cooled at 10 °C per minute to -150 °C, heated at 10 °C per minute to the annealing temperature, held isothermally for 1 hour, cooled rapidly to -150 °C, and heated through the melt at 10 °C per minute. The reported data reflect this final heating scan. Thermogravimetric Analysis (TGA) was performed on a TA Instruments Q5000 IR using the dynamic high-resolution analysis mode and a two point Curie temperature calibration (alumel alloy and high purity nickel).

Materials.

Unless otherwise stated, all reagents were purchased from Aldrich and used without further purification. Grubbs' 1st generation catalyst was a gift from Materia, Inc. Diene alcohols 3-1a,b and 3-2a,b and oligoethoxy-*p*-tosylates were synthesized according to the literature.[13, 17, 59]

General Procedure for the Synthesis of Methoxy Terminated PEG Grafted Diene Monomers (3-3a-d, 3-4a-d)

Anhydrous DMF (40 mL) was cannula transferred into an oven dried, 3-neck round-bottom flask equipped with a magnetic stirrer and gas inlet, and was charged with 2 equivalents of sodium hydride (60% dispersion in mineral oil). The slurry was cooled to 0°C and 1 equivalent of 1 in 20 mL of anhydrous DMF was added via syringe. When gas evolution (monitored by bubbler) ceased, 1.2 equivalents of 2 in 20 mL of anhydrous DMF were added via syringe. The reaction was stirred for 17 hours at 0 °C and quenched by pouring into 600 mL of water. The resulting mixture was extracted with diethyl ether and the combined organics washed with brine. Concentration afforded a yellow oil which was further purified by column chromatography.

9-(tetra (ethylene glycol) monomethyl ether)-1,16-heptadecadiene (6,6TEGOMe2, 3-3a).

Column Chromatography:40% ethyl acetate 60% hexane eluent yielding 1g (38% yield) of colorless oil. ^{1}H NMR ($CDCl_3$): δ (ppm) 1.21-1.52 (br, 20H), 2.01 (q, 4H), 3.21 (m, 1H), 3.35 (s, 3H), 3.50-3.75 (br, 16H) 4.98 (m, 4H), 5.82 (m, 2H) ^{13}C NMR ($CDCl_3$): .δ (ppm) 25.55, 29.08, 29.32, 28.89, 33.97, 34.16, 59.19, 68.23, 70.72, 70.84, 71.10, 72.16, 80.27, 114.35, 139.31. ESI/HRMS: $[M+NH_4]^+$ calcd for $NH_4C_{26}H_{50}O_5$, 460.3937; found 460.4048. Anal. (CH) calcd for $C_{26}H_{50}O_5$: C, 70.54; H, 11.38. Found C, 70.38; H, 11.57.

12-(tetra (ethylene glycol) monomethyl ether)-1,22-tricosadiene (9,9TEGOMe2, 3-3b).

Column Chromatography:25% ethyl acetate 75% hexane eluent afforded .734g (30% yield) of colorless oil. ^{1}H NMR ($CDCl_3$): δ (ppm) 1.21-1.52 (br, 32H), 2.01 (q, 4H), 3.21 (m, 1H), 3.35 (s, 3H), 3.50-3.75 (br, 16H) 4.98 (m, 4H), 5.82 (m, 2H). ^{13}C NMR ($CDCl_3$): δ (ppm) 25.63, 29.16, 29.35, 29.71, 29.79, 29.86, 30.07, 34.02, 34.19, 59.23, 68.19, 70.75, 70.83, 70.85, 71.11, 72.17, 80.35, 114.31, 139.42 ESI/HRMS: $[M+NH4]^+$ calcd for $NH_4C_{32}H_{62}O_5$, 544.4936; found 544.4938. Anal. (CH) calcd for $C_{32}H_{62}O_5$: C, 72.95; H, 11.86. Found C, 73.48; H, 12.12.

9-(tri (ethylene glycol) monomethyl ether)-1,16-heptadecadiene (6,6TrEGOMe2, 3-3c).

Column Chromatography: 40% ethyl acetate 60% hexane eluent yielding 1.2g (51% yield) of colorless oil. ^{1}H NMR ($CDCl_3$): δ (ppm) 1.21-1.52 (br, 20H), 2.01 (q, 4H), 3.21 (m, 1H), 3.35 (s, 3H), 3.50-3.75 (br, 12H) 4.98 (m, 4H), 5.82 (m, 2H). ^{13}C NMR ($CDCl_3$): .δ (ppm) 25.52, 29.05, 29.28, 28.84, 33.94, 34.12, 59.16, 68.18, 70.72, 70.79, 70.82, 71.06, 72.12, 80.24, 114.29, 139.28. ESI/HRMS: $[M+Na]^+$ calcd for $C_{24}H_{46}O_4$ Na, 416.3734; found 421.3288. Anal. (CH) calcd for $C_{24}H_{46}O_4$: C, 72.31; H, 11.63. Found C, 72.72; H, 11.64.

12-(tri (ethylene glycol) monomethyl ether)-1,22-tricosadiene (9,9TrEGOMe2 3-3d).

Column Chromatography: 25% ethyl acetate 75% hexane eluent afforded 1.01g (34% yield) of colorless oil. ^{1}H NMR ($CDCl_3$): δ (ppm) 1.21-1.52 (br, 32H), 2.01 (q, 4H), 3.21 (m, 1H), 3.35 (s, 3H), 3.50-3.75 (br, 12H) 4.98 (m, 4H), 5.82 (m, 2H). ^{13}C NMR ($CDCl_3$): δ (ppm) 25.56, 29.10, 29.30, 29.65, 29.73, 29.80, 30.01, 33.96, 34.13, 59.16, 68.14, 70.71, 70.77, 70.83, 71.06, 72.12, 80.27, 114.24, 139.32 ESI/HRMS: $[M+ NH_4]^+$ calcd for $NH_4C_{30}H_{58}O_4$, 500.4673; found 500.4676. Anal. (CH) calcd for $C_{30}H_{58}O_4$: C, 74.63; H, 12.11. Found C, 74.83; H, 12.37.

2-(7-octenyl)-9-decenyl-1-tetra(ethylene glycol) monomethyl ether (6,6TEGOMe, 3-4a).

Column Chromatography 40% ethyl acetate 60% hexane eluent yielding 1.03g (55% yield) of colorless oil. ^{1}H NMR ($CDCl_3$): δ (ppm) 1.21-1.52 (br, 21H), 1.98 (q, 4H), 3.21 (d, 2H), 3.35 (s, 2H), 3.50-3.71 (br, 16H) 4.98 (m, 4H), 5.82 (m, 2H). ^{13}C NMR ($CDCl_3$): .δ (ppm) 26.90, 29.09, 29.28, 30.07, 31.48, 33.95, 38.26, 59.17, 70.55, 70.68, 70.75, 70.79, 72.81, 74.90, 114.27, 139.32. ESI/HRMS: $[M+NH_4]^+$ calcd for $NH_4C_{27}H_{52}O_5$474.4153; found 474.4220. Anal. (CH) calcd for $C_{27}H_{52}O_5$: C, 71.01; H, 11.48. Found C, 71.12; H, 11.67.

2-(10-undecenyl)-12-tridecenyl-1-tetra (ethylene glycol) monomethyl ether (9,9TEGOMe, 3-4b).

Column Chromatography: 25% ethyl acetate 75% hexane eluent afforded .560g (63% yield) of colorless oil. ^{1}H NMR ($CDCl_3$): δ (ppm) 1.21-1.52 (br, 33H), 2.01 (q, 4H), 3.29 (d, 2H), 3.35 (s, 3H), 3.50-3.75 (br, 16H) 4.98 (m, 4H), 5.82 (m, 2H). ^{13}C NMR ($CDCl_3$): δ (ppm) 26.92, 29.06, 29.27, 29.63, 29.73, 29.76, 30.20, 31.45, 33.94,38.22, 59.13, 70.50, 70.64, 70.71, 70.75, 72.07, 74.88, 114.21, 139.29 ESI/HRMS: $[M+NH4]^+$ calcd for $NH_4C_{33}H_{64}O_5$, 558.5092; found 558.5088. Anal. (CH) calcd for $C_{33}H_{64}O_5$: C, 73.28; H, 11.93. Found C, 73.14; H, 12.05.

2-(7-octenyl)-9-decenyl-1-tri(ethylene glycol) monomethyl ether (6,6TrEGOMe, 3-4c).

Column Chromatography: 25% ethyl acetate 75% hexane eluent yielding 1.02g (60% yield) of colorless oil. ^{1}H NMR ($CDCl_3$): δ (ppm) 1.21-1.52 (br, 21H), 1.98 (q, 4H), 3.29 (d, 2H), 3.35 (s, 2H), 3.50-3.71 (br, 12H) 4.98 (m, 4H), 5.82 (m, 2H). ^{13}C NMR ($CDCl_3$): .δ (ppm) 27.31, 29.49, 29.68, 30.47, 31.88, 34.35, 38.67, 59.52, 70.95, 71.09, 71.16, 71.20, 72.52, 75.29, 114.67, 139.70. ESI/HRMS: $[M+NH_4]^+$ calcd for $NH_4C_{25}H_{48}O_4$ 430.3891; found 430.3954. Anal. (CH) calcd for $C_{25}H_{48}O_4$: C, 72.77; H, 12.72. Found C, 72.91; H, 12.88.

2-(10-undecenyl)-12-tridecenyl-1-tri (ethylene glycol) monomethyl ether (9,9TrEGOMe, 3-4d).

Column Chromatography: 25% ethyl acetate 75% hexane eluent afforded .1.01g (55% yield) of colorless oil. ^{1}H NMR ($CDCl_3$): δ (ppm) 1.21-1.52 (br, 33H), 2.01 (q, 4H), 3.29 (d, 2H), 3.35 (s, 3H), 3.50-3.75 (br, 12H) 4.98 (m, 4H), 5.82 (m, 2H). ^{13}C NMR ($CDCl_3$): δ (ppm) 26.95, 29.09, 29.30, 29.66, 29.76, 29.79, 30.23, 31.49, 33.96, 38.26, 59.16, 70.53, 70.69, 70.75, 70.79, 70.83, 72.11, 74.91, 114.24, 139.33 ESI/HRMS: $[M+NH4]^+$ calcd for $NH_4C_{31}H_{60}O_5$, 514.4830; found 514.4869. Anal. (CH) calcd for $C_{31}H_{60}O_5$: C, 74.95; H, 12.17. Found C, 74.83; H, 12.33.

General Procedure for ADMET Polymerizations

Monomers were dried under vacuum at 80 °C for 48 hours prior to polymerization and subsequently transferred to a 50 mL round-bottom flask equipped with a magnetic stir bar. Grubbs 1st generation catalyst (300:1 monomer:catalyst ratio) was added and the flask was stirred under vacuum at 45 °C for 4 days. Polymerizations were quenched with ethyl vinyl ether (5 drops in degassed toluene), precipitated into cold, acidic methanol to remove catalyst residue, and isolated as an adhesive gum.

Polymerization of 9-(tetra (ethylene glycol) monomethyl ether)-1,16-heptadecadiene (TEGOMe15u2, 3-5a).

^{1}H NMR ($CDCl_3$): δ (ppm) 1.21-1.52 (br, 20H), 2.01 (q, 4H), 3.21 (m, 1H), 3.29 (s, 3H), 3.50-3.75 (br, 16H), 5.35 (m, 2H). ^{13}C NMR ($CDCl_3$): .δ (ppm) 25.63, 27.44, 29.47, 29.90, 29.97, 32.82, 34.23, 59.21, 68.20, 70.72, 70.82, 70.84, 71.94, 72.16, 80.35, 130.04 (cis olefin), 130.50 (trans olefin). IR (ν cm-1) 2923, 2853, 1464, 1350, 1115, 967, 886, 721. GPC (THF vs. Polystyrene standards): M_w = 88700 ; PDI (M_w/M_n) = 1.75

Polymerization of 12-(tetra (ethylene glycol) monomethyl ether)-1,22-tricosadiene (TEGOMe21u2, 3-5b).

^{1}H NMR ($CDCl_3$): δ (ppm) 1.21-1.52 (br, 32H), 2.01 (q, 4H), 3.21 (m, 1H), 3.29 (s, 3H), 3.50-3.75 (br, 16H) 5.35 (m, 2H). ^{13}C NMR ($CDCl_3$): δ (ppm) 25.67, 27.36, 29.46, 29.58, 29.77, 29.87, 29.92, 30.02, 30.12, 32.85, 34.22, 59.24, 68.19, 70.74, 70.83, 70.85, 71.11, 72.17, 80.38, 130.05 (cis olefin), 130.54 (trans olefin). IR (ν̣ cm-1) 2923, 2853, 1464, 1350, 1115, 967, 886, 721. GPC (THF vs. Polystyrene standards): M_w = 114500 ; PDI (M_w/M_n) = 1.78

Polymerization of 9-(tri (ethylene glycol) monomethyl ether)-1,16-heptadecadiene (TrEGOMe15u2, 3-5c).

^{1}H NMR ($CDCl_3$): δ (ppm) 1.21-1.52 (br, 20H), 2.01 (q, 4H), 3.21 (m, 1H), 3.29 (s, 3H), 3.50-3.75 (br, 12H), 5.35 (m, 2H). ^{13}C NMR ($CDCl_3$):.δ (ppm) 25.63, 27.44, 29.47, 29.90, 29.97, 32.82, 34.23, 59.22, 68.21, 70.67, 70.82, 70.87, 71.11, 72.17, 80.34, 130.09 (cis olefin), 130.51 (trans olefin). IR (ν̣ cm-1) 2923, 2853, 1464, 1350, 1115, 967, 886, 721. GPC (THF vs. Polystyrene standards): M_w = 79500; PDI (M_w/M_n) = 1.85

Polymerization of 12-(tri (ethylene glycol) monomethyl ether)-1,22-tricosadiene (TrEGOMe21u2, 3-5d).

^{1}H NMR ($CDCl_3$): δ (ppm) 1.21-1.52 (br, 32H), 2.01 (q, 4H), 3.21 (m, 1H), 3.29 (s, 3H), 3.50-3.75 (br, 12H) 5.35 (m, 2H). ^{13}C NMR ($CDCl_3$): δ (ppm) 25.67, 27.44, 29.44, 29.56, 29.76, 29.86, 29.91, 30.01, 30.11, 32.84, 34.22, 59.22, 68.16, 70.77, 70.82, 70.87, 71.10, 72.17, 80.36, 130.07 (cis olefin), 130.53 (trans olefin). IR (ν̣ cm-1) 2923, 2853, 1464, 1350, 1115, 967, 886, 721. GPC (THF vs. Polystyrene standards): M_w = 108700 ; PDI (M_w/M_n) = 1.69

Polymerization of 2-(7-octenyl)-9-decenyl-1-tetra(ethylene glycol) monomethyl ether (TEGOMe15u, 3-6a).

^{1}H NMR ($CDCl_3$): δ (ppm) 1.21-1.52 (br, 21H), 1.98 (q, 4H), 3.21 (d, 2H), 3.35 (s, 2H), 3.50-3.71 (br, 16H), 5.35 (m, 2H). ^{13}C NMR ($CDCl_3$): .δ (ppm) 26.60, 27.02, 29.06, 29.52, 29.78, 31.16, 32.43, 37.92, 58.79, 70.15, 70.29, 70.36, 70.39, 71.72, 74.51, 129.89 (cis olefin), 130.08 (trans olefin). IR (ν cm-1) 2923, 2853, 1464, 1350, 1115, 967, 886, 721. GPC (THF vs. Polystyrene standards): M_w = 100400 ; PDI (M_w/M_n) = 1.74

Polymerization of 2-(10-undecenyl)-12-tridecenyl-1-tetra (ethylene glycol) monomethyl ether (TEGOMe21u, 3-6b).

^{1}H NMR ($CDCl_3$): δ (ppm) 1.21-1.52 (br, 33H), 2.01 (q, 4H), 3.29 (d, 2H), 3.35 (s, 3H), 3.50-3.75 (br, 16H), 5.35 (m, 2H). ^{13}C NMR ($CDCl_3$): δ (ppm) 27.03, 29.45, 29.76, 29.81, 29.90, 30.00, 30.32, 31.54, 32.83, 38.30, 59.22, 70.55, 70.71, 70.76, 70.80, 72.12, 74.96, 130.05 (cis olefin), 130.52 (trans olefin). IR (ν cm-1) 2923, 2853, 1464, 1350, 1115, 967, 886, 721. GPC (THF vs. Polystyrene standards): M_w = 96200 ; PDI (M_w/M_n) = 1.76

Polymerization of 2-(7-octenyl)-9-decenyl-1-tri(ethylene glycol) monomethyl ether (TrEGOMe15u, 3-6c).

^{1}H NMR ($CDCl_3$): δ (ppm) 1.21-1.52 (br, 21H), 1.98 (q, 4H), 3.21 (d, 2H), 3.35 (s, 2H), 3.50-3.71 (br, 12H), 5.35 (m, 2H). ^{13}C NMR ($CDCl_3$): .δ (ppm) 27.02, 27.09, 29.48, 29.94, 30.20, 31.59, 32.85, 38.35, 59.22, 70.58, 70.74, 70.79, 70.85, 70.87, 71.16, 74.94, 130.06 (cis olefin), 130.51 (trans olefin). IR (ν cm-1) 2923, 2853, 1464, 1350, 1115, 967, 886, 721. GPC (THF vs. Polystyrene standards): M_w = 37200 ; PDI (M_w/M_n) = 1.74

Polymerization of 2-(10-undecenyl)-12-tridecenyl-1-tri (ethylene glycol) monomethyl ether (TrEGOMe21u, 3-6d).

^{1}H NMR ($CDCl_3$): δ (ppm) 1.21-1.52 (br, 33H), 2.01 (q, 4H), 3.29 (d, 2H), 3.35 (s, 3H), 3.50-3.75 (br, 12H), 5.35 (m, 2H). ^{13}C NMR ($CDCl_3$): δ (ppm) 27.06, 27.51 29.46, 29.78, 29.83,

29.92, 30.34, 31.57, 32.85, 38.35, 59.24, 70.58, 70.75, 70.80, 70.84, 70.88, 72.16, 74.97, 130.08 (cis olefin), 130.54 (trans olefin). IR (ν cm-1) 2923, 2853, 1464, 1350, 1115, 967, 886, 721. GPC (THF vs. Polystyrene standards): M_w = 57700 ; PDI (M_w/M_n) = 1.72

General Procedure for the Hydrogenation of Unsaturated Polymers

Unsaturated polymers were dissolved in dry *o*-xylene. *p*-toluenesulfonyl hydrazide (TSH) and tripropyl amine (TPA) were added with stirring (3 equivalents each). The resulting solution was refluxed for 3-4 hours while monitoring nitrogen evolution with a bubbler. When gas evolution ceased, the solution was cooled to room temperature, an additional 3 equivalents of TSH and TPA were added, and the solution was refluxed for another 3 hours. The solutions were then concentrated to one-half of the original volume and precipitated into cold, acidic methanol. The polymers were isolated as elastic, adhesive gums.

TEGOMe152 (3-5a).

^{1}H NMR ($CDCl_3$): δ (ppm) 1.21-1.52 (br, 28H), 3.21 (m, 1H), 3.29 (s, 3H), 3.50-3.75 (br, 16H). ^{13}C NMR ($CDCl_3$): .δ (ppm) 25.67, 29.93, 30.12, 34.22, 59.21, 68.18, 70.72, 70.82, 71.09, 72.16, 80.35. IR (ν cm-1) 2923, 2853, 1464, 1350, 1115, 886, 721. GPC (THF vs. Polystyrene standards): M_w = 92200 ; PDI (M_w/M_n) = 1.71

TEGOMe212 (3-5b).

^{1}H NMR ($CDCl_3$): δ (ppm) 1.21-1.52 (br, 40H), 2.01, 3.21 (m, 1H), 3.29 (s, 3H), 3.50-3.75 (br, 16H). ^{13}C NMR ($CDCl_3$): δ (ppm) 25.68, 29.96, 30.12, 30.12, 34.22, 59.23, 68.19, 70.74, 70.85, 71.11, 72.17, 80.38. IR (ν cm-1) 2923, 2853, 1464, 1350, 1115, 886, 721. GPC (THF vs. Polystyrene standards): M_w = 127500 ; PDI (M_w/M_n) = 1.44

TrEGOMe152 (3-7c).

^{1}H NMR ($CDCl_3$): δ (ppm) 1.21-1.52 (br, 28H), 3.21 (m, 1H), 3.29 (s, 3H), 3.50-3.75 (br, 12H). ^{13}C NMR ($CDCl_3$): .δ (ppm) 25.67, 29.93, 30.12, 34.23, 59.22, 68.19, 70.76, 70.82, 71.11, 72.18, 80.37. IR (ν cm-1) 2923, 2853, 1464, 1350, 1115, 886, 721. GPC (THF vs. Polystyrene standards): M_w = 86700 ; PDI (M_w/M_n) = 1.85

TrEGOMe212 (3-7d).

^{1}H NMR ($CDCl_3$): δ (ppm) 1.21-1.52 (br, 40H), 2.01, 3.21 (m, 1H), 3.29 (s, 3H), 3.50-3.75 (br, 12H). ^{13}C NMR ($CDCl_3$): δ (ppm) 25.67, 29.96, 30.12, 30.12, 34.23, 59.24, 68.19, 70.74, 70.83, 70.85,70.88, 71.11, 72.18, 80.38. IR (ν cm-1) 2923, 2853, 1464, 1350, 1115, 886, 721. GPC (THF vs. Polystyrene standards): M_w = 117300; PDI (M_w/M_n) = 1.55

TEGOMe15 (3-8a).

^{1}H NMR ($CDCl_3$): δ (ppm) 1.21-1.52 (br, 29H), 3.21 (d, 2H), 3.35 (s, 2H), 3.50-3.71 (br, 16H). ^{13}C NMR ($CDCl_3$): .δ (ppm) 27.08, 29.98, 30.37, 31.61, 38.37, 59.23, 70.59, 70.74, 70.81, 70.84, 72.16, 74.98. IR (ν cm-1) 2923, 2853, 1464, 1350, 1115, 886, 721. GPC (THF vs. Polystyrene standards): M_w = 117400 ; PDI (M_w/M_n) = 1.50

TEGOMe21 (3-8b).

^{1}H NMR ($CDCl_3$): δ (ppm) 1.21-1.52 (br, 41H), 3.29 (d, 2H), 3.35 (s, 3H), 3.50-3.75 (br, 16H). ^{13}C NMR ($CDCl_3$): δ (ppm) 27.08, 29.98, 30.37, 31.36, 38.37, 59.25, 70.61, 70.76, 70.83, 70.86, 72.18, 75.03. IR (ν cm-1) 2923, 2853, 1464, 1350, 1115, 886, 721. GPC (THF vs. Polystyrene standards): M_w = 146500 ; PDI (M_w/M_n) = 1.25

TrEGOMe15 (3-8c).

^{1}H NMR ($CDCl_3$): δ (ppm) 1.21-1.52 (br, 29H), 3.21 (d, 2H), 3.35 (s, 2H), 3.50-3.71 (br, 12H). ^{13}C NMR ($CDCl_3$): .δ (ppm) 27.06, 29.96, 30.35, 31.59, 38.35, 59.22, 70.58, 70.74, 70.81,

70.84, 72.16, 74.97. IR (ν cm-1) 2923, 2853, 1464, 1350, 1115, 886, 721. GPC (THF vs. Polystyrene standards): M_w = 42600 ; PDI (M_w/M_n) = 1.71

TrEGOMe21 (3-8d).

^{1}H NMR ($CDCl_3$): δ (ppm) 1.21-1.52 (br, 41H), 3.29 (d, 2H), 3.35 (s, 3H), 3.50-3.75 (br, 12H). ^{13}C NMR ($CDCl_3$): δ (ppm) 27.05, 29.96, 30.35, 31.57, 38.34, 59.23, 70.58, 70.75, 70.81, 70.85, 70.88, 72.17, 74.99. IR (ν cm-1) 2923, 2853, 1464, 1350, 1115, 886, 721. GPC (THF vs. Polystyrene standards): M_w = 117300 ; PDI (M_w/M_n) = 1.55

Results and Discussion

Synthesis and Structural Analysis

Figure 3-2 describes the synthesis of the ADMET amphiphiles used in this study. Monomers 3-3a-d and 3-4a-d were prepared via Williamson etherification of primary and secondary diene alcohols 3-1a,b and 3-2a,b (synthsized as previously reported)[13, 17] with oligoethoxy-*p*-tosylates.[59] The use of the primary diene alcohol places a carbon atom directly off the backbone of the resulting polymer; throughout this report the monomers and polymers produced in this fashion will be described as "primary." Using a secondary alcohol places an oxygen atom directly off the backbone, monomers and polymer produced in this fashion will be described as "secondary' throughout this report. Monomer structures were confirmed by ^{1}H and ^{13}C NMR, elemental analysis, and high resolution mass spectrometry. Polymerization with Grubbs' 1st generation catalyst affords the unsaturated polymers 3-5a-d and 3-6a-d, which were quantitatively hydrogenated with *p*-toluenesulfonyl hydrazide. Polymer structures were confirmed by ^{1}H and ^{13}C NMR and FTIR. Molecular weights, (Table 3-1) were measured using gel permeation chromatography (THF vs. polystyrene standards).

To simplify the discussion, a systematic nomenclature was adopted for these polymers and monomers. Monomers are named with a prefix for the number of methylene carbons between the PEG branch and the olefin (n in Figure 3-2), followed by the identity of the branch (TEGOMe for tetra ethylene glycol (x = 4), methoxy terminated; TrEGOMe for tri ethylene glycol (x = 3), methoxy terminated). Polymers are named first for the identity of the branch, followed by a number indicating the frequency of the branch. Unsaturated polymers are denoted with the suffix "u." Finally, monomers and polymers made from the secondary diene alcohols 3-1a-b are given the additional suffix "2." For example, monomers 3-3a and 3-4a are 6,6TEGOMe2 and 6,6TEGOMe, polymers 3-5a and 3-6a TEGOMe15u2 and TEGOMe15u, polymers 3-7a and 3-8a TEGOMe15 and TEGOMe152, respectively.

The slight structural differences between the primary and secondary monomers are apparent in both the ^{1}H and ^{13}C NMR spectra. Figure 3-3 shows the ^{1}H NMR spectra of monomers 3-3a and 3-4a, chosen arbitrarily as examples. The signal at 3.28 ppm in the bottom spectrum, corresponding to the methylene spacer, does not appear in the 3-3a spectrum. Also, the resonance for the methine proton shifts from 1.54 ppm in the 3-4a spectrum to 3.22 ppm in the 3-3a spectrum. The olefin and glycol region proton signals remain mostly unchanged between the two monomers. The broad overlapping signal for the aliphatic protons emphasizes the limitation of ^{1}H NMR in the structural analysis of ADMET monomers and the need for thorough ^{13}C NMR analysis.

Figure 3-4 shows the ^{13}C NMR spectra for monomers 3-3a and 3-4a. As in the proton spectra, the ^{13}C NMR spectra for the primary and secondary monomers show significant differences. The position of the methine carbon shifts from 38.26 ppm in the spectrum of 3-4a to 80.27 in the spectrum of 3-3a. The resonance at 74.90 in the spectrum for 3-4a, absent in the

spectrum for 3-3a, corresponds to the methylene spacer carbon. The resonance at 68.22 in the spectrum for 3-3a but absent in the spectrum of 3-4a corresponds to the first methylene carbon in the glycol branch. The symmetric nature of the glycol branches results in the overlapping of the remaining glycol carbon signals in both monomers (70.50-70.75 ppm), except for the methyl endgroup carbon (59.16 ppm in both spectra) and the glycol carbon closest to the branch terminus (72.15 ppm in both spectra, unlabeled in Figure 3-3).

Expansion of the aliphatic region (Figure 3-5) again reveals the effect of the slight structural variation of the methylene spacer. Monomer 3-3a shows a strong downfield shift for the methylene carbons adjacent to the central methine carbon when compared to 3-4a. There is also an upfield shift for the next adjacent carbons in the spectrum for 3-3a compared to 3-4a, due again to a difference in the magnetic environments of the two monomers' methine carbons. However, past this the resonances are consistent for the remaining aliphatic carbons and the allylic carbons.

The progression from monomer 3-4a to fully saturated polymer 3-8a (chosen as an example), monitored by ^{1}H and ^{13}C NMR, is shown in Figure 3-6. Polymerization to 3-6a results in the convergence of terminal olefin signals in the monomer spectra (4.89, 5.74 ppm in the ^{1}H spectrum, 114.26 and 139.31 ppm in the ^{13}C spectrum) to a single internal olefin peak for the unsaturated polymer (5.38 ppm in the ^{1}H spectrum, 130.08 ppm in the ^{13}C spectrum). Saturation to form 3-8a results in the complete disappearance of any olefin signal in the spectra of the final polymer. Coalescence of several individual backbone carbon peaks into a single peak, due to the symmetric nature of the repeat unit, highlights the ability of ADMET chemistry to create pristine polymer microstructures. The appearance of only the resonances predicted by the repeating unit confirms the absence of side reactions or structural irregularities.

Typically, the quantitative hydrogenation of ADMET polymers is confirmed using FTIR by the absence of the out-of-plane C-H wagging vibrational mode at 967 cm^{-1}. This also occurs with this family of polymers. However, a combination of NMR and IR is needed, because the signal at 967 cm^{-1} is complicated by overlapping polyether stretches, which prevent baseline resolution (Figure 3-7). However, the IR spectra serve to verify the absence of moisture in the polymer films (no hydrogen bonding seen). This result helps confirm the interpretation of the DSC data (discussed in the subsequent section), which indicate that the thermal behavior is due to the bulk morphology of the polymer and is not a result of moisture content in the polyether phase.

Thermal Analysis

Previous ADMET studies have shown that both melting temperature and melting enthalpy decrease as the size of the pendant moieties increases.[10] Interestingly, this trend is not observed in the series of polymers described here. The tri ethylene glycol and tetra ethylene glycol grafts show nearly identical peak melting temperatures and enthalpies when the branch distribution is held constant (3-8a,c; 3-7a,c; 3-6b,d; 3-8b,d; 3-7b,d). This is compelling evidence that the model presented above is correct, as the length of the graft doesn't alter the behavior of the crystallizing backbone. Noticeable differences in glass transition between the tri ethylene glycol and tetra ethylene glycol grafts support this model. Referring to Figure 3-8, which shows DSC plots for polymers with tri ethylene glycol and tetra ethylene glycol grafts, in all cases the longer graft results in a higher amorphous content and a more distinct glass transition.

There are also remarkable differences in the thermograms for the saturated and unsaturated polymers. Comparing the melting temperatures in Table 3-2 for the unsaturated polymers to the values for the saturated analogues (3-6b and 3-8b, 3-5b and 3-7b, 3-6d and 3-8d, 3-5d and 3-7d), differences of more than 30 ºC are observed, but the Tg's remain essentially unchanged, an

indication that only the crystalline region (i.e., the PE backbone) is affected by the degree of unsaturation and not the amorphous part. This once again supports our crystallization model: the internal olefin acts a defect witch interrupts the all trans configuration of the methylene sequences between branches, thus impeding crystallization.

The differences between in thermal response depending on the nature of the attachment of the PEG branch (primary or secondary), and especially for the unsaturated polymers, further support our model. The unsaturated primary polymers (Figure 3-8B) display rather complex thermograms with multimodal melting profiles, while the secondary analogues (Figure 3-8A) display a single melting peak characteristic of most ADMET polymers. The corresponding saturated polymers show a difference between primary and secondary branch attachment, albeit less significant. A decrease in melting enthalpy and a broadening of the endotherm is witnessed for the secondary polymers, indicating a less perfectly formed crystal. This is definitive evidence that the point of branching is affecting the folding of the chains and therefore the crystallization and melting behavior.

The interesting melting behavior for TEGOMe21u (3-6b) and TrEGOMe21u (3-6d) were further investigated using MDSC and selective annealing experiments. MDSC provide increased sensitivity over conventional DSC, as well as the separation of kinetic and thermodynamic components of the total heat flow. This allows for the resolution of weak or overlapping transions.[51, 60-62] MDSC data (Figure 3-9A), confirmed the existence of two separate melting endotherms in these unsaturatued polymers. During the dual annealing experiment we discovered that the polymers could be conditioned thermally to prefer either of these two different crystalline forms. The DSC thermograms obtained after annealing temperatures at -37ºC (just below the higher temperature endotherm but above the lower temperature endotherm), at -57ºC

(just below the lower melting endotherm), and at -37ºC followed by -57ºC are shown in Figure 3-10B, (refer to Figure 3-8B for the unannealed curve).

Annealing at -37ºC results in a marked increase in the melting enthalpy for the higher temperature transition compared to the unannealed polymer. The lower temperature peak remains unaffected during this treatment. If the bimodal melt were the result of a melting and recrystallization mechanism, the lower temperature endotherm would be suppressed by this treatment, as crystallization would occur at temperatures above the melting point of these crystallites. This is not the case. Similarly, annealing at -57ºC results in an increase in the melting enthalpy of the lower temperature transition compared to the unannealed polymer, while leaving the higher temperature transition unaffected. Annealing at both temperatures, first -37ºC followed -57ºC produces two very sharp, distinct melting transitions. Further, the MDSC experiment shows no crystallization occurring simultaneously along with melting, noted by the absence of any exothermic transitions in any of the three heat flow signals. This confirms that the bimodal melt must be due to different crystallite populations and not to a melting and concurrent crystallization process. This again supports our current model of small, isolated crystallites.

The thermograms for the polymers with 15 carbons between the PEG grafts are shown in Figure 3-10. When comparing the unsaturated polymers in Figure 3-10 to the unsaturated polymers in Figure 3-8 (20 carbons between branch points), it becomes clear that the site of unsaturation in the 15 family disrupts crystallization, resulting in completely amorphous materials. The difference in the nature of the branch attachment (primary versus secondary) is also witnessed in the 15 family, but the trend is opposite to that of the 21 family. The secondary polymers (Figure 3-10A) exhibit a sharper, more defined melt with a greater melting enthalpy compared to the primary polymers (Figure 3-10B). The peak melting temperature however, is

slightly depressed from the primary polymer, implying a thinner crystal. The reason for the opposite trend for the 15 and 21 series is not clear at this point; however it is again evident that the nature of the attachment of the PEG plays a crucial role in the crystallization of the backbone.

Despite the differences in the crystallinity, the behavior of the amorphous content for each material is nearly identical for these polymers, the only exception being the tri ethylene glycol grafted polymers, which exhibit a smaller ΔC_p than the tetra ethylene glycol grafted polymers. This is a clear indication that the amorphous regions across this entire family of polymers, which remain unaffected with significant changes in the structure of the backbone and the observed crystallinity, are primarily polyether. The DSC data for all of the polymers discussed is summarized in Table 3-2 below.

The thermal stabilities are similar for all of the saturated polymers in this family. All are stable up to 380 °C, above which a single-stage, rapid decomposition is observed (Figure 3-11).

Conclusions

This chapter described the synthesis of a family of PEG grafted polyethylene amphiphilic copolymers using ADMET chemistry. The graft length and graft distribution have been perfectly controlled during the synthesis of the monomers. By altering several structural parameters we have shown that the PEG branches are inducing folds in the backbone, resulting in small paraffin like crystallites composed of the methylene sequences between branches. The site of unsaturation in the backbone of the polymer plays an important role in the ability of the polymer to crystallize. Likewise, the manner in which the PEG branch is connected to the backbone changes the sterics and electronics as this fold point and alters the observed crystallinity. The size of the PEG branch, however, does not affect this behavior significantly. These slight variations in structure ultimately provide tunability over the properties of the final materials; the

melting point of the resulting materials can be controlled over a range of 60 °C, or rendered fully amorphous. Experiments involving PEG branches with different end groups, designed to induce interactions of the branches within the amorphous phase of the polymer, are described in chapter 4.

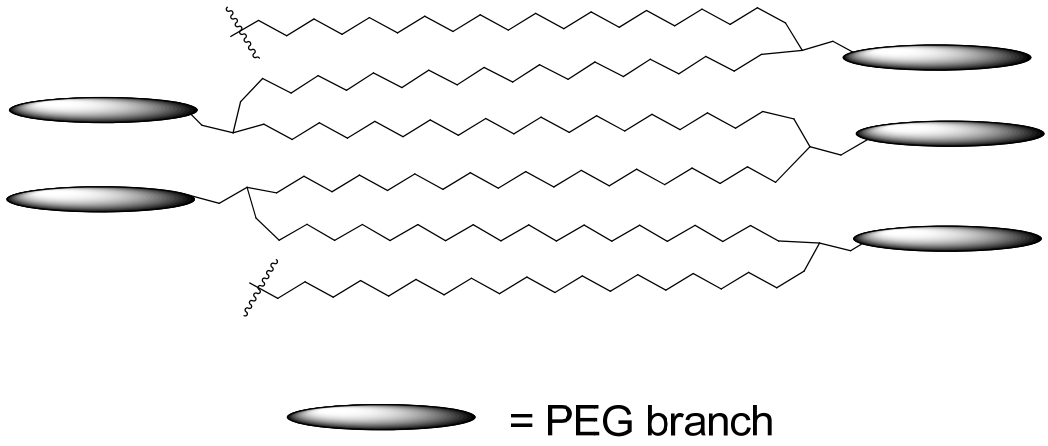

Figure 3-1: Model for chain folding and crystallization in ADMET amphiphiles.

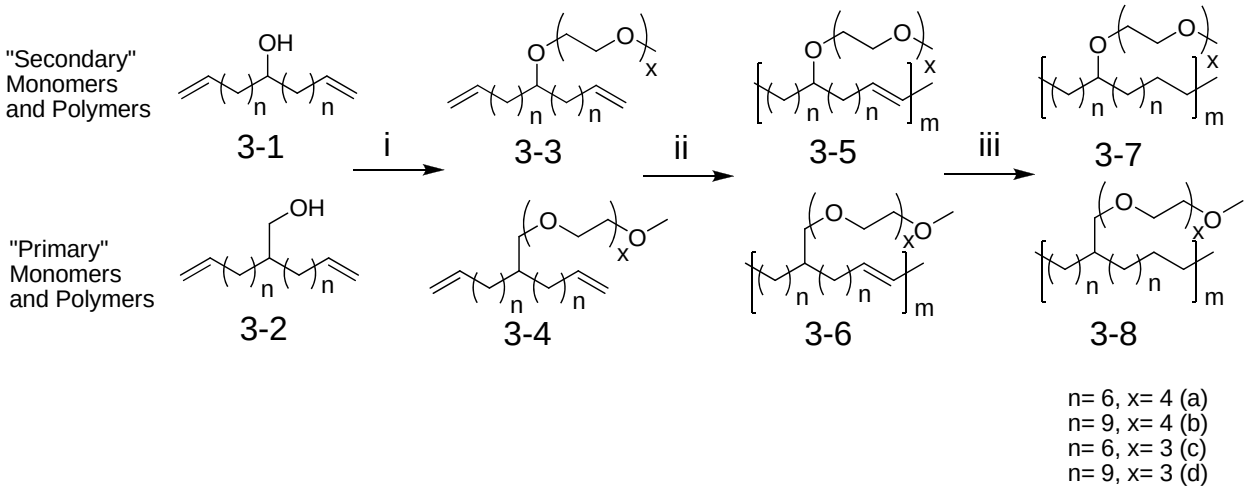

Figure 3-2: ADMET amphiphile synthesis. i: NaH, DMF, $TsO(CH_2CH_2O)_xCH_3$; ii: Grubbs' 1st generation catalyst, 45 °C, vacuum; iii: TSH, TPA, o-xylenes 140 °C.

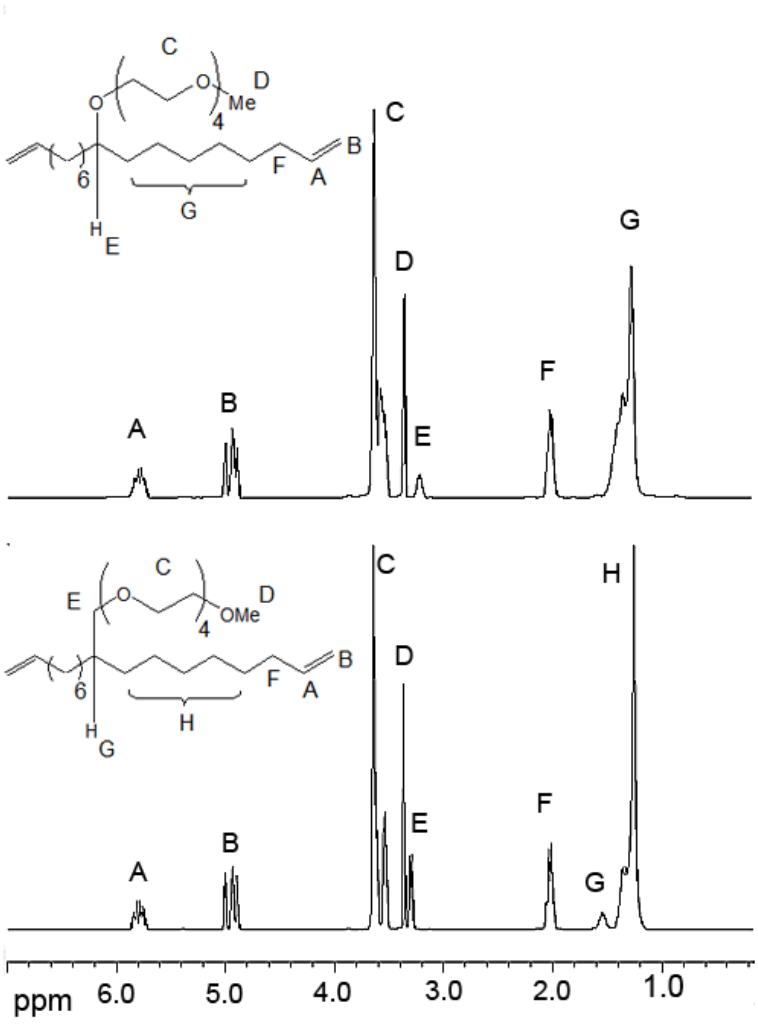

Figure 3-3: ^{1}H NMR spectra of monomers 3-3a and 3-4a.

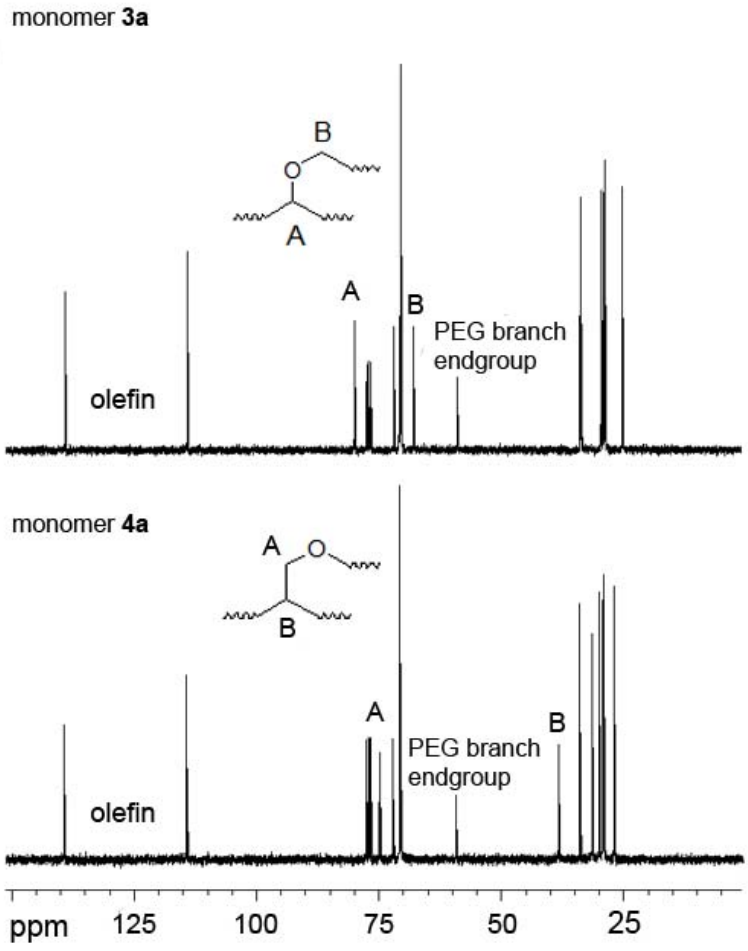

Figure 3-4: ^{13}C NMR for monomers 3-3a and 3-4a.

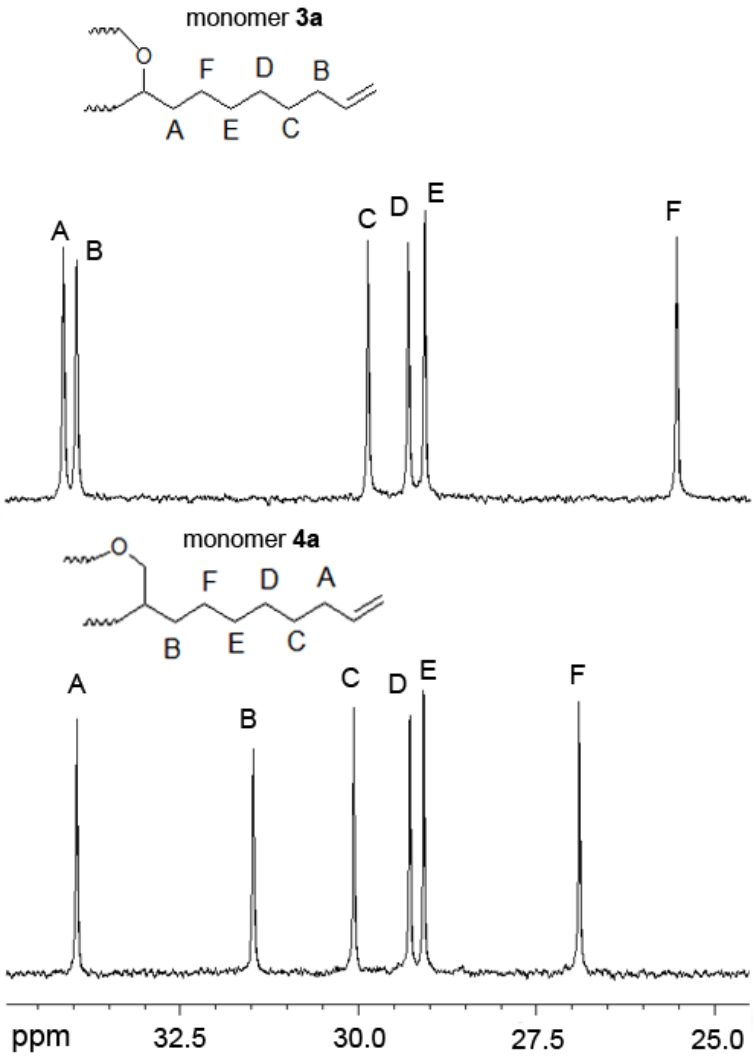

Figure 3-5: Assignment of aliphatic resonances in the ^{13}C NMR spectra of monomers 3-3a and 3-4a.

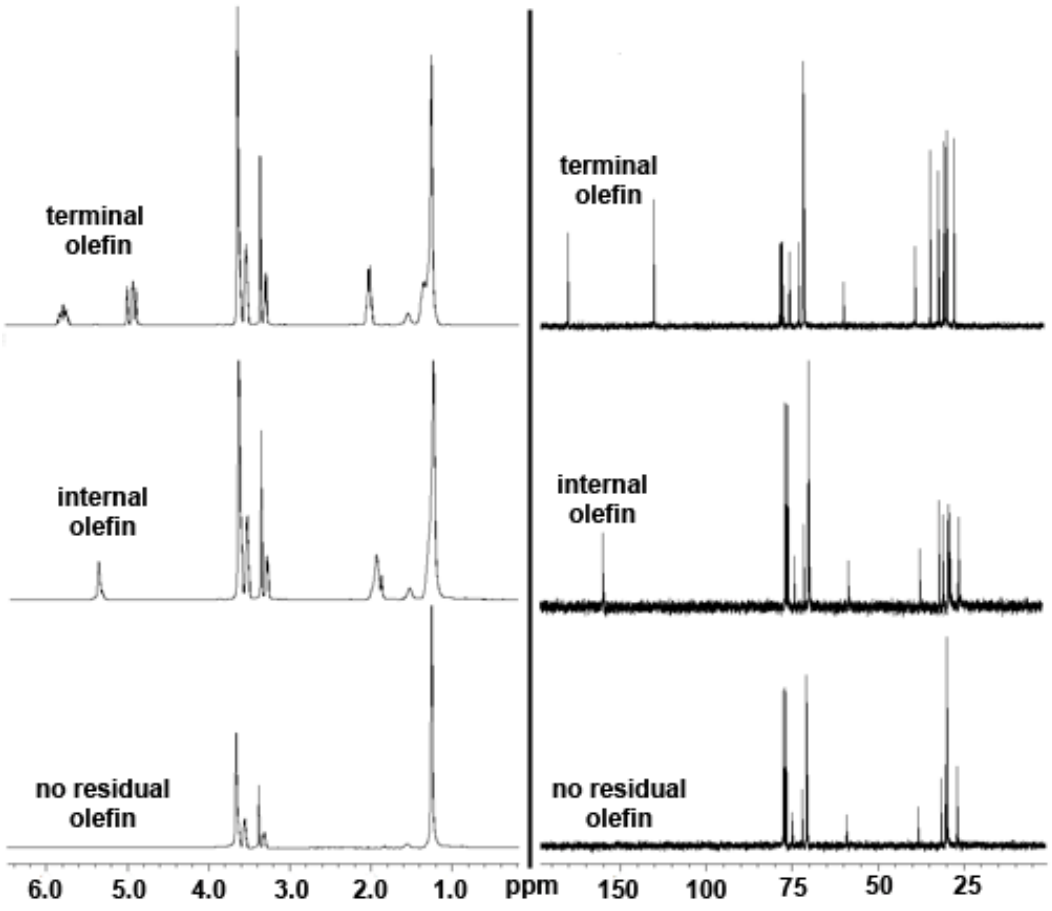

Figure 3-6: Progression from monomer 4a to polymer 8a monitored by ^{1}H and ^{13}C NMR.

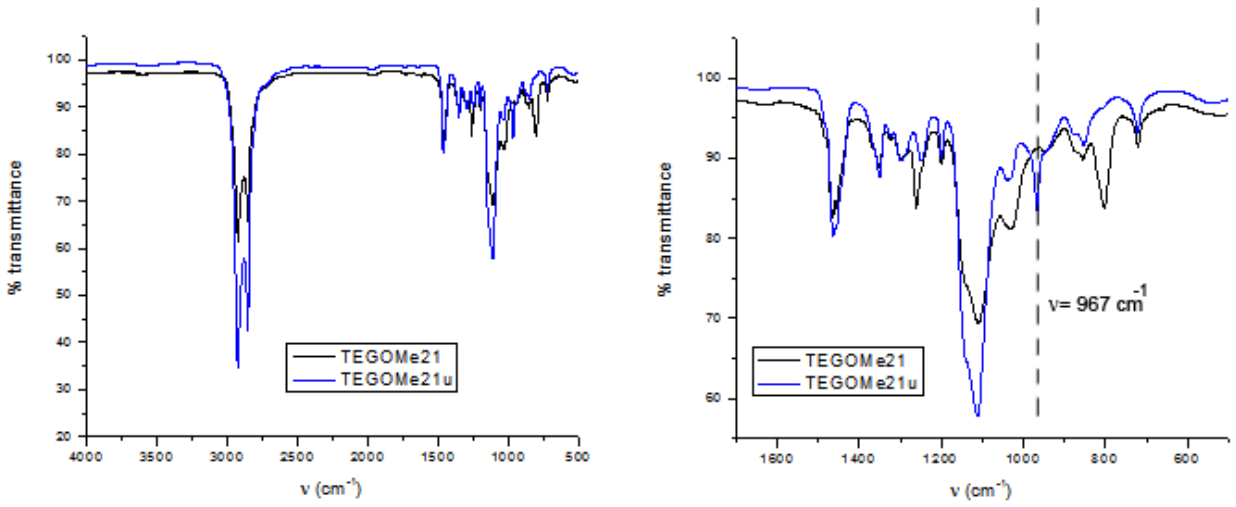

Figure 3-7: FTIR of TEGOMe21 and TEGOMe21u

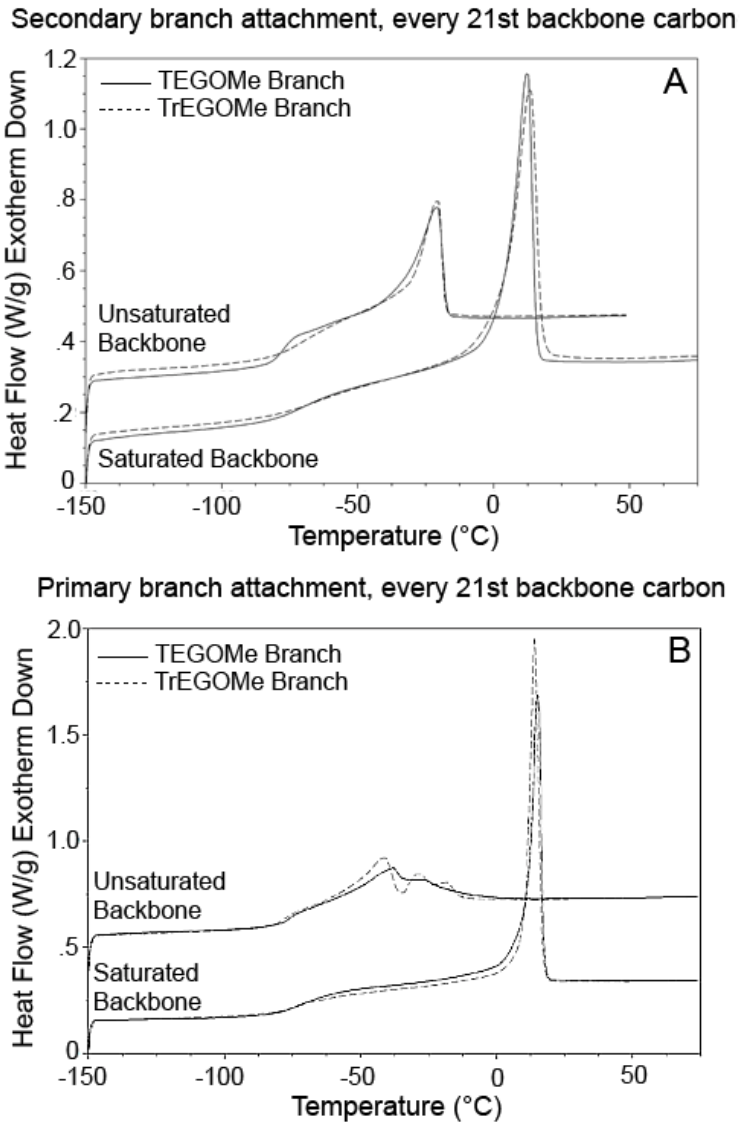

Figure 3-8: DSC comparison of secondary A) and primary B) polymers with PEG grafts every 21st backbone carbon.

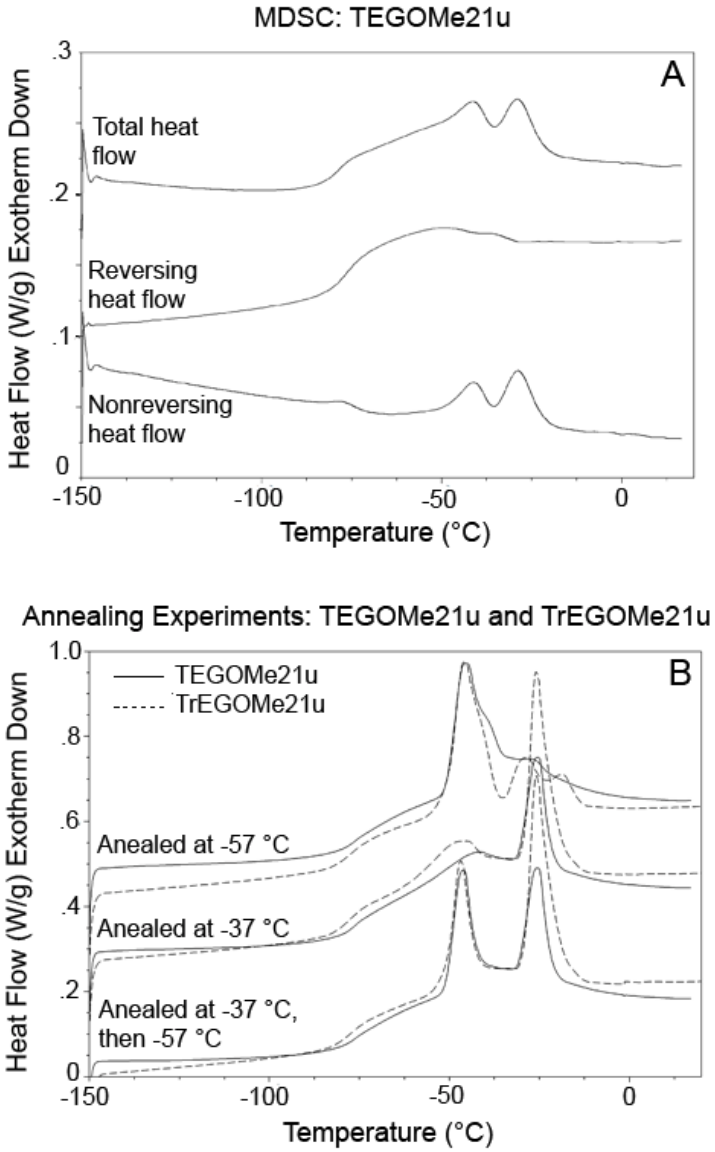

Figure 3-9: MDSC for TEGOMe21u A) and DSC annealing experiments for TEGOMe21u and TrEGOMe21u B).

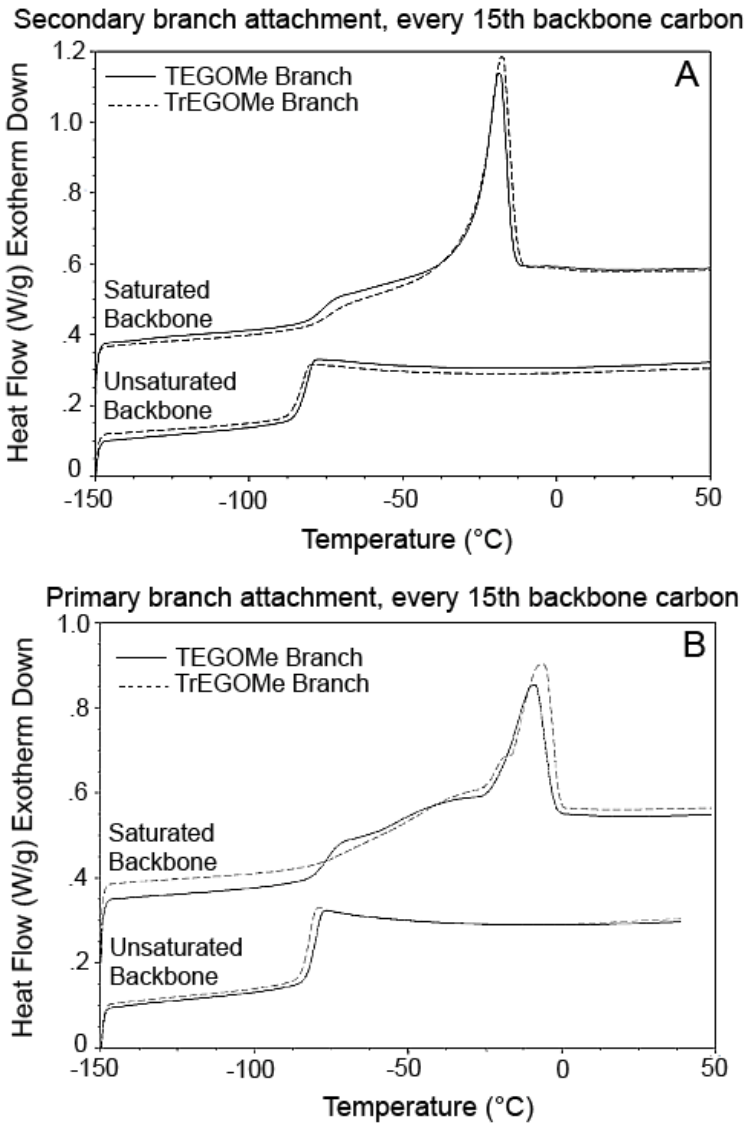

Figure 3-10: DSC comparison of secondary A) and primary B) polymers with PEG grafts every 15^{th} backbone carbon.

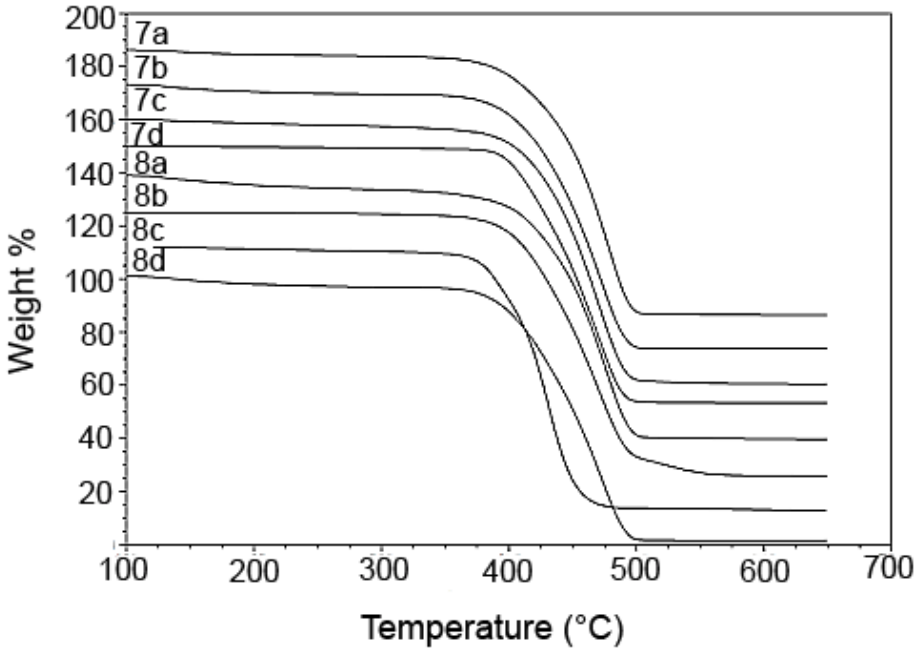

Figure 3-11: Thermo gravimetric analysis of saturated polymers (arbitrary vertical offsets for clarity)

Table 3-1: Molecular weight data for polymers described in chapter 3

Polymer	M_n[a] (kg/mol)	M_w[a] (kg/mol)	PDI[b]
TEGOMe15u **(3-6a)**	62.7	100.4	1.60
TrEGOMe15u **(3-6c)**	21.4	37.2	1.74
TEGOMe15u2 **(3-5a)**	50.7	88.7	1.75
TrEGOMe15u2 **(3-5c)**	42.9	79.5	1.85
TEGOMe15 **(3-8a)**	78.1	117.4	1.5
TrEGOMe15 **(3-8c)**	24.9	42.6	1.71
TEGOMe152 **(3-7a)**	53.9	92.2	1.71
TrEGOMe152 **(3-7c)**	46.8	86.7	1.85
TEGOMe21u **(3-6b)**	54.8	96.2	1.76
TrEGOMe21u **(3-6d)**	33.5	57.7	1.72
TEGOMe21u2 **(3-5b)**	64.1	114.5	1.78
TrEGOMe21u2 **(3-5d)**	64.1	108.7	1.69
TEGOMe21 **(3-8b)**	117.2	146.5	1.25
TrEGOMe21 **(3-8d)**	41.1	70.3	1.71
TEGOMe212 **(3-7b)**	87.9	127.5	1.44
TrEGOMe212 **(3-7d)**	75.6	117.3	1.55

[a] GPC vs. polystyrene standards; [b] M_w/M_n

Table 3-2: DSC data for polymers described in chapter 3

Polymer	T_g (°C)	ΔC_p (J/g·°C)	T_m (°C)	ΔH_m (J/g)	T_c (°C)	ΔH_c (J/g)
TEGOMe15u **(3-6a)**	-80	1.0	n/a	n/a	n/a	n/a
TrEGOMe15u **(3-6c)**	-81	1.0	n/a	n/a	n/a	n/a
TEGOMe15u2 **(3-5a)**	-81	1.0	n/a	n/a	n/a	n/a
TrEGOMe15u2 **(3-5c)**	-81	0.9	n/a	n/a	n/a	n/a
TEGOMe15 **(3-8a)**	-76	0.5	-9	21	-36	27
TrEGOMe15 **(3-8c)**	-70	0.2	-6	24	-36	32
TEGOMe152 **(3-7a)**	-76	0.4	-19	31	-28	31
TrEGOMe152 **(3-7c)**	-74	0.3	-18	40	-29	38
TEGOMe21u **(3-6b)**	-76	0.3	-38	18	-46	17
TrEGOMe21u **(3-6d)**	-76	0.3	-41	22	-49	23
TEGOMe21u2 **(3-5b)**	-76	0.4	-21	21	-37	22
TrEGOMe21u2 **(3-5d)**	-70	0.3	-20	20	-36	22
TEGOMe21 **(3-8b)**	-74	0.4	15	44	7	43
TrEGOMe21 **(3-8d)**	-74	0.2	14	45	8	45
TEGOMe212 **(3-7b)**	-71	0.3	12	45	-1	45
TrEGOMe212 **(3-7d)**	-65	0.2	13	50	-1	50

CHAPTER 4
INDUCING PENDANT BRANCH SELF ASSEMBLY IN ADMET AMPHIPHILES

Introduction

It is well understood that highly regular macromolecular structures result in predictable and controllable behavior. This is especially true with amphiphilic copolymers, for which minor alterations in structure can induce a broad range of responses in the bulk and in solution.[63-67] The amount of research on the synthesis and self assembly of amphiphilic block copolymers alone is remarkable.[35, 37, 41, 46, 67-69] Living radical,[37, 70] cationic,[36, 41] anionic,[71] and even metathesis[72] polymerizations have been extensively utilized in creating well defined structures that can self assemble to form interesting and useful morphologies.

The use of acyclic diene metathesis (ADMET) to create highly regular, precisely defined structures is also well known.[9-11] These materials, while often structurally related to copolymers made via chain copolymerization of ethylene and vinyl comonomers, possess properties that set them apart as a completely separate class of materials.[9, 12-14, 16-19, 28, 31, 53] These properties are highly tunable with minor structural alterations, imparted during the synthesis of the symmetrical terminal diolefin monomer. Two parameters are generally altered: the identity of the pendant functional moiety and the static methylene sequence length between this functional group and the terminal olefin. When the pendant moiety is a methyl group, systematically changing the methylene sequence length from branches every 7^{th} carbon to branches every 21^{st} carbon results in a control of melting point over a range of 200 °C.[19, 24] Likewise, alteration of the pendant group size and polarity allow tunability of the properties when the methylene sequence length is held constant. In all ADMET copolymers observed previously, an increase in defect size results in a systematic decrease in melting temperature.[13, 14, 18]

The previous chapters described the use of ADMET to synthesize a family of amphiphilic graft copolymers with polyethylene (PE) backbones and hydrophilic polyethylene glycol (PEG) branches. By combining the structural regularity available with ADMET and the ability of amphiphiles to phase separate and self assemble we have created semicrystalline materials in which the PE backbone crystallizes, forming pure hydrocarbon crystallites excluding the polyether branches.[15] This chapter describes the expansion of this area of research by altering the pendant PEG chain end group to create copolymers with PE backbones and AB amphiphilic grafts. Two of the polymers reported have the A-*g*-(B-*b*-A) motif, where an oligoethylene chain is affixed to the end of the PEG branch directly attached to the PE backbone. The third has a pyrene group attached to the end of the PEG chain. Labeling in the fashion allows the aggregation of these graft end groups to be examined using fluorescence measurements. To assess the influence of these pendant groups on the PE backbone accurately, the distance between pendant groups was kept constant in this chapter. A 21-carbon distance between pendant branches was chosen to ensure the crystallization of the backbone because previous ADMET polymers with this functional group distribution have always been semicrystalline.[9-11]

All monomer and precursor structures were confirmed by ^{1}H and ^{13}C NMR, elemental analysis and high resolution mass spectrometry. The structures of the corresponding polymers were confirmed by ^{1}H and ^{13}C NMR, and FTIR. Differential Scanning Calorimetry (DSC) and temperature modulated DSC (MDSC) were used to study the behavior of these materials in the bulk. The observed thermal behavior indicates that the three materials have very different morphologies. Affixing the PEG branch with a pyrene end group results in the complete exclusion of the pendant moiety from the crystal, simultaneously inducing their aggregation. Changing the end group to an n-hexyl chain results in crystallization of the pendant branch

separately from the PE backbone. Extending this olgioethylene chain from *n*-hexyl to *n*-tetradecyl allows the pendant moiety to extend back into the polymer crystal, thereby increasing the melting point compared to the polymer with the 6-carbon terminus. The inclusion of the tetradecyl group into the crystal and resultant increase in melting point compared to the other materials presented here is significant because it breaks the usual trend for ADMET polymers, which show a decrease in melting point and melting enthalpy with increasing pendant group size.

Experimental Section

Instrumentation

All ^{1}H NMR (300 MHz) and ^{13}C NMR (75 MHz) spectra were recorded on a Varian Associates Mercury 300 spectrometer. Chemical shifts for ^{1}H and ^{13}C NMR were referenced to residual signals from $CDCl_3$ (^{1}H: δ= 7.27 ppm and ^{13}C: δ = 77.23 ppm) with 0.03% v/v TMS as an internal reference. Thin layer chromatography (TLC) was performed on EMD silica gel coated (250 μm thickness) glass plates. Developed TLC plates were stained with iodine adsorbed on silica to produce a visible signature. Reaction conversions and relative purity of crude products were monitored by TLC and ^{1}H NMR. Fourier transform infrared (FT-IR) measurements were conducted with a Bruker Vector 22 Infrared Spectrophotometer using polymer films cast from chloroform onto KBr plates using . High resolution mass spectrometry analyses were performed on a Bruker APEX II 4.7 T Fourier Transform Ion Cyclotron Resonance mass spectrometer (Bruker Daltonics, Billerica, MA) using electrospray ionization (ESI). Elemental analysis was carried out at Atlantic Microlab Inc. (Norcross, GA).

Molecular weights and molecular weight distributions (M_w/M_n) were determined by gel permeation chromatography (GPC) using a Waters Associates GPCV2000 liquid chromatography system with an internal differential refractive index detector (DRI) and two

Waters Styragel HR-5E columns (10 micron particle diameter, 7.8 mm ID, 300 mm length) at 40 °C. The mobile phase was HPLC grade tetrahydrofuran at a flow rate of 1.0 mL/minute). Retention times were calibrated versus polystyrene standards (Polymer Laboratories; Amherst, MA).

Differential scanning calorimetry (DSC) and temperature modulated differential scanning calorimetry (MDSC) were performed on a TA Instruments Q1000 equipped with a liquid nitrogen cooling accessory calibrated using sapphire and high purity indium metal. All samples were prepared in hermetically sealed pans (4-7 mg/sample) and were referenced to an empty pan. Samples were run under s purge of helium gas. A scan rate of 10 °C per minute was used unless otherwise specified. Modulated experiments were scanned with a 3 °C per minute linear heating rate with modulation amplitude of .45 °C and period of 30 seconds. Melting temperatures are taken as the peak of the melting transition, glass transition temperatures as the mid point of a step change in heat capacity.

Materials

Unless otherwise stated, all reagents were purchased from Aldrich and used without further purification. Grubbs' 1st generation catalyst was a gift from Materia, Inc. Diene alcohol 4-1 was synthesized as previously reported.[17]

Synthesis of 2-(10-undecenyl)-12-tridecenyl-1-tetra(ethylene glycol)-*p*-tosylate (4-2).

Anhydrous DMF (30 mL) was cannula transferred into an oven dried, 3-neck round-bottom flask equipped with a magnetic stirrer and gas inlet, and was charged with 2 equivalents of sodium hydride (60% dispersion in mineral oil). The slurry was cooled to 0°C and 1 equivalent of 4-1 in 20 mL of anhydrous DMF was added via syringe. When hydrogen gas evolution (monitored by bubbler) ceased, the solution was cannula transferred into a well-stirred flask containing 4.5 equivalents of tetraethylene glycol di-p-tosylate in 50 mL of anhydrous

DMF. The reaction was stirred for 17 hours at 0 °C and quenched by pouring into 300 mL of water. The resulting mixture was extracted with diethyl ether and the combined organics washed with brine. Concentration afforded a yellow oil which was further purified by column chromatography, 30% ethyl acetate 70% hexane eluent, yielding 1.5g (52%) of colorless oil. ^{1}H NMR ($CDCl_3$): δ (ppm) 1.21-1.52 (br, 33H), 2.01 (q, 4H), 2.42 (s, 3H), 3.29 (d, 2H), 3.50-3.75 (br, 15H), 4.18 (d, 2H), 4.98 (m, 4H), 5.82 (m, 2H), 7.31 (d, 2H), 7.79 (d, 2H). ^{13}C NMR ($CDCl_3$): δ (ppm) 21.82, 27.01, 29.15, 29.35, 29.70, 20.80, 29.83, 30.28, 31.55, 34.00, 38.32, 68.89, 69.39, 70.57, 70.74, 70.79, 70.80, 70.88, 70.97, 75.01, 114.28, 128.18, 129.99, 133.33, 139.43, 144.92. ESI/HRMS: $[M+NH4]^+$ calcd for $NH_4C_{39}H_{68}O_7S$, 698.5024; found 698.5023. Anal. (CH) calcd for $C_{39}H_{68}O_7S$: C, 68.78; H, 10.06. Found C, 58.51; H, 9.95.

General Procedure for Preparation of Monomers

Anhydrous DMF (45 mL) was cannula transferred into an oven dried, 3-neck round-bottom flask equipped with a magnetic stirrer and gas inlet, and was charged with 2 equivalents of sodium hydride (60% dispersion in mineral oil). The slurry was cooled to 0°C and 3 was added in 20 mL of anhydrous DMF via syringe. When hydrogen gas evolution (monitored by bubbler) ceased, 1 equivalent of 4-2 in 30 mL of anhydrous DMF was added via syringe. The reaction was stirred for 17 hours at 0 °C and quenched by pouring into 300 mL of water. The resulting mixture was extracted with diethyl ether and the combined organics washed with brine. Concentration afforded a yellow oil which was further purified by column chromatography.

2-(10-undecenyl)-12-tridecenyl-1-tetra (ethylene glycol) methenyl pyrene (9,9TEGOPy, 4-3a).

Column Chromatography:30% ethyl acetate 70% hexane eluent afforded .475g (29% yield) of colorless oil. ^{1}H NMR ($CDCl_3$): δ (ppm) 1.21-1.52 (br, 33H), 2.01 (q, 4H), 3.29 (d, 2H), 3.50-3.75 (br, 12H) 4.98 (m, 4H), 5.28 (s, 2H), 5.82 (m, 2H), 7.61-8.79 (m, 4H), 8.13-8.20 (m,

4H), 8.37 (d, 1H). ^{13}C NMR ($CDCl_3$): δ (ppm) 26.96, 29.14, 29.35, 29.71, 20.82, 29.85, 30.28, 31.52, 34.01, 38.28, 69.72, 70.54, 70.75, 70.83, 70.87, 70.95, 72.04, 74.96, 114.28, 123.75, 124.64, 124.92, 125.36, 126.09, 127.22, 127.60, 127.83, 131.03, 131.47, 131.62, 139.43. ESI/HRMS: $[M+NH4]^+$ calcd for $NH_4C_{49}H_{72}O_5$, 758.5718; found 758.5735. Anal. (CH) calcd for $C_{49}H_{72}O_5$: C, 79.41; H, 9.79. Found C, 79.00; H, 9.80.

2-(10-undecenyl)-12-tridecenyl-1-tetra (ethylene glycol) mono *n*-hexyl ether (9,9TEGOHex, 4-3b).

Column Chromatography: 20% ethyl acetate 80% hexane eluent afforded .144g (17% yield) of colorless oil. ^{1}H NMR ($CDCl_3$): δ (ppm) 0.82 (t, 3H), 1.21-1.61 (br, 41H), 2.01 (q, 4H), 3.29 (d, 2H), 3.41 (t, 2H), 3.50-3.71 (br, 16H) 4.98 (m, 4H), 5.82 (m, 2H). ^{13}C NMR ($CDCl_3$): δ (ppm) 14.21, 22.78, 25.95, 26.92, 29.12, 29.33, 29.68, 29.79, 29.82, 30.26, 31.53, 31.87, 33.98, 38.31, 70.26, 70.57, 70.78, 70.81, 70.83, 71.71, 74.98, 114.25, 139.33. ESI/HRMS: $[M+NH4]^+$ calcd for $NH_4C_{38}H_{74}O_5$, 628.5875; found 628.5887. Anal. (CH) calcd for $C_{38}H_{74}O_5$: C, 74.70; H, 12.21. Found C, 74.84; H, 12.36.

2-(10-undecenyl)-12-tridecenyl-1-tetra (ethylene glycol) mono *n*-tetradecyl ether (99TEGOC$_{14}$, 4-3c).

Column Chromatography: 20% ethyl acetate 80% hexane eluent afforded .400g (34% yield) of colorless oil. ^{1}H NMR ($CDCl_3$): δ (ppm) 0.82 (t, 3H), 1.21-1.61 (br, 57H), 2.01 (q, 4H), 3.29 (d, 2H), 3.41 (t, 2H), 3.50-3.71 (br, 16H) 4.98 (m, 4H), 5.82 (m, 2H). ^{13}C NMR ($CDCl_3$): δ (ppm) 14.29, 22.88, 26.31, 27.03, 29.16, 29.36, 29.55, 29.71, 29.82, 29.85, 29.87, 30.29, 31.57, 32.13, 34.01, 38.35, 70.29, 70.60, 70.79, 70.84, 70.86, 71.75, 75.01, 114.27, 139.40. ESI/HRMS: $[M+NH4]^+$ calcd for $NH_4C_{38}H_{74}O_5$, 628.5875; found 628.5887. Anal. (CH) calcd for $C_{38}H_{74}O_5$: C, 74.70; H, 12.21. Found C, 74.84; H, 12.36.

General Procedure for ADMET Polymerizations

Monomers were dried under vacuum at 80 °C for 48 hours prior to polymerization and subsequently transferred to a 50 mL round-bottom flask equipped with a magnetic stir bar. Grubbs 1st generation catalyst (300:1 monomer:catalyst ratio) was added and the flask was stirred under vacuum at 45 °C for 4 days. Polymerizations were quenched with ethyl vinyl ether (5 drops in degassed toluene), precipitated into cold, acidic methanol to remove catalyst residue, and isolated as adhesive gums.

Polymerization of 2-(10-undecenyl)-12-tridecenyl-1-tetra (ethylene glycol) methenyl pyrene (TEGOPy21u, 4-4a).

^{1}H NMR ($CDCl_3$): δ (ppm) 1.21-1.52 (br, 33H), 2.01 (q, 4H), 3.29 (d, 2H), 3.50-3.75 (br, 12H) , 5.28 (s, 2H), 5.35 (m, 2H), 7.61-8.79 (m, 4H), 8.13-8.20 (m, 4H), 8.37 (d, 1H). ^{13}C NMR ($CDCl_3$): δ (ppm) 27.05, 27.46, 29.46, 29.35, 29.59, 29.78, 29.92, 30.02, 30.35, 31.57, 32.86, 38.33, 69.73, 70.54, 70.76, 70.83, 70.87, 70.95, 72.05, 74.96, 123.75, 124.64, 124.93, 125.13, , 125.33, 125.38, 126.10, 127.23, 127.57, 127.60, 127.84, 129.60, 130.08 (cis olefin), 130.53 (trans olefin), 131.03, 131.44, 131.47, 131.62. IR (ν cm-1) 2923, 2853, 1464, 1350, 1260, 1115, 967, 846, 802, 721. GPC (THF vs. Polystyrene standards): M_w = 80300 ; PDI (M_w/M_n) = 1.90

Polymerization of 2-(10-undecenyl)-12-tridecenyl-1-tetra (ethylene glycol) mono *n*-hexyl ether (TEGOHex21u, 4-4b).

^{1}H NMR ($CDCl_3$): δ (ppm) 0.82 (t, 3H), 1.21-1.61 (br, 41H), 2.01 (q, 4H), 3.29 (d, 2H), 3.41 (t, 2H), 3.50-3.71 (br, 16H), 5.35 (m, 2H). ^{13}C NMR ($CDCl_3$): δ (ppm) 14.26, 22.83, 25.99, 27.08, 29.49, 29.83, 29.97, 30.36, 31.61, 31.91, 32.87, 38.38, 70.29, 70.60, 70.86, 71.63, 75.06, 130.09(cis olefin), 130.55 (trans olefin). IR (ν cm-1) 2923, 2853, 1464, 1350, 1260, 1115, 967, 846, 802, 721. GPC (THF vs. Polystyrene standards): M_w = 84800 ; PDI (M_w/M_n) = 1.98

Polymerization of 2-(10-undecenyl)-12-tridecenyl-1-tetra (ethylene glycol) mono *n*-tetradecyl ether (TEGOC$_{14}$21u, 4-4c).

^{1}H NMR ($CDCl_3$): δ (ppm) 0.82 (t, 3H), 1.21-1.61 (br, 57H), 2.01 (q, 4H), 3.29 (d, 2H), 3.41 (t, 2H), 3.50-3.71 (br, 16H), 5.35 (m, 2H). ^{13}C NMR ($CDCl_3$): δ (ppm) 14.29, 22.88, 26.31, 27.03, 29.16, 29.36, 29.55, 29.71, 29.82, 29.85, 29.87, 30.29, 31.57, 32.13, 34.01, 38.35, 70.29, 70.61, 70.79, 70.84, 70.86, 71.76, 75.01, 130.08 (trans olefin), 130.54 (trans olefin). IR (ν cm-1) 2923, 2853, 1464, 1350, 1260, 1115, 967, 846, 802, 721. GPC (THF vs. Polystyrene standards): M_w = 61900 ; PDI (M_w/M_n) = 1.71

General Procedure for the Hydrogenation of Unsaturated Polymers

Unsaturated polymers were dissolved in dry *o*-xylene. *P*-toluenesulfonyl hydrazide (TSH) and tripropyl amine (TPA) were added with stirring (3 equiv each). The resulting solution was refluxed for 3-4 hours while monitoring nitrogen evolution with a bubbler. When gas evolution ceased, the solution was cooled to room temperature, an additional 3 equivalents of TSH and TPA were added, and the solution was refluxed for another 3 hours. The solutions were then concentrated to one-half of the original volume and precipitated into cold, acidic methanol. The polymers were isolated as elastic, adhesive gums.

TEGOPy21, (4-5a).

^{1}H NMR ($CDCl_3$): δ (ppm) 1.21-1.52 (br, 41H), 3.29 (d, 2H), 3.50-3.75 (br, 12H) , 5.28 (s, 2H), 7.61-8.79 (m, 4H), 8.13-8.20 (m, 4H), 8.37 (d, 1H). ^{13}C NMR ($CDCl_3$): δ (ppm) 27.05, 29.96, 30.02, 30.35, 31.59, 38.34, 69.76, 70.56, 70.78, 70.85, 70.87, 70.97, 72.05, 74.97, 123.75, 124.64, 124.95, 125.15, , 125.33, 125.38, 126.10, 127.23, 127.57, 127.61, 127.84, 129.60, 131.05, 131.44, 131.48, 131.66. IR (ν cm-1) 2923, 2853, 1464, 1350, 1260, 1115, 846, 802, 721. GPC (THF vs. Polystyrene standards): M_w = 60400 ; PDI (M_w/M_n) = 1.93

TEGOHex21 (4-5b).

^{1}H NMR ($CDCl_3$): δ (ppm) 0.82 (t, 3H), 1.21-1.61 (br, 49H), 3.29 (d, 2H), 3.41 (t, 2H), 3.50-3.71 (br, 16H). ^{13}C NMR ($CDCl_3$): δ (ppm) 14.28, 22.85, 25.99, 27.07, 29.83, 29.97, 30.38, 31.58, 31.93, 38.35, 70.29, 70.60, 70.84, 70.86, 71.77, 75.02. IR (ν cm-1) 2923, 2853, 1464, 1350, 1260, 1115, 846, 802, 721. GPC (THF vs. Polystyrene standards): M_w = 79200 ; PDI (M_w/M_n) = 1.78

TEGOC$_{14}$21 (4-5c).

^{1}H NMR ($CDCl_3$): δ (ppm) 0.82 (t, 3H), 1.21-1.61 (br, 65H), 3.29 (d, 2H), 3.41 (t, 2H), 3.50-3.71 (br, 16H), 5.35 (m, 2H). ^{13}C NMR ($CDCl_3$): δ (ppm) 14.29, 22.88, 26.31, 27.03, 29.55, 29.71, 29.82, 29.87, 29.97, 30.35, 31.60, 32.13, 38.38, 70.28, 70.61, 70.86, 71.76, 75.01. IR (ν cm-1) 2923, 2853, 1464, 1350, 1260, 1115, 846, 802, 721. GPC (THF vs. Polystyrene standards): M_w = 65800; PDI (M_w/M_n) = 1.76

Results and Discussion

Synthesis and Structural Analysis

Figure 4-1 describes the synthesis of these unique materials. First, diene alcohol 4-1 (prepared as previously described[17]) is attached to the PEG branch via Williamson etherification with tetra(ethylene glycol)di *p*-tosylate. Disubstitution is avoided using careful stoichiometry. The hydrophobic endgroup is then attached to 4-2 with a second Williamson by using the appropriate alcohol. This synthetic method is general and can potentially be applied to prepare an array of ADMET monomers and subsequent polymers having a variety of functional groups separated from the PE backbone by a PEG spacer. Monomers 4-3a-c are polymerized in the bulk at 45 °C under high vacuum using Grubbs' first generation catalyst to afford the unsaturated

ADMET polymers 4-4a-c. Subsequent hydrogenation with *p*-toluenesulfonyl hydrazide results in the final fully saturated polymers 4-5a-c.

For simplicity, a systematic nomenclature has been adopted for these monomers and polymers. Monomers are given the prefix "9,9" to indicate the number of methylene carbons between the branch and the olefin, followed by the identity of the pendant group (TEGO for tetra ethylene glycol and either Py, Hex, or C_{14} for pyrene, *n*-hexyl or *n*-tetradecyl). Polymers are named first for the identity of the pendant defect, followed by the branch frequency. Unsaturated polymers are denoted with the suffix "u." For example, monomer 4-3a is named "9,9TEGOPy," polymer 4-4a "TEGOPy21u," and polymer 4-5a "TEGOPy21."

The ^{1}H and ^{13}C NMR spectra for 9,9TEGOTs (4-2) are shown in Figure 4-2. In the proton spectrum the tosyl end group is clearly identified by the two doublets at 7.32 and 7.72 ppm, as well as the singlet at 2.45 ppm. The triplet at 4.16 ppm corresponds to the methylene protons adjacent to the tosyl group, shifted downfield from the overlapping glycol proton signals which appear from 3.55 to 3.61 ppm. The doublet at 3.30 ppm corresponds to the methylene protons separating the glycol moiety from the backbone. The allylic protons display a quartet at 2.03 ppm, the central methine carbon shows a multiplet at 1.56 ppm, and the characteristic terminal olefin peaks are seen at 4.91 and 5.80 ppm. Finally, the remaining methylene protons of the diene main chain overlap into a single broad peak at 1.26 ppm. In the carbon spectra for 99TEGOTs the resonances for the tosyl group are seen at 144.92, 133.33, 129.99, 128.18 ppm (aromatic carbons) and 21.83 ppm (methyl carbon). Terminal olefin signals appear at 114.28 and 139.43 ppm, the methylene carbon connecting the branch to the backbone appears at 75.01 ppm, and the glycol carbons overlap from 70.58 to 70.97 ppm. The glycol carbons closest to the tosyl group appear at 68.90 ppm, the central methine carbon is at 38.32 ppm, and the allylic carbons

are at 34.01 ppm. The remaining resonances for the internal methylene carbons appear from 27 to 32 ppm and are all individually resolved. This highlights the need for thorough ^{13}C analysis in the ADMET synthesis of precise polyolefins, because simply investigating the ^{1}H spectra can lead to ambiguities due to overlapping resonances.

The ^{1}H and ^{13}C NMR spectra of 9,9TEGOPy (4-3a) are shown in Figure 4-3. In the proton spectrum the aromatic pyrene protons appear from 8.02 to 8.43 ppm. The methylene protons between the pyrene and glycol branch appear as a singlet at 5.30 ppm. The resonances for the glycol region, terminal olefin, allylic, and aliphatic protons remain mostly unchanged compared to the ^{1}H spectrum of 9,9TEGOTs. The case is similar for the carbon spectrum of 9,9TEGOPy. The aromatic pyrene carbons appear from 123.74 to 131.61 ppm, and the methylene carbon between the pyrene and glycol moieties is seen at 72.04 ppm. As in the proton spectrum, the terminal olefin, allylic, and aliphatic carbons remain mostly unchanged compared to the carbon spectrum of 9,9TEGOTs.

Figures 4-4 and 4-5 show the ^{1}H and ^{13}C NMR spectra of 9,9TEGOHex (4-3b) and 9,9TEGOC_{14} (4-3c), respectively. In the proton spectra the n-hexyl and n-tetradecyl methyl end groups appear at 0.87 ppm, and the methylene protons adjacent to the glycol portion of the branch appear as triplets at 3.44 ppm. The rest of the *n*-hexyl protons overlap with the internal methylene protons of the diene main chain. The remaining resonances are unchanged as described in the previous example. The carbon spectra for these monomers are nearly identical except for the aliphatic regions, which are complicated by the overlapping diene main chain and aliphatic branch carbon resonances.

An expanded view of the aliphatic regions in the ^{13}C NMR spectra of 9,9TEGOHex, 9,9TEGOC_{14}, and 9,9TEGOPy is shown in Figure 4-6. Comparing 9,9TEGOPy to the two

monomers with aliphatic branch end groups allows the resonances for the diene main chain to be separated from the aliphatic end group resonances. Still, particularly in the case of 9,9TEGOC$_{14}$, the number of overlapping resonances greatly complicates the interpretation of this region.

The progression from diene monomer through unsaturated polymer, to saturated polymer (monitored by ^{1}H and ^{13}C NMR) is shown in Figure 4-7 for 9,9TEGOC$_{14}$ (4-3c) through TEGOC$_{14}$21 (4-5c) (arbitrarily chosen as an example). Polymerization to 4-4c results in convergence of the terminal olefin signals in the monomer spectrum to a single peak for internal olefin seen in both the ^{1}H and ^{13}C spectra. Hydrogenation results in the complete elimination of any olefin signal in either the proton or the carbon spectra. The appearance of only the resonances predicted by the fundamental repeat unit confirm the absence of side reactions and structural irregularities, again highlighting the effectiveness of ADMET chemistry in the synthesis of pristine, highly regular polymer structures. Molecular weight data (GPC in THF vs. polystyrene standards) are displayed in Table 4-1.

Thermal Analysis

The DSC data for the new polymers are presented in Table 4-2. The polymers exhibit remarkably different thermal behavior, a clear indication that changing the graft end group moiety has significant effects on the morphology of these systems. The difference in behavior between the saturated and unsaturated polymers is also significant, emphasizing the role of the PE backbone on the crystallization in these materials.

The DSC profiles for TEGOPy21 and TEGOPy21u are shown in Figure 4-8. The heating and cooling curves show that the saturation of the backbone allows for crystallization to occur, while the unsaturated polymer remains completely amorphous. This is clear evidence that the pendant defect is not involved in the crystallization and therefore must be excluded from the crystal. The T_g of the saturated polymer is also slightly increased compared to the unsaturated

analogue, an indication that segmented motion of the grafts is restricted by the crystallinity. The completely amorphous behavior of TEGOPy21u is an interesting result, considering that previous reported unsaturated ADMET polymers with the same distribution of pendant functionality are semi crystalline.[9-11] The lack of crystallinity in TEGOPy21u, as well as the significantly depressed melting point for the saturated analogue compared to our previous ADMET amphiphilic copolymers[15] is a result of pyrene aggregation impeding segmental motion as well as backbone crystallization. This is confirmed by pyrene excimer formation seen in the fluorescence spectra for both the unsaturated and saturated polymers (Figure 4-9).

The DSC curves for TEGOHex21 and TEGOHex21u are shown in Figure 4-10. The difference in behavior between the saturated and unsaturated polymers is especially interesting in this pair. The unsaturated polymer is semicrystalline with a melting endotherm at -13 °C. There is significant amorphous content to this material as well, indicated by the distinct T_g at -76 °C. The heating and cooling profiles are typical for unsaturated ADMET polymers. The thermal behavior of the saturated analogue is completely different, however. A single, bimodal crystallization at -4ºC is witnessed on cooling. Upon heating a small exotherm is barely observed at -91 °C, followed by a bimodal melting endotherm with peaks at -48 °C and -37 °C. A second bimodal melting endotherm occurs with peaks at 4 °C and 11 °C.

The complex behavior of TEGOHex21 was further investigated by MDSC, which provides increased sensitivity compared to traditional DSC and allows for resolution of overlapping transitions.[51, 60-62] The MDSC heating traces are shown in Figure 4-11. In the nonreversing and total heat flow signals the cold crystallization event, barely perceptible in Figure 4-10, is clearly visible. This is followed by the first bimodal melting endotherm, which is observed in all three signals. In the nonreversing signal this transition is first exothermic, then endothermic, indicating

that the bimodal melt is actually the result of a melting and concurrent crystallization mechanism.[60] The same is true for the higher temperature bimodal endotherm; clear exothermic activity in both the total and nonreversing signals indicates melting and simultaneous crystallization. Because the melting enthalpy of this higher temperature peak (21 J/g) matches the enthalpy of crystallization (21 J/g), and also because its metling temperature and enthalpy (4ºC and 27 J/g) are in good agreement with those of TEGOPy21 (9ºC and 24 J/g), it can be concluded that this behavior is a result of crystallization of the backbone excluding the pendant branch. The backbone crystallizes during cooling. Then during subsequent heating, the excluded branches gain sufficient mobility to self crystallize, noted by the exotherm at -100ºC. The pendant crystals then melt at about -50ºC, followed by the melting of the backbone crystals.

The thermal behavior of TEGOC$_{14}$21u and TEGOC$_{14}$21 (Figure 4-12) differs significantly from the previous two examples. Both polymers exhibit extremely sharp melting transitions at temperatures much higher than the other polymers in this family. This deviates from the well known trend for ADMET polymers, which show a decrease in T_m and ΔH_m as the defect size increases. For TEGOC$_{14}$21u and TEGOC$_{14}$21, the increase in pendant group length results in marked increases in both melting temperature and enthalpy. Further, no T_g is observed in either the saturated or unsaturated analogues, indicating greatly reduced amorphous content for these polymers. Thus, the long alkyl chains must also be crystallizing. Since there is only one melting peak the C$_{14}$ chain must be long enough to extend back into the crystallizing PE backbone, forming a single crystallized region.

Conclusions

The synthesis of polyethylene with precise placement of amphiphilic grafts has been achieved. These polymers feature PEG grafts attached to the polyolefin backbone with different hydrophobic groups affixed to the end of the PEG chains. These structural differences induce

significant changes in the thermal behavior of the corresponding materials. When the graft end group is a pyrene moiety, the polyolefin backbone crystallizes excluding the pendant branch. When the end group is changed to an *n*-hexyl chain, the branches and the backbone crystallize separately, forming two different crystalline regions. Extending this end group from an n-hexyl to an *n*-tetradecyl chain allows the branches and backbone to crystallize together, resulting in the inclusion of the branch within the PE crystal. This material breaks the well known trend for ADMET polymers, which show a decrease in T_m and ΔH_m as the defect size increases. Most importantly we have demonstrated that a pendant group can be intentionally excluded from the crystallized polyethylene backbone and induced to self interact. This displays the promise such architectures could have in advanced applications such as membrane technologies or polymer electrolytes.

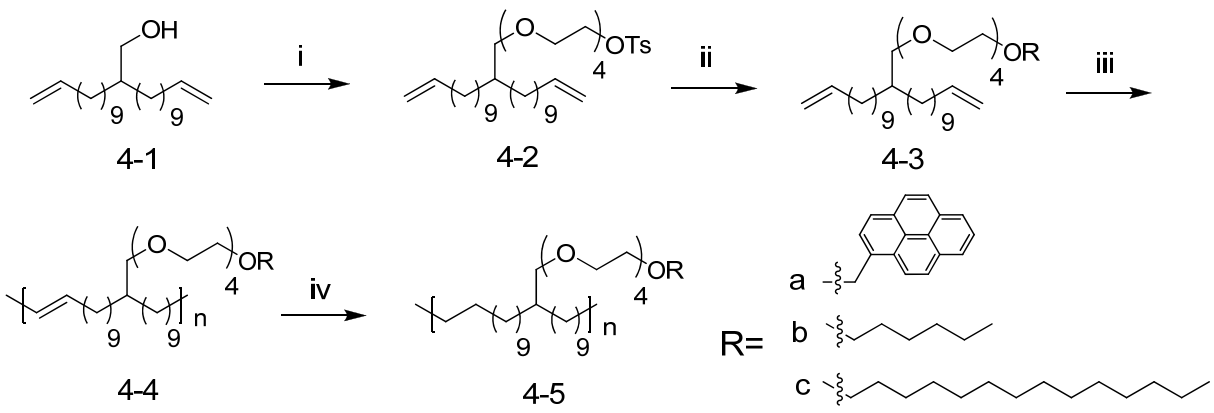

Figure 4-1: Synthesis of polyethylene with precisely placed amphiphilic branches. i: NaH, tetra(ethylene glycol)di-*p*-tosylate, DMF; ii: NaH, ROH, DMF; iii: Grubbs' 1st generation catalyst, 45 °C, vacuum; iv: TSH, TPA, *o*-xylene, 140 °C.

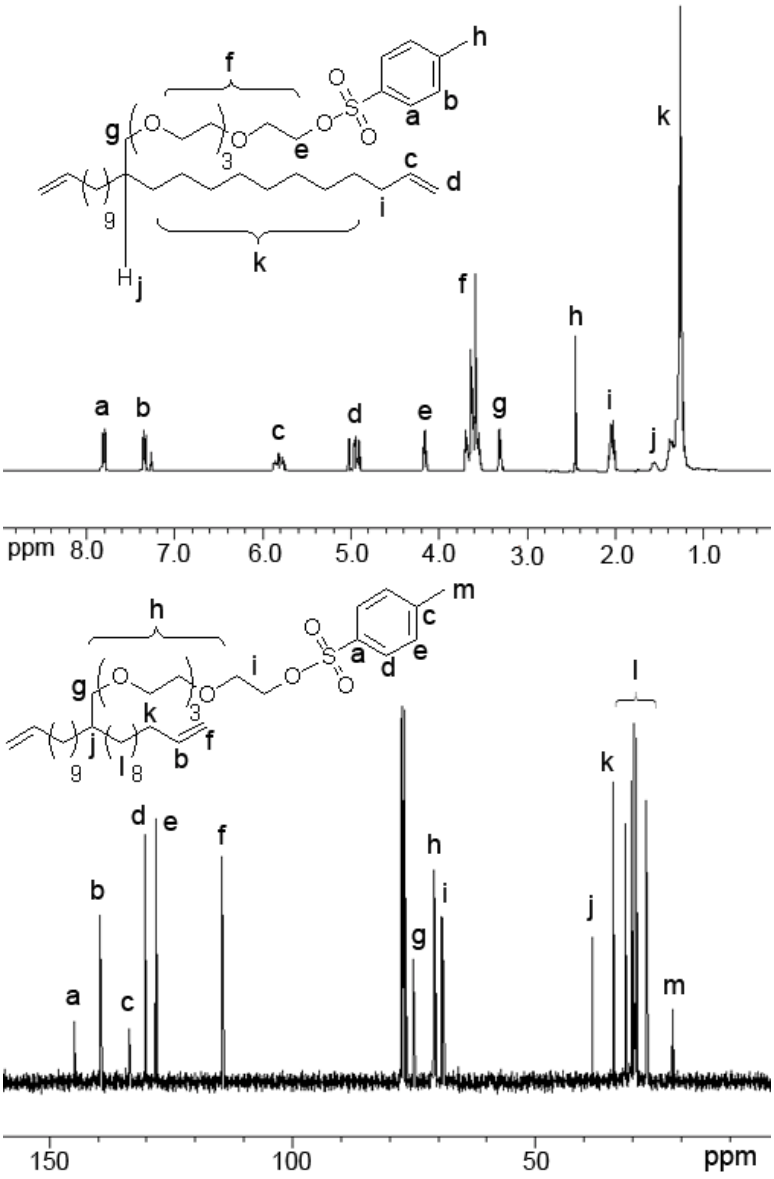

Figure 4-2: ^{1}H and ^{13}C NMR spectra of 9,9TEGOTs (4-2).

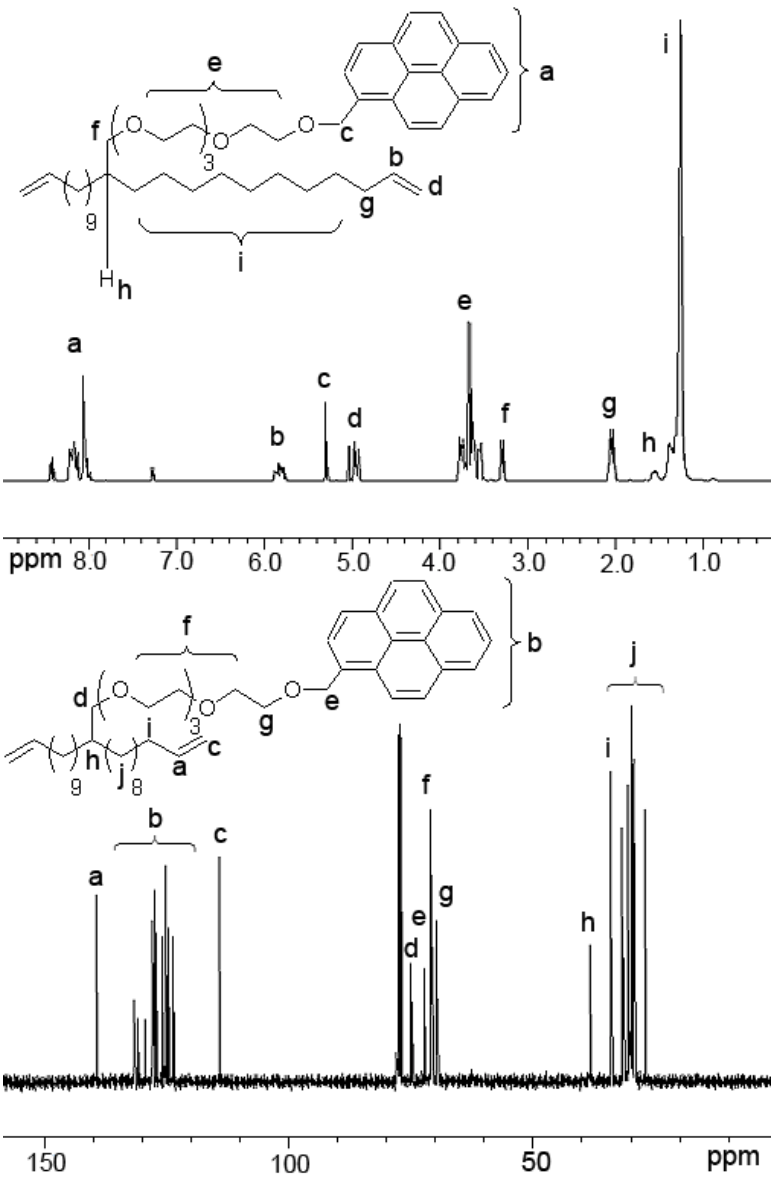

Figure 4-3: ^{1}H and ^{13}C NMR spectra of 9,9TEGOPy (4-3a).

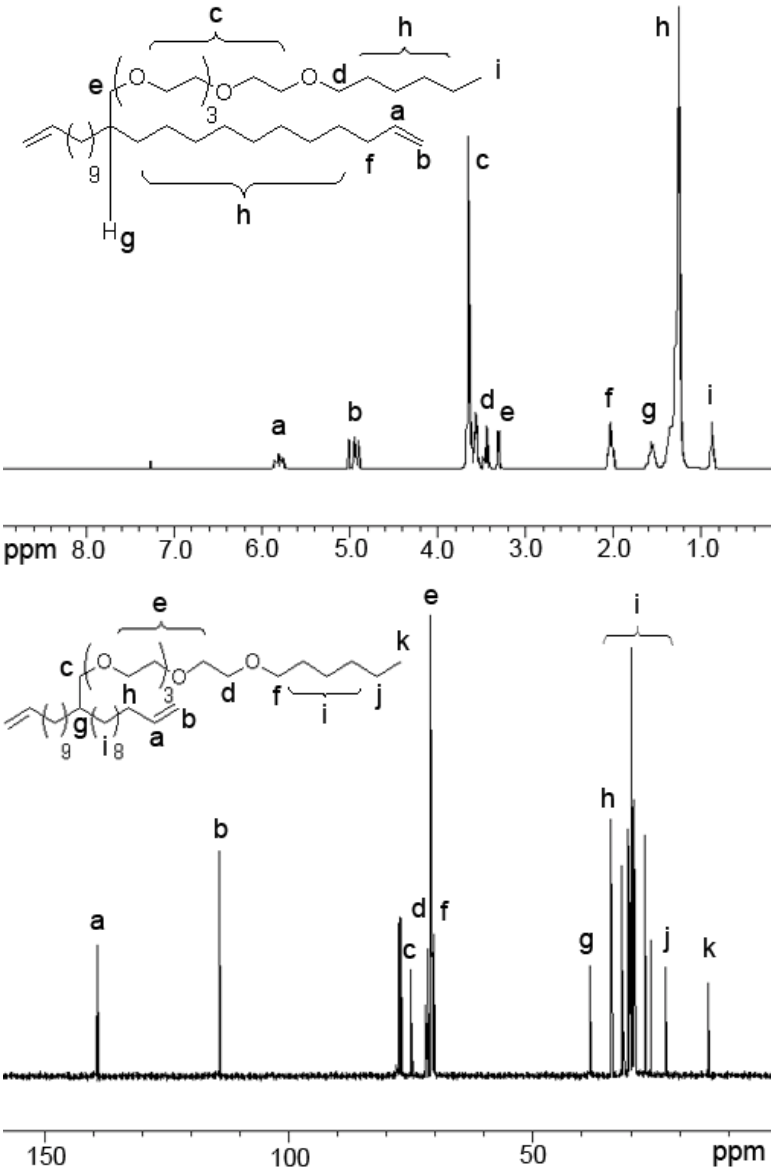

Figure 4-4: ^{1}H and ^{13}C NMR spectra of 9,9TEGOHex (4-3b).

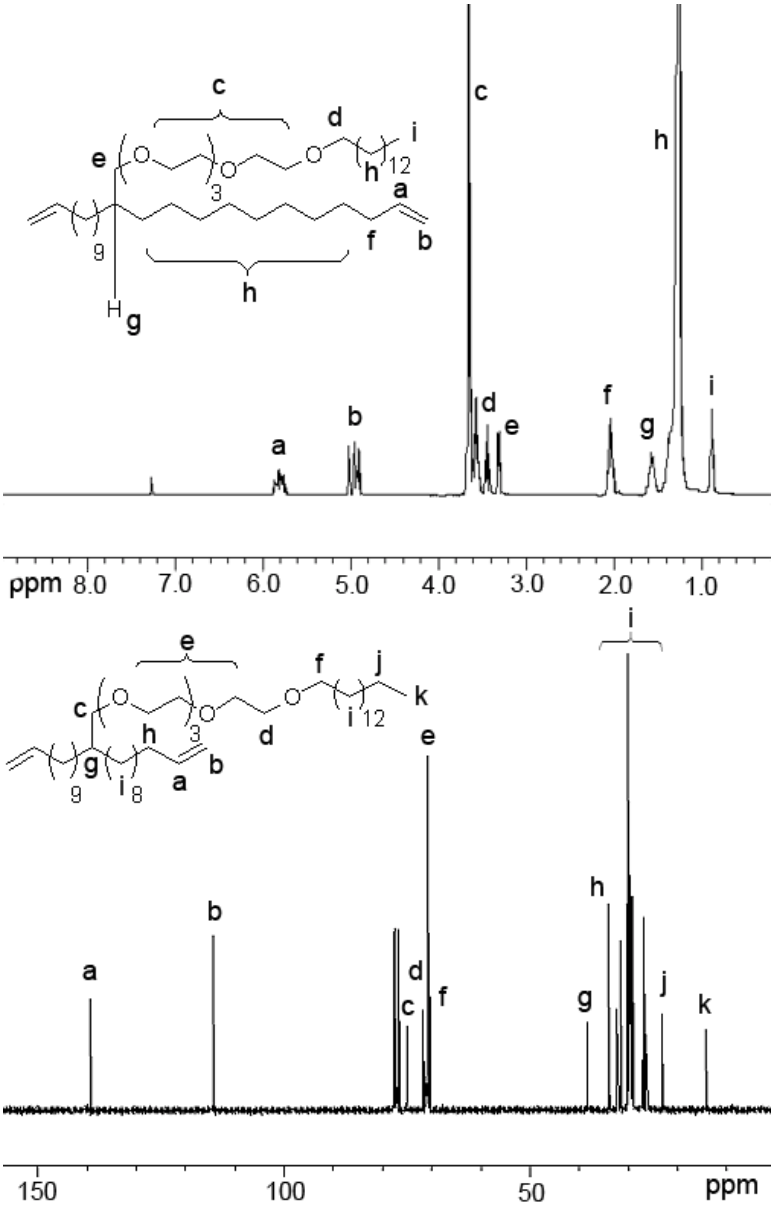

Figure 4-5: ^{1}H and ^{13}C NMR spectra of 9,9TEGOC14 (4-3c).

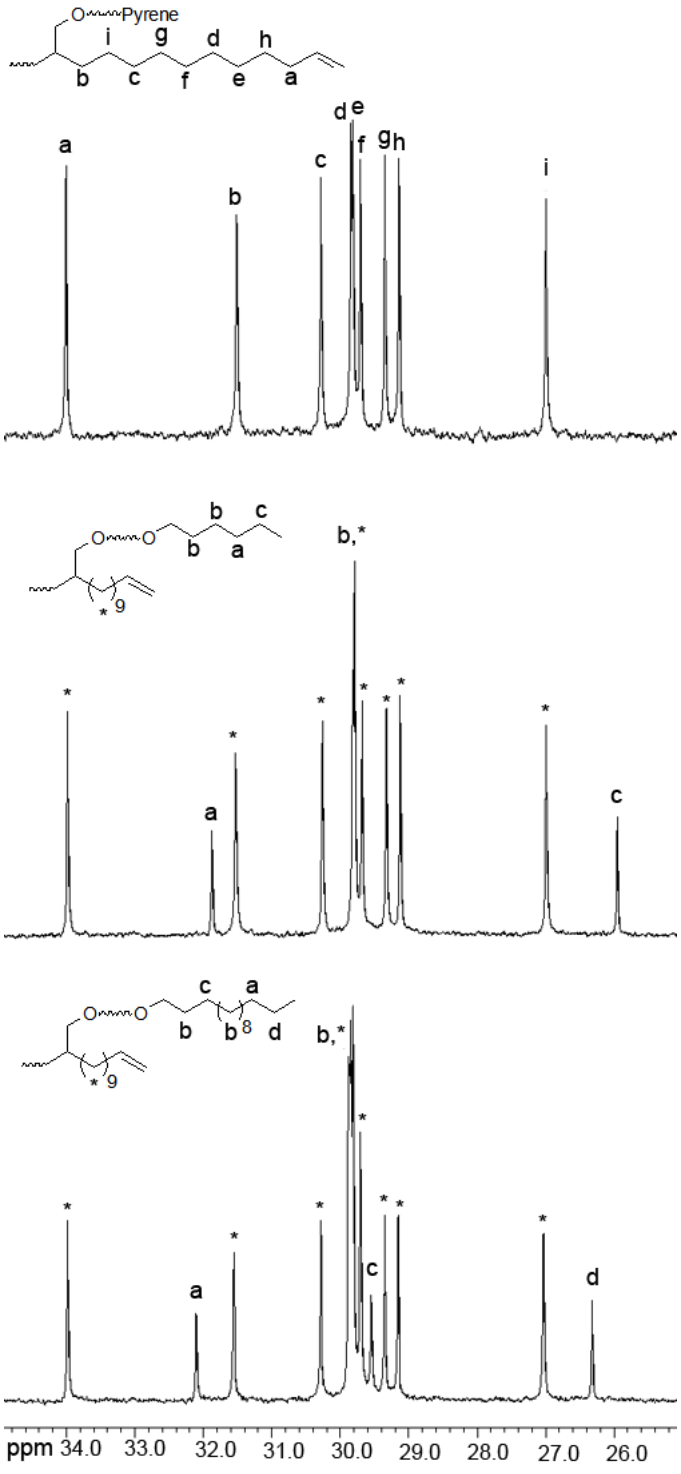

Figure 4-6: Expansion of the aliphatic regions of the ^{13}C spectra of 9,9TEGOPy, 9,9TEGOHex, and 9,9TEGOC_{14} (3a-c).

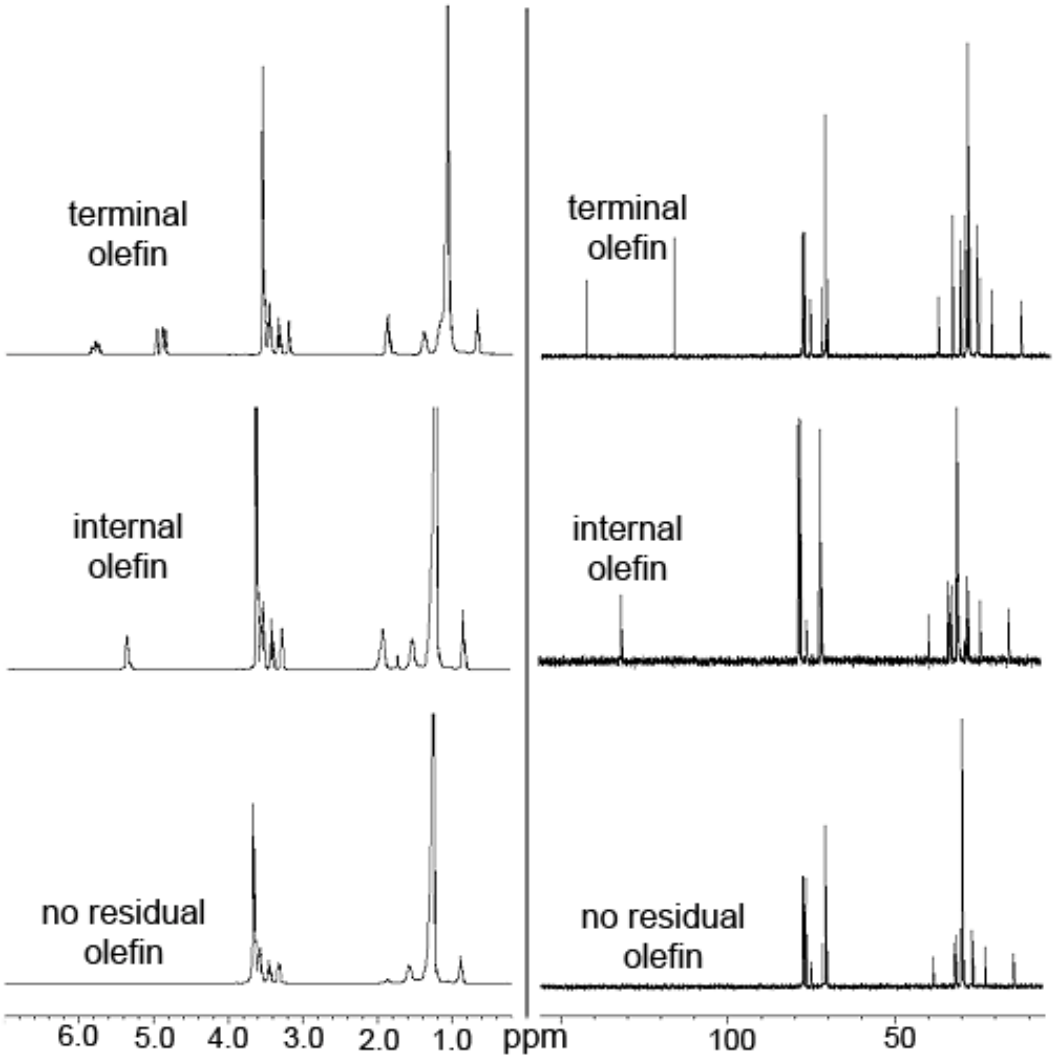

Figure 4-7: Progression from monomer 4-3c to saturated polymer 4-5c monitored by NMR.

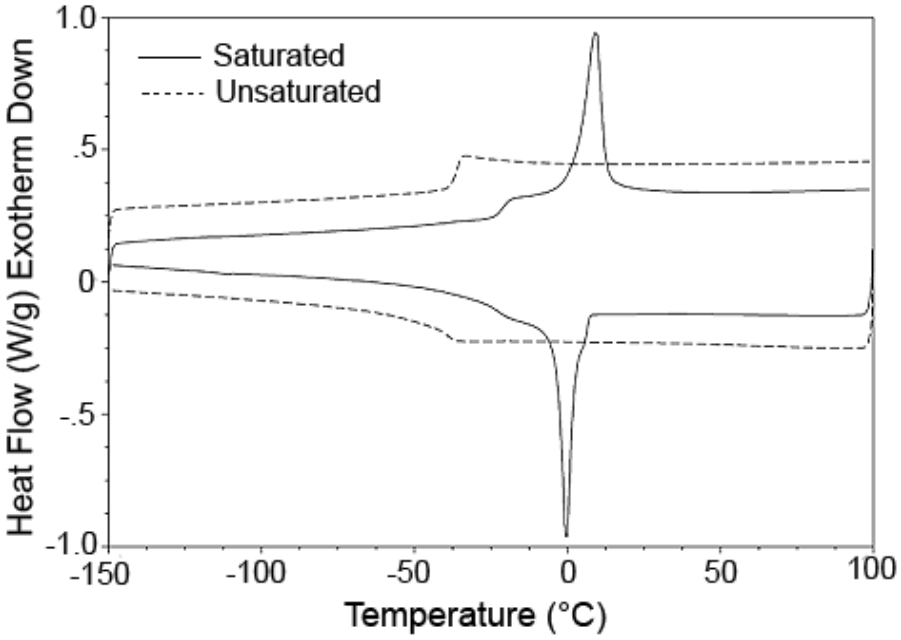

Figure 4-8: DSC heating and cooling traces for TEGOPy21u (4-4a) and TEGOPy21 (4-5a).

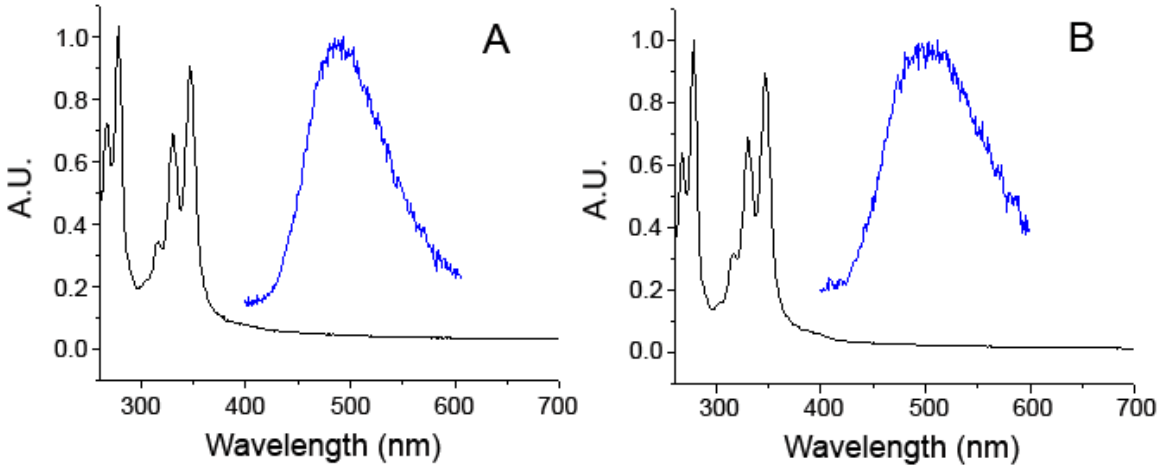

Figure 4-9: Absorption and fluorescence spectra for TEGOPy21 A) and TEGOPy21u B)

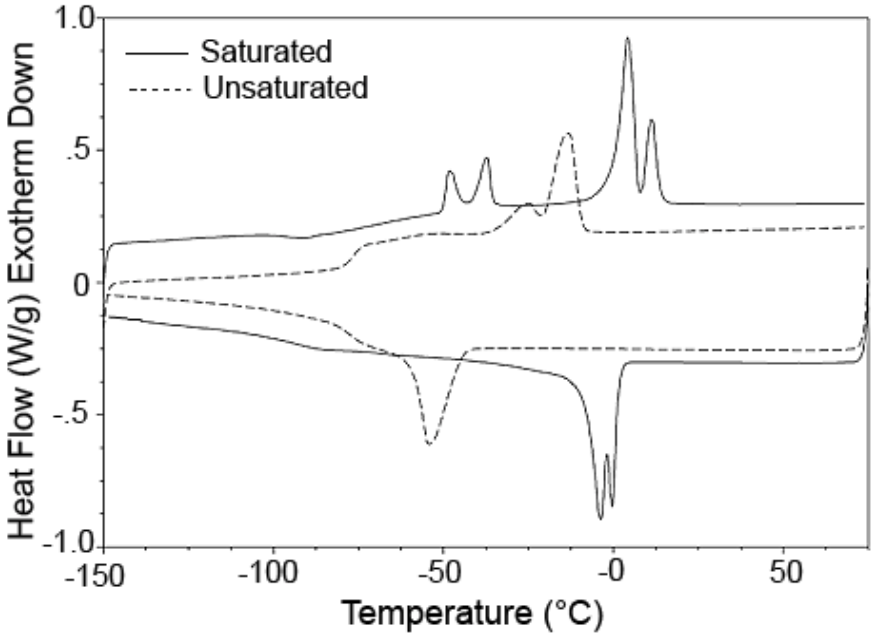

Figure 4-10: DSC heating and cooling traces for TEGOHex21u (4-4b) and TEGOHex21 (4-5b).

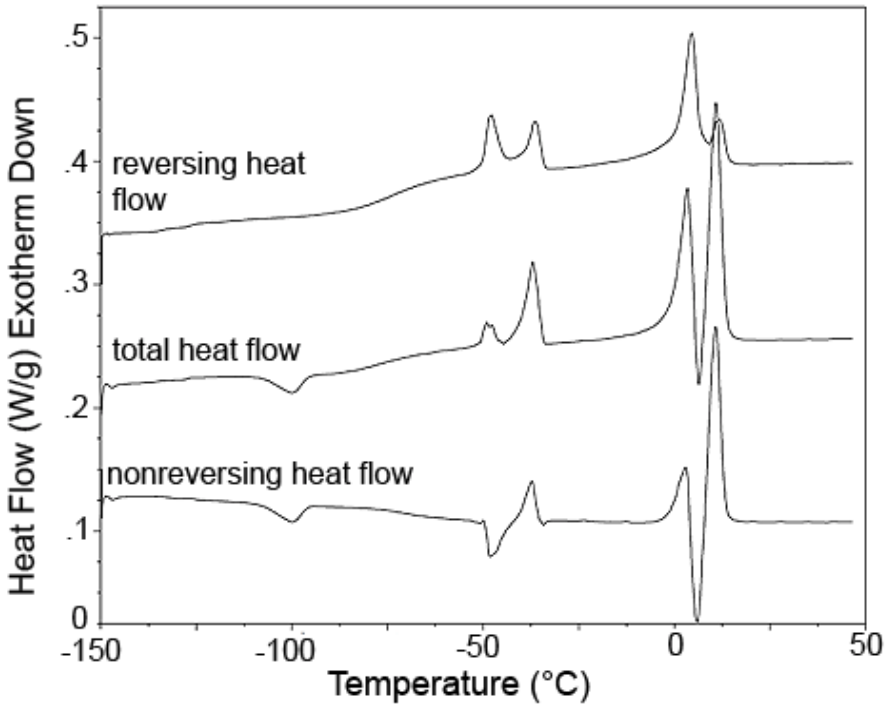

Figure 4-11: MDSC heating traces for TEGOHex21 (4-5b).

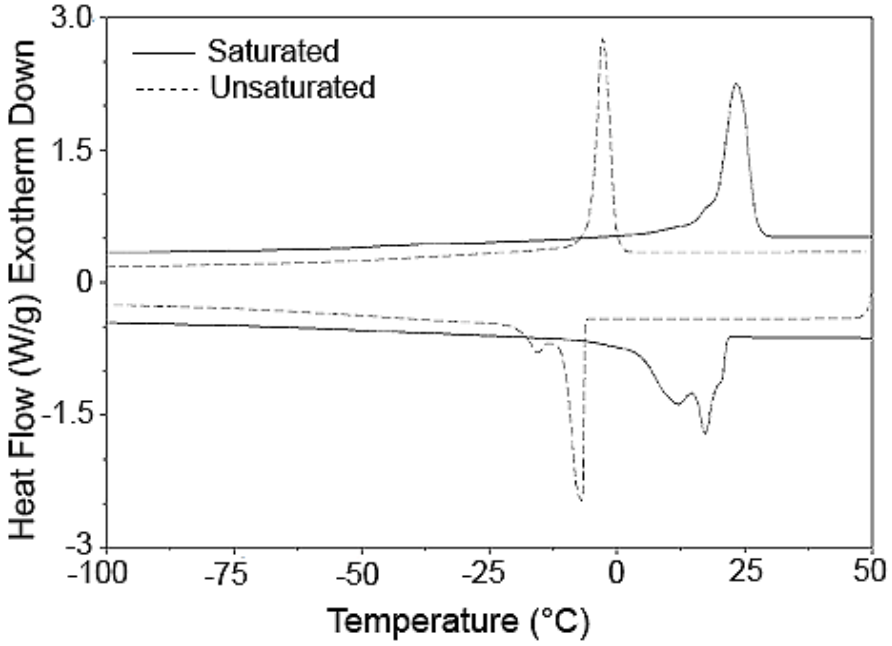

Figure 4-12: DSC heating and cooling traces for $TEGOC_{14}21u$ (4-4c) and $TEGOC_{14}21$ (4-5c).

Table 4-1: Molecular weight data for polymers described in chapter 4.

Polymer	M_n[a] (kg/mol)	M_w[a] (kg/mol)	PDI[b]
TEGOPy21u (4a)	42.2	80.3	1.9
TEGOPy21 (5a)	31.2	60.4	1.93
TEGOHex21u (4b)	42.8	84.8	1.98
TEGOHex21 (5b)	44.4	79.2	1.78
$TEGOC_{14}21u$ (4c)	36.2	61.9	1.71
$TEGOC_{14}21$ (5c)	37.3	65.8	1.76

[a] GPC vs. polystyrene standards; [b] M_w/M_n

Table 4-2: DSC data for polymers described in chapter 4.

Polymer	T_g (°C)	ΔC_p (J/g·°C)	T_m (°C)	ΔH_m (J/g)	T_c (°C)	ΔH_c (J/g)
TEGOPy21u	-36	0.76	n/a	n/a	n/a	n/a
TEGOPy21	-21	0.36	9	24	-12	25
TEGOHex21u	-76	0.49	-13	21	-54	21
TEGOHex21	n/a	n/a	-37, 4	8, 27	-4	28
$TEGOC_{14}21u$	n/a	n/a	-3	50	-7	51
$TEGOC_{14}21$	n/a	n/a	23	71	17	72

CHAPTER 5
SYNTHESIS OF DEUTERIUM LABELED ADMET AMPHIPHILES

Introduction

This dissertation explores the effects that altering various parameters have on the overall response in a family of materials with related structures. Chapter 2 outlines the basics of this study where altering the distribution of the hydrophilic branch as well as the identity of the branch end group could affect the ability of the polymer backbone to crystallize. This is further explored in chapter 3 by examining the effect the length of the graft and the manner of its connection to the backbone has on thermal behavior while keeping the graft end group constant. Chapter 3 also showed that the saturation of the internal olefin influenced thermal behavior: when the site of unstauration remains the polymers ability of to crystallize is greatly hindered or suppressed completely. By considering these data we are able to constructe a model for the manner in which the chains fold to allow the crystallization of the backbone and the exclusion of the pendant branch. This chapter briefly describes the synthesis of deuterium labeled polymers based on TEGOMe21 (structure 3-8b, presented in chapter 3). Solid state ^{2}H NMR has been utilized in the past to gain information on polymer molecular motions and dynamics.[73-77] Since TEGOMe21 presents both a well defined glass transition and melting endotherm it is an excellent candidate for deuterium labeling and subsequent solid state ^{2}H NMR motion studies on the crystalline and amorphous regions of the polymer. Three labeled TEGOMe21analogues are presented in this chapter. The backbone (midway between defects), the point of branch connection, and the branch end group were chosen as labeling points since the previous chapters have proven these locations are critical in the thermal behavior of these materials (Figure 5-1). Only the synthesis of these polymers is discussed here, the solid state NMR experiments are beyond the scope of this dissertation.

Experimental Section

Instrumentation

All ^{1}H NMR (300 MHz) and ^{13}C NMR (75 MHz) spectra were recorded on a Varian Associates Mercury 300 spectrometer. Chemical shifts for ^{1}H and ^{13}C NMR were referenced to residual signals from $CDCl_3$ (^{1}H: δ= 7.27 ppm and ^{13}C: δ = 77.23 ppm) with 0.03% v/v TMS as an internal reference. Thin layer chromatography (TLC) was performed on EMD silica gel coated (250 μm thickness) glass plates. Developed TLC plates were stained with iodine adsorbed on silica to produce a visible signature. Reaction conversions and relative purity of crude products were monitored by TLC and ^{1}H NMR. Fourier transform infrared (FT-IR) measurements were conducted with a Bruker Vector 22 Infrared Spectrophotometer using polymer films cast from chloroform onto KBr plates. High resolution mass spectrometry analyses were performed on a Bruker APEX II 4.7 T Fourier Transform Ion Cyclotron Resonance mass spectrometer (Bruker Daltonics, Billerica, MA) using electrospray ionization (ESI). Elemental analysis was carried out at Atlantic Microlab Inc. (Norcross, GA).

Molecular weights and molecular weight distributions (M_w/M_n) were determined by gel permeation chromatography (GPC) using a Waters Associates GPCV2000 liquid chromatography system with an internal differential refractive index detector (DRI) and two Waters Styragel HR-5E columns (10 micron particle diameter, 7.8 mm ID, 300 mm length) at 40 °C. The mobile phase was HPLC grade tetrahydrofuran at a flow rate of 1.0 mL/minute. Retention times were calibrated versus polystyrene standards (Polymer Laboratories; Amherst, MA).

Differential scanning calorimetry (DSC) and temperature modulated differential scanning calorimetry (MDSC) were performed on a TA Instruments Q1000 equipped with a liquid

nitrogen cooling accessory and calibrated using sapphire and high purity indium metal. All samples were prepared in hermetically sealed aluminum pans (4-7 mg/sample) and were referenced to an empty pan. Samples were run under a purge of helium gas. Scan rates of 10ºC/min and 3ºC/min were used for DSC and MDSC, respectively. Melting temperatures were evaluated as the peak of the melting transition and glass transition temperatures as the mid-point of a step change in heat capacity.

Materials.

Unless otherwise stated, all reagents were purchased from Aldrich and used without further purification. Grubbs' 1st generation catalyst was a gift from Materia, Inc. Oligoethoxy-*p*-tosylates[59] and diene acid 5-4[49] were prepared according to the literature. 99TEGOMe (3-4b) and 99TEGOTs (4-2) were synthesized as described in chapters 3 and 4 of this dissertation, respectively. 99CD_2OH (5-4) was prepared as described in the PhD dissertation of John Sworen.[76] TEGOMe21u (3-6b) was obtained from the polymerization of 99TEGOMe as described in chapter 3 of this dissertation.

Synthesis of 99CD_2TEGOMe (5-5).

Anhydrous DMF (40 mL) was cannula transferred into an oven dried, 3-neck round-bottom flask equipped with a magnetic stirrer and gas inlet, and was charged with 2 equivalents of sodium hydride (60% dispersion in mineral oil). The slurry was cooled to 0°C and 2g (5.6 mmol) of 5-4 in 20 mL of anhydrous DMF was added via syringe. When gas evolution (monitored by bubbler) ceased, 2.94g (8.1 mmol) of tetraethylene glycol monomethylether *p*-toluenesulfonate in 20 mL of anhydrous DMF was added via syringe. The reaction was stirred for 17 hours at 0 °C and quenched by pouring into 300 mL of water. The resulting mixture was extracted with diethyl ether and the combined organics washed with brine. Concentration afforded a yellow oil which was further purified by column chromatography. 25% ethyl acetate

75% hexane eluent afforded .710g (23% yield) of colorless oil. ^{1}H NMR ($CDCl_3$): δ (ppm) 1.21-1.52 (br, 33H), 2.01 (q, 4H), 3.35 (s, 3H), 3.50-3.75 (br, 16H) 4.98 (m, 4H), 5.82 (m, 2H). ^{2}H NMR ($CDCl_3$): δ (ppm) 3.30 ^{13}C NMR ($CDCl_3$): δ (ppm) 26.92, 29.06, 29.27, 29.63, 29.73, 29.76, 30.20, 31.45, 33.94,38.22, 59.13, 70.50, 70.64, 70.71, 70.75, 72.07, 114.21, 139.29 ESI/HRMS: $[M+H]^+$ calcd for $H^+C_{33}H_{62}D_2O_5$, 543.4592; found 543.4933. Anal. (CH) calcd for $C_{33}H_{64}O_5$: C, 73.01; H or D, 12.25. Found C, 72.94; H, 11.83.

Synthesis of 99TEGOCD$_3$ (5-2)

Anhydrous DMF (40 mL) was cannula transferred into an oven dried, 3-neck round-bottom flask equipped with a magnetic stirrer and gas inlet, and was charged with 2 equivalents of sodium hydride (60% dispersion in mineral oil). The slurry was cooled to 0°C and .270g (7.5 mmol) of deuterated methanol was added via syringe. When gas evolution (monitored by bubbler) ceased, 1g (1.5 mmol) of 99TEGOTs (4-2) in 20 mL of anhydrous DMF was added via syringe. The reaction was stirred for 17 hours at 0 °C and quenched by pouring into 300 mL of water. The resulting mixture was extracted with diethyl ether and the combined organics washed with brine. Concentration afforded a yellow oil which was further purified by column chromatography. 25% ethyl acetate 75% hexane eluent afforded .300g (36% yield) of colorless oil. 1H NMR (CDCl3): δ (ppm) 1.21-1.52 (br, 33H), 2.01 (q, 4H), 3.29 (d, 2H), 3.50-3.75 (br, 16H) 4.98 (m, 4H), 5.82 (m, 2H). ^{2}H NMR ($CDCl_3$): δ (ppm) 3.38 ^{13}C NMR (CDCl3): δ (ppm) 26.92, 29.06, 29.27, 29.63, 29.73, 29.76, 30.20, 31.45, 33.94,38.22, 70.50, 70.64, 70.71, 70.75, 72.07, 74.88, 114.21, 139.29 ESI/HRMS: [M+H]+ calcd for H^+C33H64O5, 544.5015; found 544.4998. Anal. (CH) calcd for C33H61D3O5: C, 72.88; H or D, 12.42. Found C, 72.66; H or D, 11.86

General Procedure for ADMET Polymerizations

Monomers were dried under vacuum at 80 °C for 48 hours prior to polymerization and subsequently transferred to a 50 mL round-bottom flask equipped with a magnetic stir bar. Grubbs 1st generation catalyst (300:1 monomer:catalyst ratio) was added and the flask was stirred under vacuum at 45 °C for 4 days. Polymerizations were quenched with ethyl vinyl ether (5 drops in degassed toluene), precipitated into cold, acidic methanol to remove catalyst residue, and isolated as an adhesive gum.

CD_2TEGOMe21u.

^{1}H NMR (CDCl3): δ (ppm) 1.21-1.52 (br, 33H), 2.01 (q, 4H), 3.35 (s, 3H), 3.50-3.75 (br, 16H), 5.35 (m, 2H). 13C NMR (CDCl3): δ (ppm) 27.03, 29.45, 29.76, 29.81, 29.90, 30.00, 30.32, 31.54, 32.83, 38.30, 59.22, 70.55, 70.71, 70.76, 70.80, 72.12, 130.05 (cis olefin), 130.52 (trans olefin). IR (ν cm-1) 2923, 2853, 1464, 1350, 1115, 967, 886, 721. GPC (THF vs. Polystyrene standards): Mw = 63800 ; PDI (Mw/Mn) = 1.66

TEGO$CD_3$21u.

^{1}H NMR ($CDCl_3$): δ (ppm) 1.21-1.52 (br, 33H), 2.01 (q, 4H), 3.29 (d, 2H), 3.50-3.75 (br, 16H), 5.35 (m, 2H). ^{13}C NMR ($CDCl_3$): δ (ppm) 27.03, 29.45, 29.76, 29.81, 29.90, 30.00, 30.32, 31.54, 32.83, 38.30, 70.55, 70.71, 70.76, 70.80, 72.12, 74.96, 130.05 (cis olefin), 130.52 (trans olefin). IR (ν cm-1) 2923, 2853, 1464, 1350, 1115, 967, 886, 721. GPC (THF vs. Polystyrene standards): M_w = 88700 ; PDI (M_w/M_n) = 1.64

General Procedure for the TSH Hydrogenation of Unsaturated Polymers

Unsaturated polymers were dissolved in dry *o*-xylene. *p*-toluenesulfonyl hydrazide (TSH) and tripropyl amine (TPA) were added with stirring (3 equivalents each). The resulting solution was refluxed for 3-4 hours while monitoring nitrogen evolution with a bubbler. When gas

evolution ceased, the solution was cooled to room temperature, an additional 3 equivalents of TSH and TPA were added, and the solution was refluxed for another 3 hours. The solutions were then concentrated to one-half of the original volume and precipitated into cold, acidic methanol. The polymers were isolated as elastic, adhesive gums.

CD_2TEGOMe21 (5-7).

^{1}H NMR ($CDCl_3$): δ (ppm) 1.21-1.52 (br, 41H), 3.35 (s, 3H), 3.50-3.75 (br, 16H). ^{13}C NMR ($CDCl_3$): δ (ppm) 27.08, 29.98, 30.37, 31.36, 38.37, 59.25, 70.61, 70.76, 70.83, 70.86, 72.18, IR (ν cm-1) 2923, 2853, 1464, 1350, 1115, 886, 721. GPC (THF vs. Polystyrene standards): M_w = 77700 ; PDI (M_w/M_n) = 1.70

TEGO$CD_3$21 (5-3).

^{1}H NMR ($CDCl_3$): δ (ppm) 1.21-1.52 (br, 41H), 3.29 (d, 2H), 3.50-3.75 (br, 16H). ^{13}C NMR ($CDCl_3$): δ (ppm) 27.08, 29.98, 30.37, 31.36, 38.37, 70.61, 70.76, 70.83, 70.86, 72.18, 75.03. IR (ν cm-1) 2923, 2853, 1464, 1350, 1115, 886, 721. GPC (THF vs. Polystyrene standards): M_w = 107500 ; PDI (M_w/M_n) = 1.66

Parr Bomb "Deuteration" of TEGOMe21d (5-1).

Unsaturated, trityl protected polymer TEGOMe21u was dissolved in toluene and added to a glass lined Parr bomb. Wilkinson's catalyst was added and the bomb charged with 700 psi of D_2. The reaction was stirred for 3 days at room temperature. The resulting polymers were purified by precipitation into acidic methanol to remove catalyst residue and isolated as an adhesive gum. ^{1}H NMR ($CDCl_3$): δ (ppm) 1.21-1.52 (br, 39H), 3.29 (d, 2H), 3.35 (s, 3H), 3.50-3.75 (br, 16H). ^{13}C NMR ($CDCl_3$): δ (ppm) 27.08, 29.98, 30.37, 31.36, 38.37, 59.25, 70.61, 70.76, 70.83, 70.86, 72.18, 75.03. IR (ν cm-1) 2923, 2853, 1464, 1350, 1115, 886, 721. GPC (THF vs. Polystyrene standards): M_w = 81700 ; PDI (M_w/M_n) = 1.70

Results and Discussion

Synthesis and Structural Analysis

Figure 5-2 illustrates the synthesis of the deuterium labeled TEGOMe21 analogues. To label the backbone TEGOMe21u (3-6b, prepared as described in chapter 3) was simply saturated with deuterium gas using the parr bomb hydrogenation procedure found in chapter 2. Labeling the branch's methyl end group and the branch connection point were slightly more complicated. To label the branch end group 99TEGOTs (4-2, prepared as described in chapter 4) was reacted with deuterated sodium methoxide. To label the branch connection the appropriately labeled diene alcohol $99CD_2OH$ (5-5) was prepared by the LAD reduction of the diene acid 5-4. This alcohol was then used in a Williamson etherification to yield $99CD_2TEGOMe$, the reaction conditions identical to the synthesis of the corresponding unlabeled monomer described in chapter 3.

The structures of the deuterium labeled monomers were confirmed by ^{1}H, ^{13}C, and ^{2}H NMR as well as high resolution mass spectrometry and elemental analysis. Figure 5-3 shows the ^{1}H NMR spectra of the deuterium labeled monomers with the unlabeled 99TEGOMe for comparison. In the spectrum for $99CD_2TEGOMe$ the doublet at δ=3.29 ppm corresponding to the methylene unit directly off the backbone disappears confirming deuterium labeling at this location. In the spectrum of $99TEGOCD_3$ the singlet at δ=3.35 ppm corresponding to the branch methyl end group is absent, confirming the presence of deuterons at this location. Similarly, differences in the ^{13}C NMR spectra (Figure 5-4) between the labeled and unlabeled can be seen. Labeling at the methylene unit and methyl end group results in the splitting of the corresponding carbon signal, slightly visible in the spectrum for $99CD_2TEGOMe$ (δ=75 ppm)

and not visible in the spectrum for 99TEGOCD$_3$ (δ=59 ppm). In both cases the disappearance of the obvious singlets confirms deuterium labeling has occurred on these carbons

As discussed in the chapter 3 (Figure 3-6), polymerization is confirmed by the disappearance of terminal olefin signals in both the ^{1}H and ^{13}C NMR spectra. Subsequent saturation is confirmed by the disappearance of the internal olefin signal.

Thermal Analysis

Since the ultimate goal of this synthesis is to study the dynamics above and below the glass transition and melting temperatures it is essential to confirm that labeling in this fashion will not affect these polymers' thermal response. Figure 5-5 shows the DSC overlay for all three labeled polymers. It is clear looking at the thermogram that the thermal behavior is identical in all cases, showing that labeling in this fashion does not alter the thermal behavior of the polymer. Given the consistency in the thermograms it is clear these materials are appropriate for future use in solid state ^{2}H NMR motion studies.

Conclusions

The polymer TEGOMe21 was deuterium labeled in three locations that have been proven critical throughout this dissertation in the crystallization and melting behavior of this class of materials. The deuterium labeling of these ADMET amphiphiles is straight forward and requires only small alterations in synthetic method. Labeling in the fashion does not affect the thermal behavior of the final polymer. These materials could be useful in solid state ^{2}H NMR motion studies. Such studies could offer further insight into the way these specific locations on the repeat unit of ADMET polymers affect the crystallization and melting behavior.

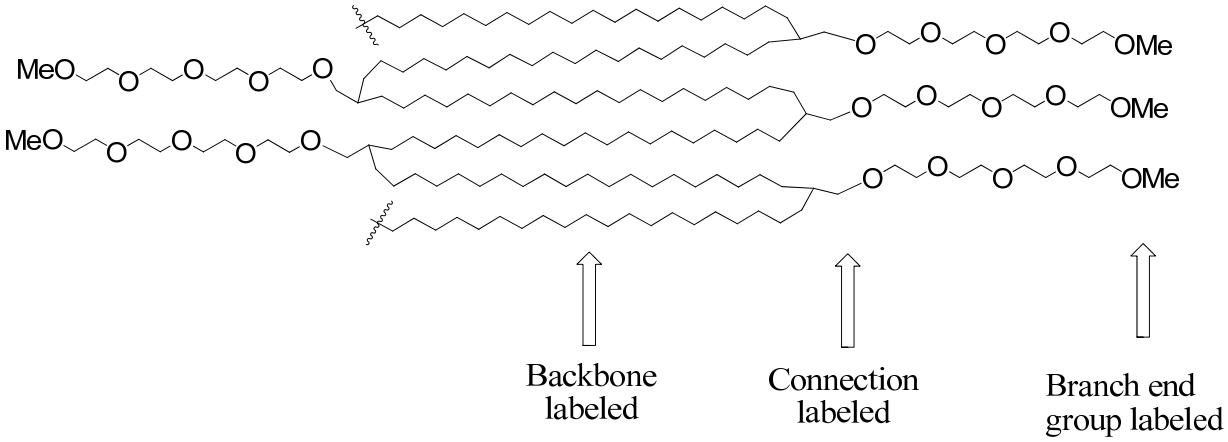

Figure 5-1: Locations chosen for deuterium labeling in TEGOMe21

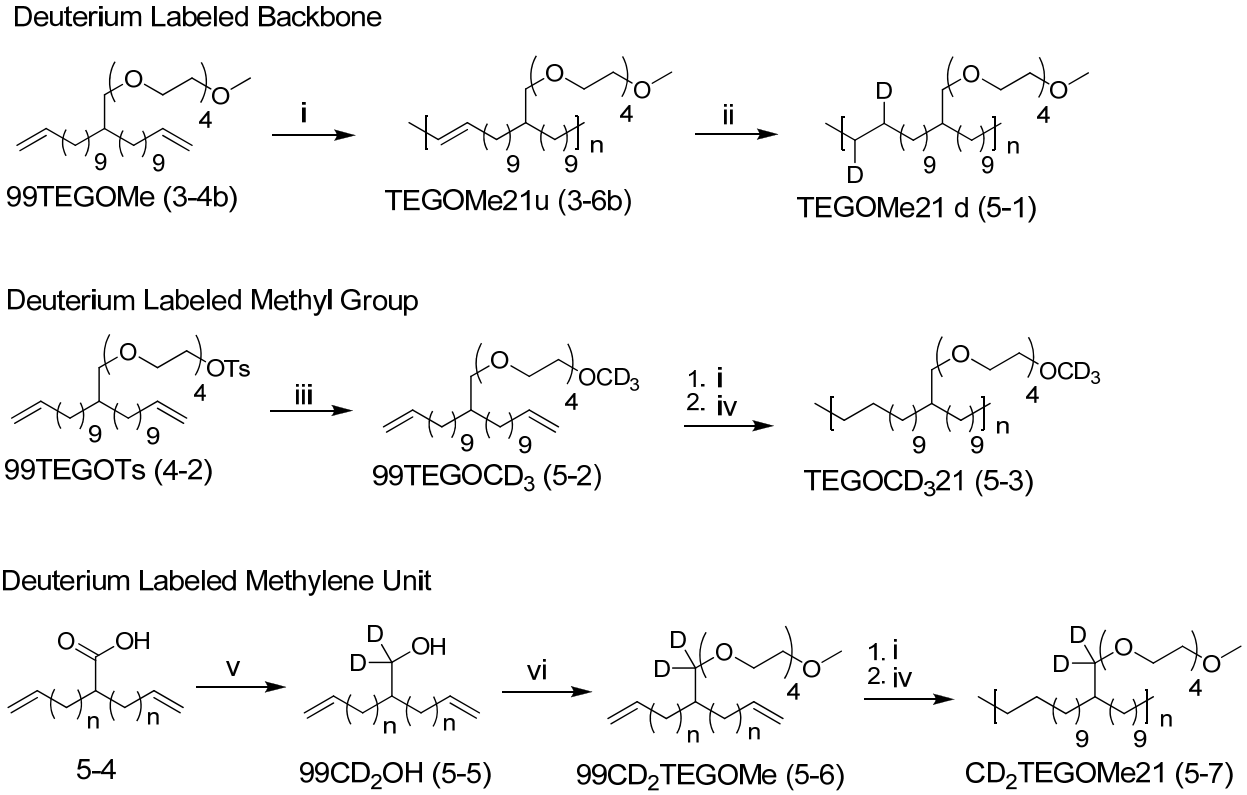

Figure 5-2: Synthesis of deuterium labeled TEGOMe21 analogues; i: Grubbs 1st generation, 45 °C, vacuum; ii: Wilkinson's catalyst; 700 psi D_2, toluene; iii: NaH, CD_3OD, DMF; iv: TSH, TPA, xylenes, 140 °C; v: LAD, THF; vi: NaH, $TsO(CH_2CH_2O)_4CH_3$, DMF

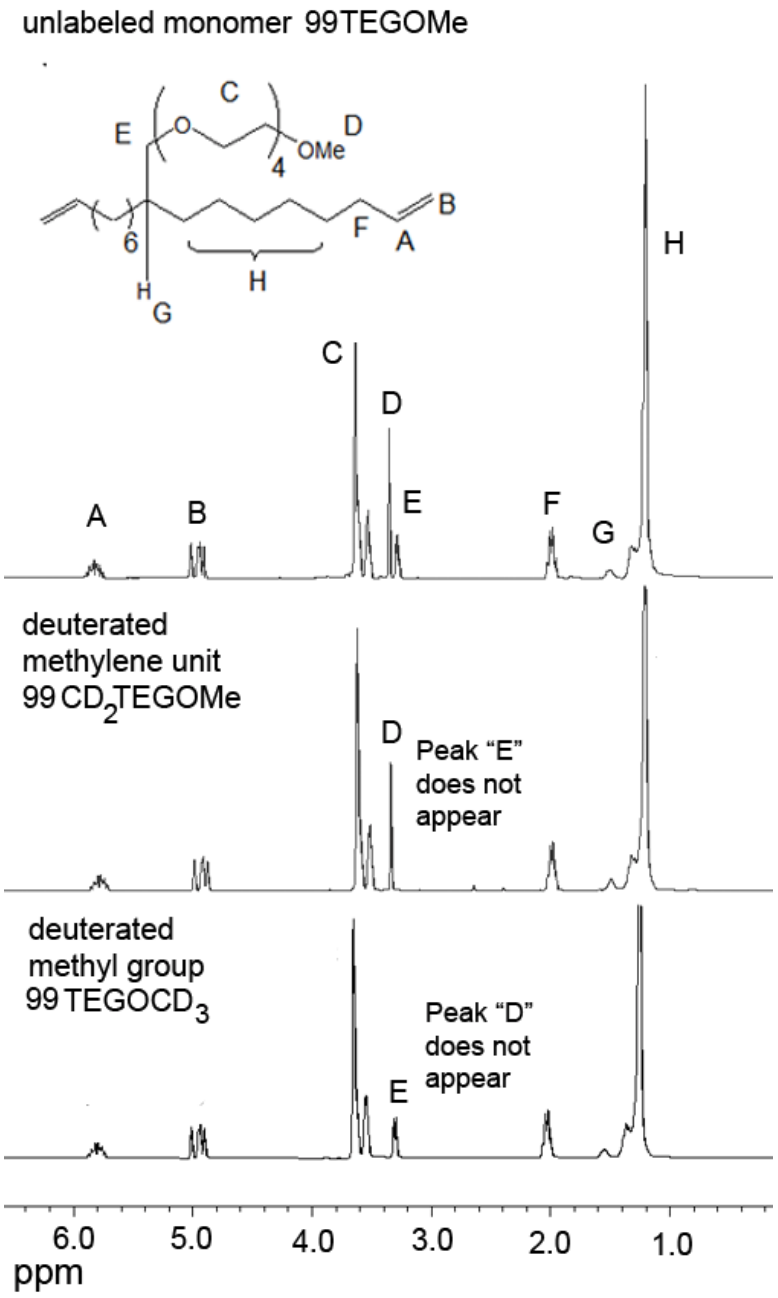

Figure 5-3: ^{1}H NMR of deuterium labeled 99TEGOMe analogues. Unlabeled 99TEGOMe shown for comparison

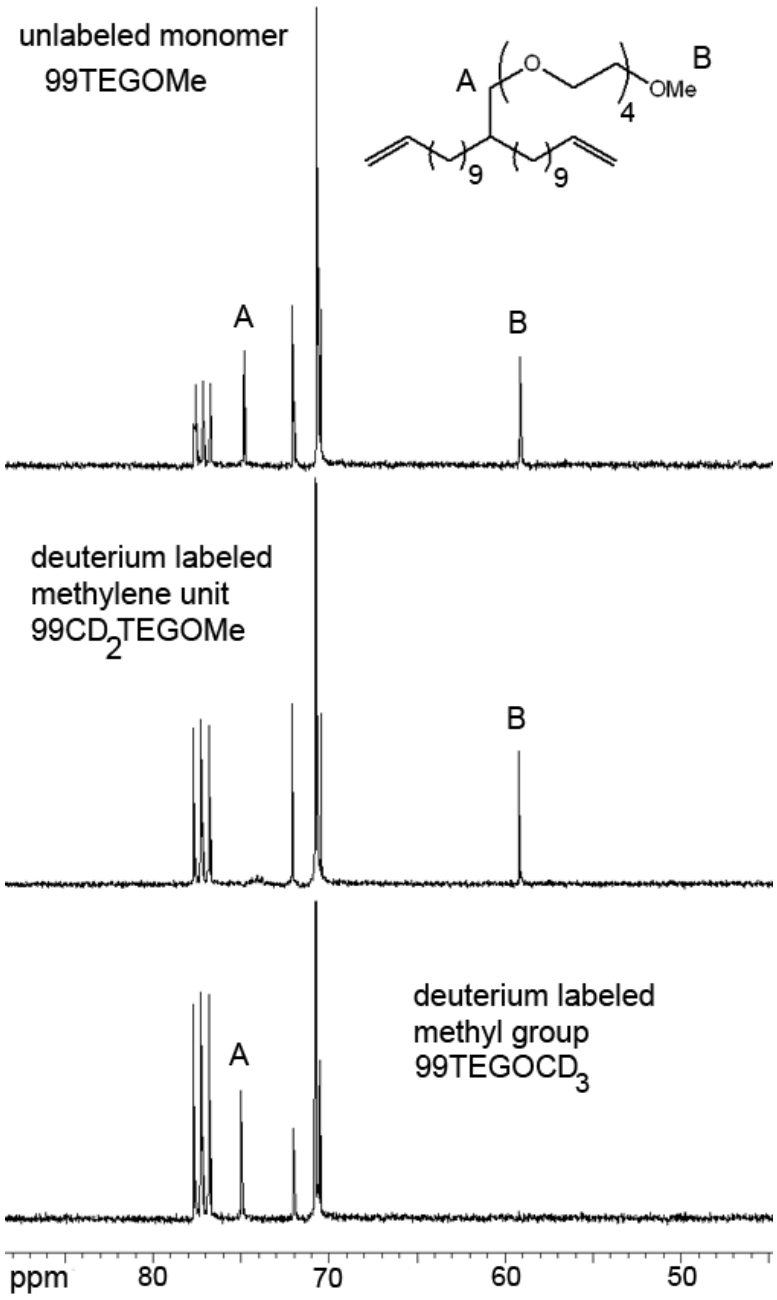

Figure 5-4: ^{13}C spectra of deuterium labeled 99TEGOMe analogues. Unlabeled 99TEGOMe shown for comparison

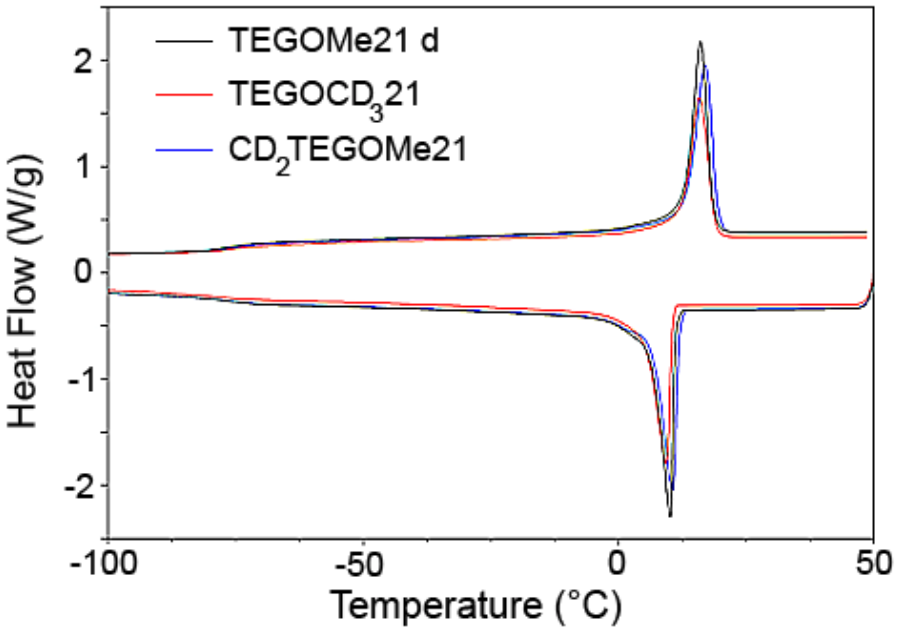

Figure 5-5: DSC overlay of the deuterium labeled TEGOMe21 analogues.

APPENDIX
IMPRESSIONS ON LIFE IN KYOTO

Hajimemashite

As long as I live I will never forget the shouts of *irrashaimassen dozo* when entering restaurants or shops, or the chants of *arigato gozimasu* received when leaving. Although I spent only one month in Japan it has left an indelible impression. The entire society is set up for efficiency and convenience. There is intense emphasis on being polite, as well as a strong feeling that the collective is much more important than the individual. This is not to say that individuality is not openly expressed and embraced. It is simply slightly more subtle than in western cultures. There are wisdoms and courtesies to Japanese culture that escape our own. People with colds, for example, wear gauze masks to protect others from infection. The emphasis on politeness can be aggravating to an unfamiliar outsider, and could even be misconstrued as open rudeness. For example, no one will tell you "no." They instead say: *musukashi desu ne* (literally "it's difficult"). *Chotto musukashi desu* (it's a little difficult) appears to mean down right impossible. Imagine asking if the train you are on goes to your destination and being told that "it's a bit difficult," only to find out after continuing to ride that is does not take you anywhere close to where you want to be. Once you begin to recognize the social rules and adopt them in your own behavior the atmosphere is warm and inviting.

Japan is not at all free of Western influence, however. Kyoto, Osaka and Nagoya have the same designer fashion boutiques as Fifth Avenue in Manhattan. The music shops are lined with rare and vintage American guitars. Camera shops contain high end professional equipment from all over the globe. Appearance, it seems, is very important. At the same time, stealing in Japan is unheard of. In Kyoto I lost a cellular phone on a bus and it was returned to me within days. The lack of thievery coupled with this emphasis on materialism perhaps reveals the most striking trait

of Japanese culture: everything from possessions to social status must be earned through hard work, honor, and integrity.

Amid the vast differences are innumerable and comforting similarities. It took no time at all for me to feel at home despite my sophomoric understanding of the language. In the following report I will briefly describe the cultural experience I had during my visit. This exchange has changed my outlook entirely. I can not wait to return for an extended visit, and I have recommended the trip to everyone I've talked to since my return. To spend time in another culture is essential to understand how small the world we share really is, how alike we all are, and how much we still have to learn from each other. For a graduate student this is of monumental importance, as many of us become the educators of future generations. We can not teach understanding and tolerance for all people until we are forced to tolerate and understand, as well as be tolerated and understood. My experience in Kyoto has promoted precisely this.

City life in Kyoto

I was immediately impressed by the cleanliness of the city, the efficiency of the public transportation, and the ease at which this city of about 1.5 million operates. The subway system consists of only 2 lines, which is in sharp contrast to the complicated network of train lines in Nagoya or Osaka. Busses are by far the easiest means of transport. They are always on time, reasonably priced (roughly 2 American dollars for most rides), and on city busses a number of stops are announced in English. Several private bus lines link to private and public train lines, making travel to surrounding areas very convenient.

Restaurants in Kyoto operate with the same efficiency as the public transportation. You are welcomed with tea, your order taken, and your check delivered with the food. There is no pressure to hurry, however the minute you stand up your table is bussed and prepared for the next customer. Tipping is not customary. The cost of food varies widely. Family sit down

restaurants (comparable to Applebee's or Ruby Tuesday's in the US) are about 30% more expensive, the cost per meal around 12-15 USD. Higher quality restaurants (comparable to our downtown restaurants like Liquid Ginger) are much more expensive, typically 30-50 USD for a meal. At some of the more famous sushi restaurants patrons can expect to pay upwards of $500 per person for the experience! Most restaurants of course feature Japanese food, however Chinese, French, and Italian cuisine are all very popular throughout Japan.

Japanese fast food is similar in cost to US fast food, depending on the meal item and portion. The food is much lower in fat content compared to US fast food. Food at grocery stores is again comparable to US prices, with the exception of beef, which is extremely expensive in Japan. Some western items are widely available such as breakfast cereal and potato chips; however it is difficult to find all of the ingredients to cook traditional American meals.

Entertainment is Kyoto is slightly lower key than other Japanese cities. There are a few pubs, bars, and night clubs. I didn't frequent these, preferring instead to explore the myriad temples, shrines, and shopping arcades for a true look into a foreign culture with a fascinating history. Perhaps the most interesting feature was the vast subterranean malls in Kyoto and Nagoya. In such a small country space is a premium, and the Japanese are experts and making the most efficient use of this resource.

Graduate School in Kyoto

The educational system in Japan is very different from our own system. Research groups are run by a team of three faculty members: one full professor, one associate professor, and one assistant professor. There is always more faculty on staff than at American research universities; Osaka University's department of Materials Engineering has 60 full professors alone (180 professors if assistant and associate professors are included!)

Students remain at the same school throughout undergraduate, masters, and PhD studies. They are required to finish masters studies before working towards a PhD; most students elect to take an industrial job rather than continuing for a PhD. Regardless of the difference in structure the time to a degree is about the same: Japanese graduate students spend 2 years in the masters course and 3 years in the PhD course. All of this time is spent on research, there is no teaching requirement.

Life as a graduate student in Japan is not at all unlike life as an American graduate student in the sciences. Most students work 10 to 12 hours days, most work at least one day on the weekend. Some students arrive early, most however begin work around 10 am. This varies from group to group, just like in the USA. The most striking difference to our university is the time for weekly group meeting: in Japan research groups meet every other Saturday to discuss research. The purpose is 2 fold, it allows every researcher ample time to discuss recent work and get advice, as well as forcing less diligent students to work at least 2 Saturdays a month! In addition, each researcher is expected to give a literature presentation every semester. There is great emphasis on being productive, and a total of 6 publications, split between undergraduate, masters, and PhD courses are expected before a PhD degree will be awarded. The length and style of PhD dissertations is very similar to those in the USA, and most are written in English.

College Sports at Kyoto University

I was fortunate enough to join Kyodai Judo Club for one of their practices and get a glimpse into role of extra curricular activities and athletics at Japanese colleges. There is really no equivalent at Japanese universities for NCAA college athletics. All sports are operated as clubs. The members, however, take them just as seriously as our college athletes (perhaps more so!) The Kyodai Judo team practices 6 days a week for at least 3 hours per session. Every other week there are 2 practice session per day Monday through Friday. This is true not only for

Japanese sports such as judo, kendo, and karate, but also western sports like boxing, fencing, volleyball, basket ball, etc. Music and art clubs operate with the same intensity. I was curious how this affected course work; apparently undergraduate studies are very different in Japan. The most rigorous part is the entrance exam. The course work is less intense than in the USA, the idea being that Undergraduate time is supposed to be enjoyed before the responsibilities of professional life set in.

Benefit to the University of Florida

The benefits of this exchange program to both the students involved as well as the University of Florida itself far outweigh the costs involved. Kyoto University is one of the top ranked schools in Asia (second only to the University of Tokyo), as well as being ranked in the top 25 schools in the world.

For students, this program allows a glimpse at a different culture with a fascinating history. For students in science particularly this is an eye opening experience, as the lingua franca for the sciences is English. At the poster sessions I attended a number of the presentations reflected this. Although a majority the lectures were in Japanese, most of the power point slides were in English, so it wasn't difficult to follow their stories. I even attended a few symposia were the language switched from Japanese to English between speakers (questions and discussions included)! Perhaps most surprising was the fact that these English lectures were usually given by Chinese or Korean speakers. It is especially important for American students to witness this. How many of us could enter into scientific discussions in multiple languages?

The University of Florida also benefits by strengthening its bond with a globally recognized institution. Kyoto University has been involved in exchange programs with Stanford, Brown, The University of Pennsylvania, the University of Michigan, Oxford, and Cambridge to

name a few. The University of Florida certainly belongs among such company, and I hope that we will continue to build this connection with colleagues at Kyoto University.

Arigato Gozaimashita

I would like to extend my gratitude to Professors Masuda, Sanda, and Shiotsuki for their hospitality, as well and the Deans office, the College of Liberal Arts and Sciences, and my advisor Ken Wagener for making this dream a reality. I am a changed person after my experience in Japan and I hope I can incorporate the lessons of patience, tolerance, respect, and curtsey I learned during my visit in all of my future endeavors.

LIST OF REFERENCES

1. Grubbs, R. H. *Tetrahedron* **2004,** 60, (34), 7117-7140.

2. Calderon, N.; Ofstead, E. A.; Ward, J. P.; Judy, W. A.; Scott, K. W. *J. Am. Chem. Soc.* **1968,** 90, (15), 4133-4140.

3. Calderon, N.; Chen, H. Y.; Scott, K. W. *Tetrahedron Letters* **1967,** 8, (34), 3327-3329.

4. Herrison, J.-L.; Chauvin, Y. *Makromol. Chem.* **1971**, (141), 161.

5. Katz, T. J.; McGinnis, J. *J. Am. Chem. Soc.* **1975,** 97, (6), 1592-1594.

6. Grubbs, R. H., *Handbook of Metathesis*. Wiley-VHC: New York, 2003.

7. Lindmark-Hamberg, M.; Wagener, K. B. *Macromolecules* **1987,** 20, (11), 2949-2951.

8. Wagener, K. B.; Boncella, J. M.; Nel, J. G.; Duttweiler, R. P.; Hillmyer, M. A. *Die Makromolekulare Chemie* **1990,** 191, (2), 365-374.

9. Berda, E. B.; Baughman, T. W.; Wagener, K. B. *Journal of Polymer Science Part A: Polymer Chemistry* **2006,** 44, (17), 4981-4989.

10. Baughman, T. W.; Wagener, K. B. *Advances in Polymer Science* **2005,** 176, (Metathesis Polymerization), 1-42.

11. Lehman, S. E.; Wagener, K. B., ADMET Polymerization. In *The Handbook of Metathesis*, Grubbs, R. H., Ed. Wiley: New York, 2003; Vol. 3.

12. Sworen, J. C.; Wagener, K. B. *Macromolecules* **2007,** 40, (13), 4414-4423.

13. Boz, E.; Nemeth, A. J.; Ghiviriga, I.; Jeon, K.; Alamo, R. G.; Wagener, K. B. *Macromolecules* **2007,** 40, (18), 6545-6551.

14. Boz, E.; Nemeth, Alexander J.; Alamo, Rufina G.; Wagener, Kenneth B. *Advanced Synthesis & Catalysis* **2007,** 349, (1-2), 137-141.

15. Berda, E. B.; Lande, R. E.; Wagener, K. B. *Macromolecules* **2007**.

16. Boz, E.; Wagener, K. B.; Ghosal, A.; Fu, R.; Alamo, R. G. *Macromolecules* **2006,** 39, (13), 4437-4447.

17. Sworen, J. C.; Smith, J. A.; Berg, J. M.; Wagener, K. B. *J. Am. Chem. Soc.***2004,** 126, (36), 11238-11246.

18. Watson, M. D.; Wagener, K. B. *Macromolecules* **2000,** 33, (24), 8963-8970.

19. Smith, J. A.; Brzezinska, K. R.; Valenti, D. J.; Wagener, K. B. *Macromolecules* **2000,** 33, (10), 3781-3794.

20. Schwendeman, J. E.; Wagener, K. B. *Macromolecular Chemistry and Physics* **2005,** 206, (15), 1461-1471.

21. Boz, E.; Nemeth, A. J.; Wagener, K. B.; Jeon, K.; Smith, R.; Nazirov, F.; Bockstaller, M. R.; Alamo, R. G. *Macromolecules* **2008**.

22. Boz, E.; Ghiviriga, I.; Nemeth, A. J.; Jeon, K.; Alamo, R. G.; Wagener, K. B. *Macromolecules* **2008,** 41, (1), 25-30.

23. Sworen, J. C.; Smith, J. A.; Wagener, K. B.; Baugh, L. S.; Rucker, S. P. *J. Am. Chem. Soc.* **2003,** 125, (8), 2228-2240.

24. Baughman, T. W.; Sworen, J. C.; Wagener, K. B. *Macromolecules* **2006,** 39, (15), 5028-5036.

25. Courchay, F. C.; Baughman, T. W.; Wagener, K. B. *Journal of Organometallic Chemistry* **2006,** 691, (4), 585-594.

26. Lieser, G.; Wegner, G.; Smith, J. A.; Wagener, K. B. *Colloid and Polymer Science* **2004,** 282, (8), 773-781.

27. Qiu, W.; Sworen, J.; Pyda, M.; Nowak-Pyda, E.; Habenschuss, A.; Wagener, K. B.; Wunderlich, B. *Macromolecules* **2006,** 39, (1), 204-217.

28. Baughman, T. W.; vanderAa, E.; Wagener, K. B. *Macromolecules* **2006,** 39, (20), 7015-7021.

29. Baughman, T. W.; vanderAa, E.; Lehman, S. E.; Wagener, K. B. *Macromolecules* **2005,** 38, (7), 2550-2551.

30. Luo, S.; Vela, J.; Lief, G. R.; Jordan, R. F. *J. Am. Chem. Soc.* **2007,** 129, (29), 8946-8947.

31. Baughman, T. W.; Chan, C. D.; Winey, K. I.; Wagener, K. B. *Macromolecules* **2007,** 40, (18), 6564-6571.

32. Baughman, T. W. Functionalized Ethylene Copolymers and Materials via Olefin Metathesis Polymerization. PhD Dissertation, University of Florida, 2006.

33. Liu, G.; Reinhout, M.; Mainguy, B.; Baker, G. L. *Macromolecules* **2006,** 39, (14), 4726-4734.

34. Iwasaki, Y.; Akiyoshi, K. *Biomacromolecules* **2006,** 7, (5), 1433-1438.

35. Wang, F.; Bronich, T. K.; Kabanov, A. V.; Rauh, R. D.; Roovers, J. *Bioconjugate Chemistry* **2005,** 16, (2), 397-405.

36. Tian, H. Y.; Deng, C.; Lin, H.; Sun, J.; Deng, M.; Chen, X.; Jing, X. *Biomaterials* **2005,** 26, (20), 4209-4217.

37. Cheng, Z.; Zhu, X.; Kang, E. T.; Neoh, K. G. *Langmuir* **2005,** 21, (16), 7180-7185.

38. Sun, L.; Liu, Y.; Zhu, L.; Hsiao, B. S.; Avila-Orta, C. A. *Polymer* **2004,** 45, (24), 8181-8193.

39. Lu, Y.; Chen, S.; Hu, Y.; Chung, T. C. *Polymer International* **2004,** 53, (12), 1963-1967.

40. Loiseau, F. A.; Hii, K. K.; Hill, A. M. *Journal of Organic Chemistry* **2004,** 69, (3), 639-47.

41. Huang, W.; Zhou, Y.; Yan, D. *Journal of Polymer Science, Part A: Polymer Chemistry* **2005,** 43, (10), 2038-2047.

42. Breitenkamp, K.; Simeone, J.; Jin, E.; Emrick, T. *Macromolecules* **2002,** 35, (25), 9249-9252.

43. O'Donnell, P. M.; Brzezinska, K.; Powell, D.; Wagener, K. B. *Macromolecules* **2001,** 34, (20), 6845-6849.

44. Chen, Y.; Baker, G. L. *Journal of Organic Chemistry* **1999,** 64, (18), 6870-6873.

45. Loiseau, F. A.; Hii, K. K.; Hill, A. M. *Journal of Organic Chemistry* **2004,** 69, (3), 639-47.

46. Schmalz, H.; Knoll, A.; Muller, A. J.; Abetz, V. *Macromolecules* **2002,** 35, (27), 10004-10013.

47. Guo, Q.; Thomann, R.; Gronski, W.; Thurn-Albrecht, T. *Macromolecules* **2002,** 35, (8), 3133-3144.

48. Fukuhara, K.; Hashiwata, K.; Takayama, K.; Matsuura, H. *Journal of Molecular Structure* **2000,** 523, (1-3), 269-280.

49. Hopkins, T. E.; Wagener, K. B. *Macromolecules* **2004,** 37, (4), 1180-1189.

50. Hopkins, T. E.; Pawlow, J. H.; Koren, D. L.; Deters, K. S.; Solivan, S. M.; Davis, J. A.; Gomez, F. J.; Wagener, K. B. *Macromolecules* **2001,** 34, (23), 7920-7922.

51. Wunderlich, B. *Journal of Thermal Analysis & Calorimetry* **2006,** 85, (1), 179-187.

52. Uehara, H.; Kanamoto, T.; Kawaguchi, A.; Murakami, S. *Macromolecules* **1996,** 29, (5), 1540-1547.

53. Lehman, S. E.; Wagener, K. B.; Baugh, L. S.; Rucker, S. P.; Schulz, D. N.; Varma-Nair, M.; Berluche, E. *Macromolecules* **2007,** 40, (8), 2643-2656.

54. Matloka, P. P.; Sworen, J. C.; Zuluaga, F.; Wagener, K. B. *Macromolecular Chemistry and Physics* **2005,** 206, (2), 218-226.

55. Lu, Y.; Hu, Y.; Wang, Z. M.; Manias, E.; Chung, T. C. *Journal of Polymer Science Part A: Polymer Chemistry* **2002,** 40, (20), 3416-3425.

56. Hu, D.; Cheng, Z.; Zhu, J.; Zhu, X. *Polymer* **2005,** 46, (18), 7563-7571.

57. Sun, L.; Liu, Y.; Zhu, L.; Hsiao, B. S.; Avila-Orta, C. A. *Macromolecular Rapid Communications* **2004,** 25, (8), 853-857.

58. Menger, F. M.; Lu, H.; Lundberg, D. *J. Am. Chem. Soc.* **2007,** 129, (2), 272-273.

59. Stone, M. T.; Moore, J. S. *Org. Lett.* **2004,** 6, (4), 469-472.

60. Shieh, Y.-T.; Liu, G.-L. *Journal of Polymer Science Part B: Polymer Physics* **2007,** 45, (4), 466-474.

61. Schawe, J. E. K. *Thermochimica Acta* **1997,** 304-305, 111-119.

62. Jones, K. J.; Kinshott, I.; Reading, M.; Lacey, A. A.; Nikolopoulos, C.; Pollock, H. M. *Thermochimica Acta* **1997,** 304-305, 187-199.

63. Rodriguez-Hernandez, J.; Checot, F.; Gnanou, Y.; Lecommandoux, S. *Progress in Polymer Science* **2005,** 30, (7), 691-724.

64. Rider, D. A.; Cavicchi, K. A.; Power-Billard, K. N.; Russell, T. P.; Manners, I. *Macromolecules* **2005,** 38, (16), 6931-6938.

65. Kim, Y.; Pyun, J.; Frechet, J. M. J.; Hawker, C. J.; Frank, C. W. *Langmuir* **2005,** 21, (23), 10444-10458.

66. Allcock, H. R.; Powell, E. S.; Chang, Y.; Kim, C. *Macromolecules* **2004,** 37, (19), 7163-7167.

67. Park, C.; Yoon, J.; Thomas, E. L. *Polymer* **2003,** 44, (22), 6725-6760.

68. Yu, Z.; Liu, L. *Journal of Biomaterials Science, Polymer Edition* **2005,** 16, (8), 957-971.

69. Hillmyer, M. A.; Bates, F. S. *Macromolecules* **1996,** 29, (22), 6994-7002.

70. Fu, G. D.; Phua, S. J.; Kang, E. T.; Neoh, K. G. *Macromolecules* **2005,** 38, (7), 2612-2619.

71. Vlcek, P.; Otoupalova, J.; Sikora, A.; Kriz, J. *Macromolecules* **1995,** 28, (21), 7262-7265.

72. Singh, R.; Verploegen, E.; Hammond, P. T.; Schrock, R. R. *Macromolecules* **2006,** 39, (24), 8241-8249.

73. Pschorn, U.; Roessler, E.; Sillescu, H.; Kaufmann, S.; Schaefer, D.; Spiess, H. W. *Macromolecules* **1991,** 24, (2), 398-402.

74. Leisen, J.; Schmidt-Rohr, K.; Spiess, H. W. *Journal of Non-Crystalline Solids* **1994,** 172-174, (Pt. 2), 737-50.

75. Wiesner, U.; Spiess, H. W.; Müller, F.; Kremer, F.; Lauprêtre, F.; Halary, J. L.; Monnerie, L. *Acta Polymerica* **1996,** 47, (10), 429-435.

76. Sworen, J. C. Modeling Linear-low Density Polyethylene: Copolymers Containing Precise Structures. PhD Dissertation, Univeristy of Florida, 2004.

77. Lee, Y. J.; Murakhtina, T.; Sebastiani, D.; Spiess, H. W. *J. Am. Chem. Soc.* **2007,** 129, (41), 12406-12407.

BIOGRAPHICAL SKETCH

Erik Benjamin Berda was born in Scranton, PA on September 12th, 1980. Shortly after, parents Pat and Marybeth Berda relocated to the Northwest Suburbs of Philadelphia, where Erik spent the remainder of his youth. He discovered chemistry during sophomore year of high school and became immediately enamored. Erik graduated from Norristown Area High School in June, 1999. He began studies towards a Bachelor of Science Degree in chemistry at Penn State University (PSU), University Park Campus, in August 1999.

During his second year at PSU he joined the research group of Prof. Harry R. Allcock, studying phosphazene based polymers for advanced lithium battery applications. Erik also developed a deep passion for teaching at PSU giving guitar lessons. This translated fluidly into science while teaching a section of organic lab in the spring of his senior year.

After graduating from PSU in December 2003 Erik moved to the University of Florida in Gainesville to pursue a PhD degree in Organic Chemistry under the advisement of Prof. Kenneth B. Wagener. During his tour of duty in Gainesville, the state of Florida endured record numbers of hurricanes, wild fires, and fatal alligator attacks. Despite this, the University's own Gators managed to capture a record number of NCAA national titles.

In September 2007 Erik spent a month at Kyoto University in Kyoto, Japan. He successfully completed the requirements for the PhD degree in March of 2008. After graduation he moved to Europe with longtime girlfriend Dana Gioia to begin postdoctoral studies with Prof. Bert W. Meijer at the Technical University of Eindhoven in Eindhoven, The Netherlands.